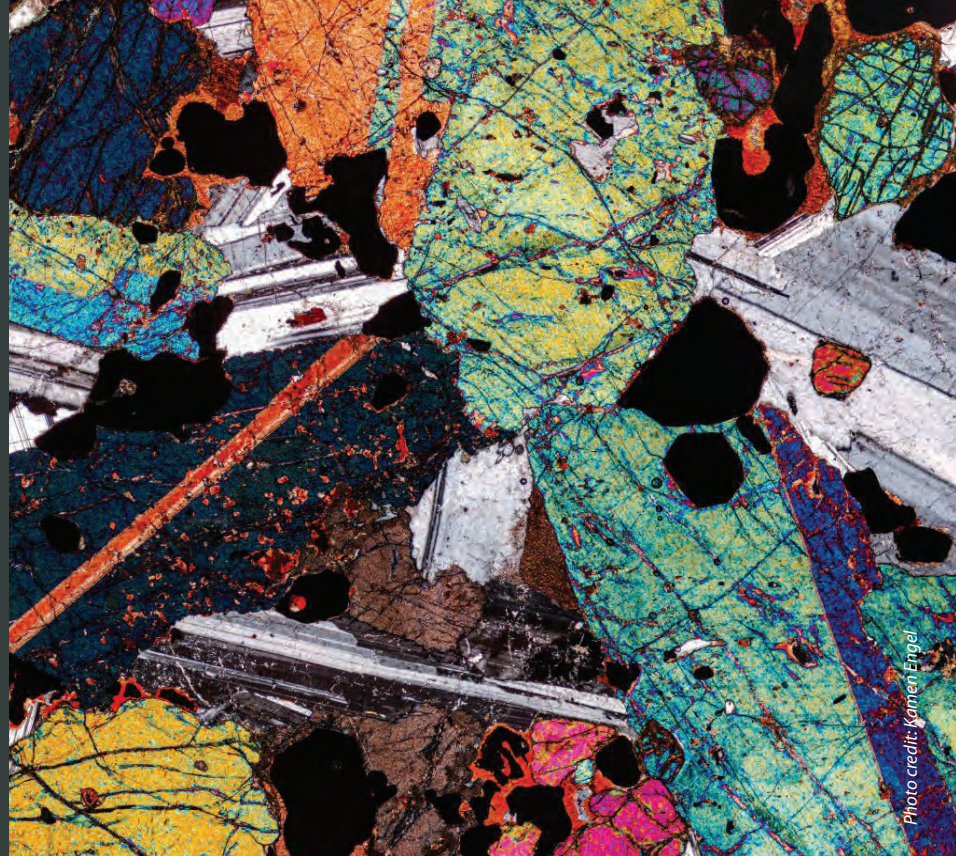




# Annual Conference 2020

22–25 November  
University of Canterbury  
Christchurch



## ABSTRACT VOLUME



[CONFER.NZ/GSNZ2020](https://confer.nz/gsnz2020)

Bibliographic reference for Field Trip Guides:

Author A.B., Author B.C. (2020). Field trip title. In: Bassett K.N., Horton T.W. eds. Geosciences 2020: Field Trip Guides. Geoscience Society of New Zealand Miscellaneous Publication 157B. Geoscience Society of New Zealand, Wellington, pp. 1–2.

Geoscience Society of New Zealand Miscellaneous Publication 157B  
ISBN (online): 978-0-473-55116-2  
ISSN (online): 2230-4495

## **LOCAL ORGANISING COMMITTEE**

### **Organising Committee Convenor**

Kari Bassett, University of Canterbury

### **Organising Committee**

Alex Nichols, Programme Committee, University of Canterbury

Clark Fenton, Programme Committee, University of Canterbury

Sacha Baldwin, University of Canterbury

Darren Gravley, University of Canterbury

Travis Horton, University of Canterbury

Ben Kennedy, University of Canterbury

Kate Pedley, University of Canterbury

Matiu Prebble, University of Canterbury

Rob Spiers, University of Canterbury

Tom Wilson, University of Canterbury

## **SESSION CONVENORS AND CHAIRS**

Peter Almond (Lincoln University), Richmond Beetham (Coffey), Mac Beggs (University of Canterbury), David Bell (University of Canterbury), Alan Bischoff (University of Canterbury), Kate Clark (GNS Science), Shaun Eaves (Victoria University of Wellington), Joanna Elliot (Todd Energy), Clark Fenton (University of Canterbury), Michael Gazley (AusIMM), Alexandra Gossart (Victoria University of Wellington), Jess Hillman (GNS Science), Jenni Hopkins (Victoria University of Wellington), Ilma Del Carmen Juarez Garfias (Victoria University of Wellington), Andy Howell (University of Canterbury/GNS Science), Katelyn Johnson (GNS Science), Richard Justice (ENGE0), Andrew La Croix (Waikato University), Rob Langridge (GNS Science), Mark Lawrence (GNS Science), Andrew Lorrey (NIWA), Sebastian Naeher (GNS Science), Karoly Nemeth (Massey University), Andy Nicol (University of Canterbury), Michael G. Petterson (Auckland University of Technology), Adrian Pittari (University of Waikato), Matiu Prebble (University of Canterbury), Heather Purdie (University of Canterbury), James Scott (University of Otago), Sarah Seabrook (NIWA / University of Auckland), Dan Sinclair (Victoria University of Wellington), Richard Smith (Resilience National Science Challenge), Mark Stirling (University of Otago), James Thompson (Canterbury Emergency Management Office), Lauren Vargo (Victoria University of Wellington), Emily Warren-Smith (GNS Science), Sally Watson (NIWA), Tom Wilson (University of Canterbury), Holly Winton (Victoria University of Wellington), Hisham Zarour (Stantec)

## SPONSORS

The conference organising committee acknowledges and thanks the following key sponsors for their generous support and involvement in this conference.

Their support has contributed towards our being able to provide a comprehensive programme of quality content and excellent value for all participants.

### Gold Sponsor



### Silver Sponsors



### Bronze Sponsor



### Grant Sponsor



### Supporting Sponsors and Exhibitors



**UC<sup>ED</sup> EARTH AND ENVIRONMENT**  
*Te Kura Aronukurangi*



## CONTENTS

Field Trip 1: Kaikōura earthquake surface ruptures,landslides and building damage	1
Field Trip 4: Petroleum Exploration and Production in North Canterbury	17
Field Trip 5: Banks Peninsula’s Best Bits: Volcanology, Research and Geopark	42
Field Trip 6: A Walking Tour of Christchurch CBD Rebuild	68

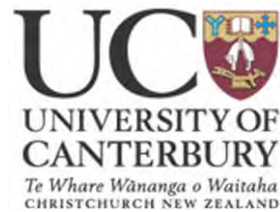
# FIELD TRIP 1: KAIKŌURA EARTHQUAKE SURFACE RUPTURES, LANDSLIDES AND BUILDING DAMAGE

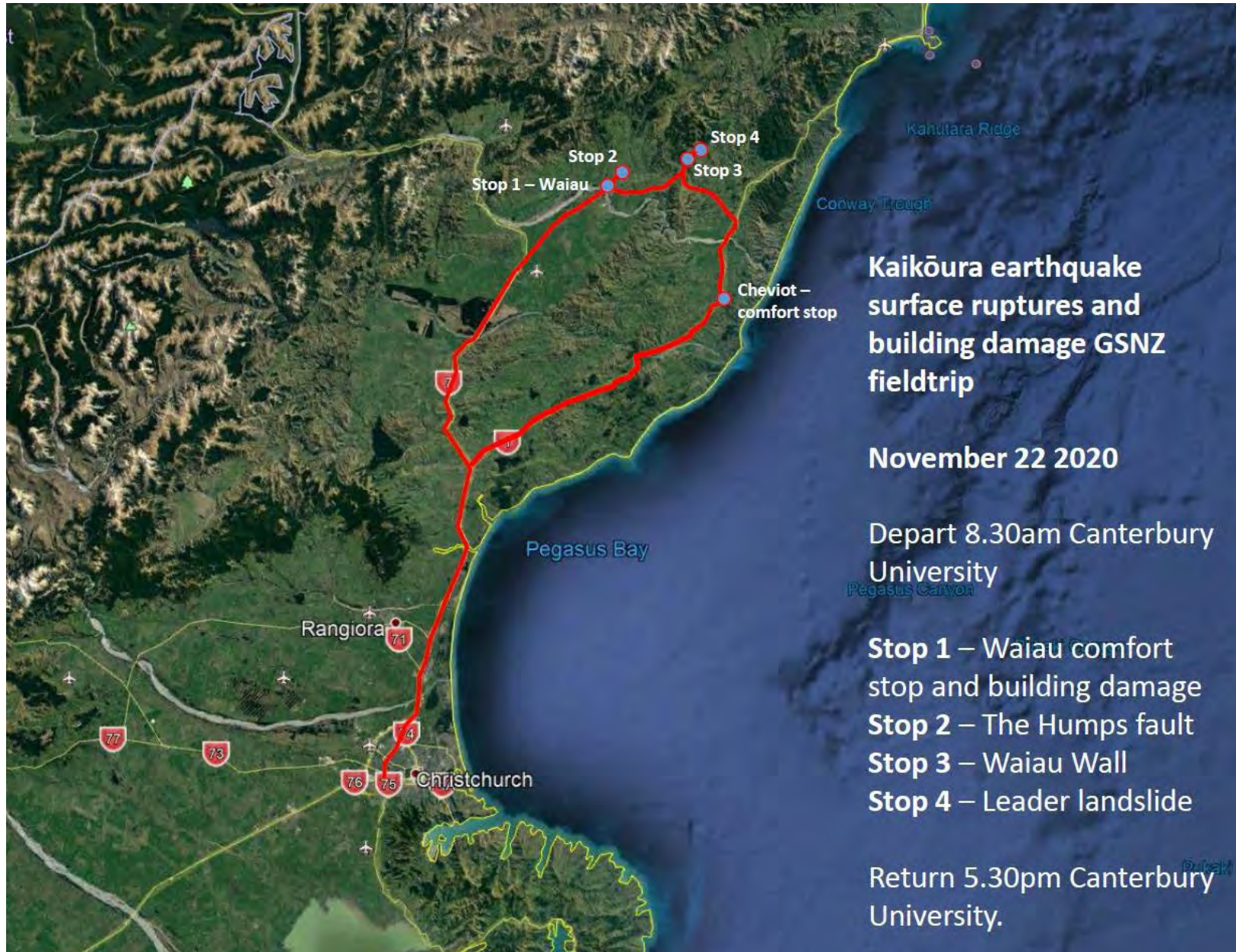
Sunday 22 November 2020

Leaders: Andy Nicol and Kate Pedley, University of Canterbury



Three-metre high fault scarp generated along the Leader Fault during the November 14<sup>th</sup> 2016 Kaikōura Earthquake. Photograph by Kate Pedley.





## Kaikōura earthquake surface ruptures and building damage GSNZ fieldtrip

November 22 2020

Depart 8.30am Canterbury University

- Stop 1** – Waiau comfort stop and building damage
- Stop 2** – The Humps fault
- Stop 3** – Waiau Wall
- Stop 4** – Leader landslide

Return 5.30pm Canterbury University.

## Kaikōura Earthquake

The Mw 7.8 Kaikōura earthquake struck at two minutes past midnight on 14 November 2016 (NZDT), almost 4 years ago to the day. Its epicentre was located near the South Island township of Waiiau (Figure 1; Figure 2) and was the largest on-land earthquake to hit New Zealand in more than a century (Downs and Dowrick, 2015). The Kaikōura earthquake ruptured at least 20 faults at the ground surface for a distance of ~165 km across the New Zealand plate boundary zone in the northeastern South Island of New Zealand. The earthquake initiated at a focal depth of ~14 km on The Humps Fault and propagated northwards with the greatest energy release occurring north of Kaikōura (Kaiser et al., 2017; Hamling et al., 2017). The complexity of the Kaikōura earthquake is partly reflected in the oblique focal mechanism, which displays approximately equal components of thrusting/reverse and right-lateral slip (e.g., Cesca et al., 2017; Kaiser et al., 2017; Wang et al., 2017). The resulting fault ruptures displaced the ground surface and sea floor with strikes varying from east-west to north-northwest. The east-northeast striking faults are primarily right-lateral strike-slip and the northerly striking faults have left-lateral reverse displacement (Stirling et al., 2017; Litchfield et al., 2018). In addition to the mapped surface faults, the spatial extent of coastal uplift and widespread occurrence of tsunamis up to ~250 km from Kaikōura have been interpreted to indicate slip on the subduction interface and/or a blind upper plate thrust(s) within the accretionary prism complex (e.g., Clark et al., 2017; Wang et al., 2017; Mouslopoulou et al., 2019).

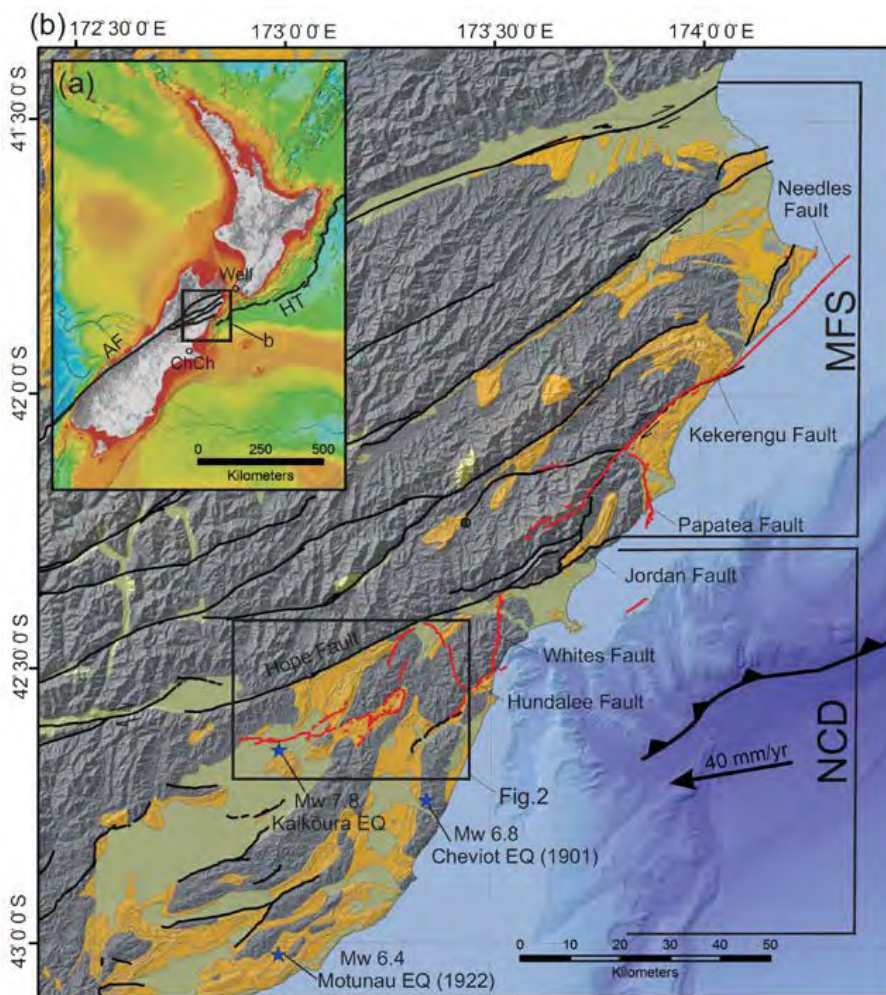


Figure 1. Maps showing the plate boundary setting of the Kaikōura earthquake. (a) New Zealand plate boundary. AF, Alpine Fault; ChCh, Christchurch; HT, Hikurangi Trough; Well, Wellington. (b) Geology (Torlesse Supergroup Basement - grey; Late Cretaceous-Cenozoic strata—orange-brown; Quaternary deposits—yellow-green; Rattenbury et al., 2006), active faults (black lines from Langridge et al. 2016) and faults that ruptured in the November 14 2016 Mw 7.8 Kaikōura earthquake (red lines with fault names) in the northeastern South Island. The Pacific Plate motion vector relative to the Australian Plate is from Beavan et al. (2002). MFS, Marlborough Fault System; NCD, North Canterbury Domain. Figure from Nicol et al. (2018).

## Earthquake Tectonic Setting

The Kaikōura earthquake produced displacement on faults that accommodate the transition from subduction beneath the North Island to continental collision and strike slip on the Alpine fault in the South Island of New Zealand (Figure 1A). Onshore in the South Island,  $\geq 80\%$  of the  $\sim 40$  mm/yr relative plate motion is transferred from subduction towards the Alpine fault via strike-slip on the Marlborough Fault System (MFS) (e.g., Beavan and Haines, 2001; Wallace et al., 2012). Offshore and east of the Kaikōura earthquake surface ruptures, plate boundary deformation is accommodated by a subduction thrust and accretionary prism complex (e.g., Barnes and Audru, 1999; Williams et al., 2013). The accretionary prism and eastern MFS are underlain by the Pacific plate which, based on seismic tomography and focal depths of historical seismicity, extends to a depth of at least 200 km beneath the northern South Island (Eberhart-Phillips and Bannister, 2010; Eberhart-Phillips and Reyners, 2012; Williams et al., 2013). These data indicate that in the epicentral area the top of the subducted Pacific plate is located at a depth of  $\sim 20$ -30 km beneath the surface ruptures and may define the lower limit of the upper-plate faults (Nicol et al., 2018).

In the epicentral area of North Canterbury, here referred to as the North Canterbury (Tectonic) Domain (NCD) (Figure 1), active faulting and Quaternary deformation has been widely reported prior to the Kaikōura earthquake (e.g., Pettinga et al., 2001; Rattenbury et al., 2006; Forsyth et al., 2008; Barrell and Townsend, 2012). The NCD accommodates transpression and is dominated by northeast-striking oblique-slip faults with components of right-lateral and reverse displacement (e.g., Nicol et al., 1994; Pettinga et al., 2001). These faults typically separate hanging-wall anticlines and footwall synclines, which are manifest in the topography as Quaternary-age basins and ranges. Late Cretaceous to Pliocene strata that predate the onset of Quaternary deformation occupy the basins, while the ranges are often cored by steeply bedded and complexly deformed Torlesse Supergroup basement (Figure 1) (e.g., Rattenbury et al., 2006; Forsyth et al., 2008). Basin and range topography primarily reflect crustal contraction and provide little evidence for a component of strike slip on the NE–ENE trending faults.

Many of the faults mapped in the NCD are associated with active fault traces, which attest to the ongoing earthquake activity of these structures (e.g., Pettinga et al., 2001; Rattenbury et al., 2006; Forsyth et al., 2008; Barrell and Townsend, 2012). Quantitative data constraining the displacement rates and recurrence intervals of these faults is limited, with the majority of rates estimated to be  $< 2$  mm/yr and recurrence intervals of thousands to 10s of thousands of years (Pettinga et al., 2001; Barrell and Townsend, 2012). Due in part to these long recurrence intervals the faults that ruptured in the NCD on November 14<sup>th</sup> 2016 were either, not known to be active or their lengths were poorly defined prior to the earthquake. Given these recurrence intervals it is also unsurprising that the Kaikōura earthquake is the only historical event to have produced surface rupture in the NCD. In addition to the Kaikōura earthquake the Mw 6.8 Cheviot 1901 and Mw 6.4 Motunau 1922 shallow ( $< 25$  km depth) earthquakes may have produced surface folding in the NCD due to fault displacement at depth (see Downes and Dowrick, 2015, for descriptions of the earthquakes and Figure 1 for their locations).

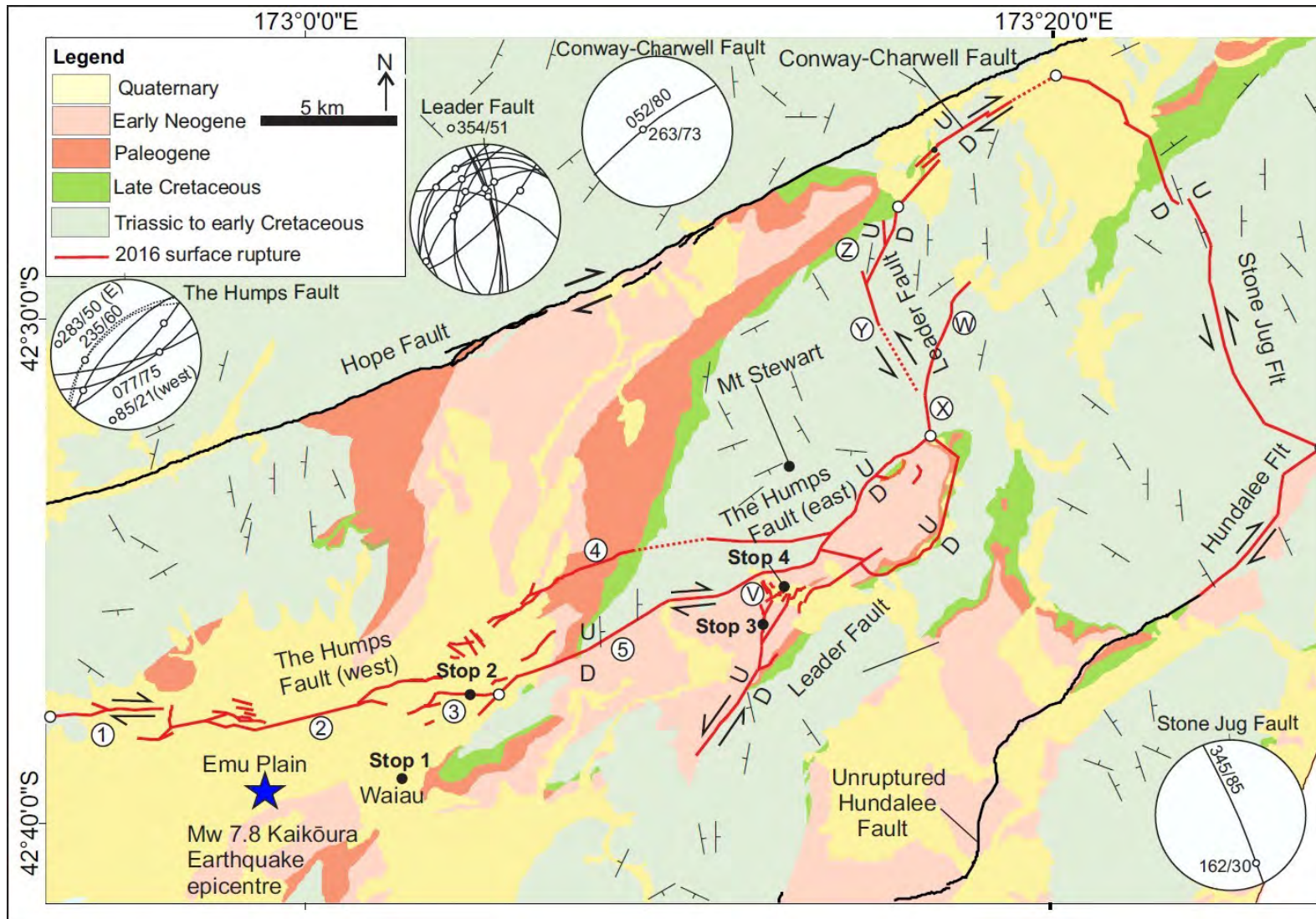


Figure 2. Geological map of rock units, active faults that did not rupture during the earthquake (dark grey lines) and surface ruptures from the Kaikōura earthquake (solid and black lines surveyed and dashed redlines inferred from deformation recorded by InSAR in the study area south of the Hope fault in the NCD (Rattenbury et al., 2006; Langridge et al., 2016). Strike and dip of bedding in Torlesse rocks is from Rattenbury et al. (2006). See Figure 1 for location of study area. Inset stereonets depict fault planes (great circles) and slip vectors (white filled circles) for The Humps, Leader, Conway-Charwell and Stone Jug faults from field measurements. Strike-slip movement sense shown by arrows along with upthrow (U) and down throw (D) on fault traces. Locations of stops 1, 2, 3 and 4 shown. Figure modified from Nicol et al. (2018).

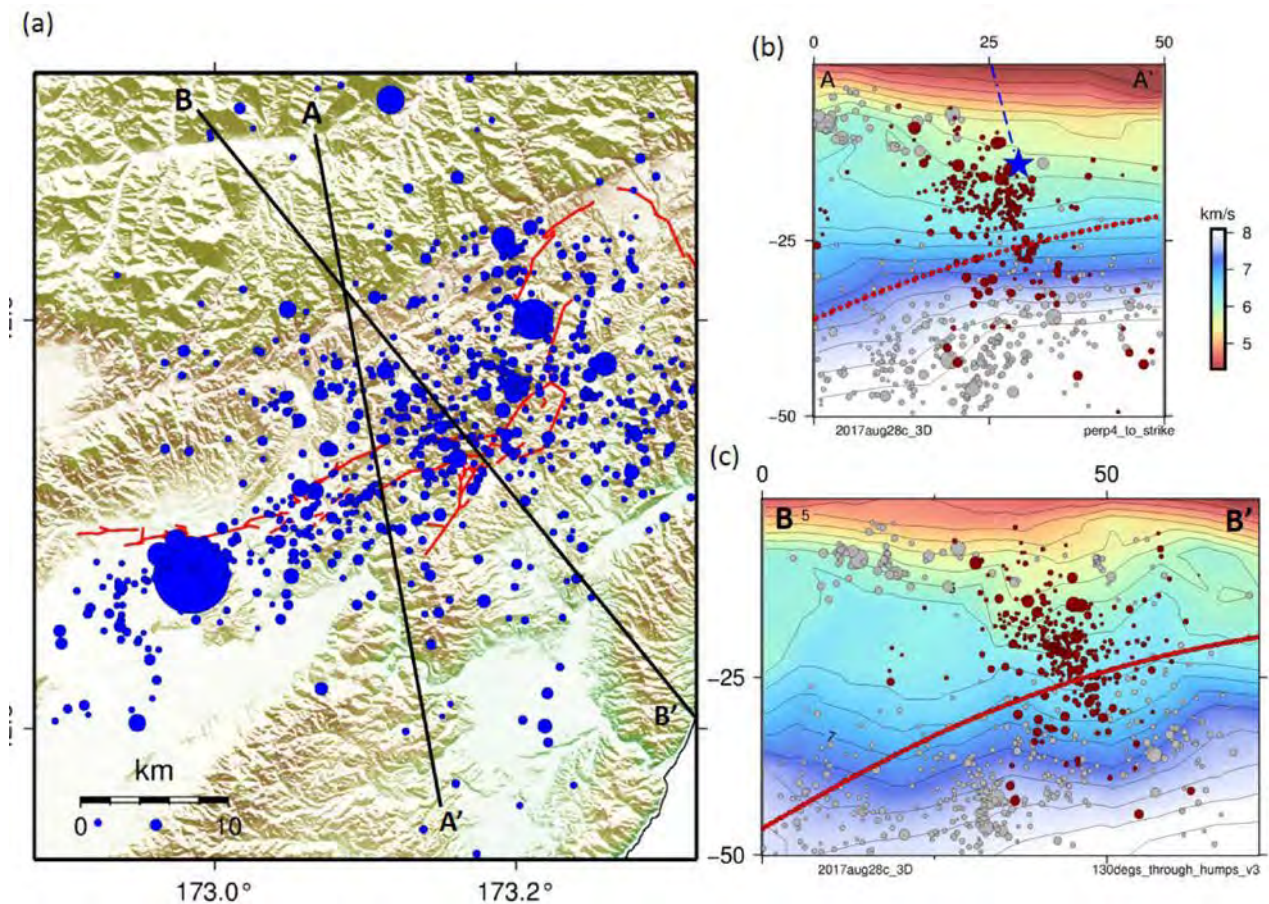


Figure 3. Main shock (large blue filled circle) and aftershock locations displayed on map (a) and cross sections (b and c) showing subsurface fault geometry of The Humps and Leader faults. Events recorded by GeoNet seismograph stations were relocated using the HypoDD relative earthquake location algorithm (Waldhauser and Ellsworth, 2000) and phase-two automatic P arrival time picks along with the New Zealand 3D velocity model now used by GeoNet for routine locations (see Nicol et al. 2018 for further discussion). Locations of cross sections A-A' and B-B' are shown on the map in (a). Surface ruptures from the Kaikōura earthquake are indicated by the red lines. Closely-spaced red dots on (b) and (c) indicate the approximate location of the subducting Pacific plate from Williams et al. (2013). Figure from Nicol et al. (2018).

## Implications of Earthquake for Seismic Hazard

The Kaikōura earthquake has implications for the identification and characterisation of seismic sources for seismic hazard analysis. Prior to the earthquake knowledge of the locations, geometries and paleoearthquake histories of the faults that ruptured was variable. North of the Hope Fault within the MFS, most of the main faults (e.g., >1 m slip) that ruptured during the earthquake had already been identified as active prior to the earthquake and incorporated into the National Seismic Hazard Model (NSHM) (Stirling et al., 2012, 2017). By contrast, in the NCD, most of the faults were either not known to be active (Leader Fault) or had poorly defined lengths compared to the 2016 ruptures. Therefore, independent of whether these faults generally rupture together or separately, their previously-assigned active fault lengths would produce minimum estimates of the earthquake magnitude. In addition, the Kaikōura earthquake supports the notion that many active faults in New Zealand

likely remain undetected and have the potential to produce future large magnitude earthquakes (Nicol et al., 2016).

The present New Zealand seismic hazard model contains over 530 individual faults and generally treats these as discrete sources (Stirling et al., 2012). Since the completion of the NSHM fault source model in 2010 the Darfield and Kaikōura earthquakes, and numerical models suggest that rare multi-fault ruptures are possible and should be included in the model (Field et al., 2013; Litchfield et al., 2018). While the 2010 NSHM includes the possibility of multi-fault rupture in the area of greatest seismic energy release during the earthquake, the full complexity of the Kaikōura earthquake could not be recognised as a viable event. The absence of complex ruptures similar to the Kaikōura earthquake in the NSHM is in part because some of the faults that ruptured were not known to be active. Estimates of recurrence intervals for faults in the study area suggest a minimum value for the recurrence interval of Kaikōura events of at least ~6000 years (i.e. this is the longest recurrence interval of the faults that ruptured; Litchfield et al., 2018). While Kaikōura events appear to occur infrequently, it remains possible that multi-fault ruptures in general are much more common than presently represented in the NSHM, a view supported by the 1987 Edegcumbe, 2010 Darfield and 2016 Kaikōura earthquakes, which all produced displacement on at least five faults (Beanland et al., 1989; Beavan et al., 2012; Litchfield et al., 2018). Future versions of the NSHM could explicitly include more multi-fault ruptures by identifying a greater number of faults that may rupture together and/or by raising the maximum magnitude of background seismicity from Mw 7.2 to at least Mw 7.8 (Nicol et al., 2016).

## Stop 1: Waiau

The township of Waiau sits in the immediate hangingwall of The Humps Fault and is approximately 5 km east of the Kaikōura Earthquake epicentre. The fault rupture of the ground surface directly impacted about a dozen residential (or residential-type) structures (Van Dissen et al., 2018), while damaging levels of ground shaking occurred throughout much of North Canterbury, eastern Marlborough and beyond (Kaiser et al., 2017). The earthquake triggered thousands of landslides (Massey et al., 2018), and locally significant liquefaction (Bastin et al., 2018). Despite its proximity to the epicentre and possible peak ground accelerations of 3g being recorded near Waiau, few buildings in the town were significantly damaged (Van Dissen et al., 2018).

Several buildings in the township of Waiau damaged during the earthquake remain unrepaired, including the Waiau Lodge Hotel (Figure 4). At the time of the earthquake the hotel was under relatively new ownership and not fully insured. The damage to hotel building is repairable and the owners are presently seeking finance to restore and relocate the business to its pre-earthquake premises.



Figure 4. Photograph of the Waiau Lodge Hotel in Waiau showing earthquake-related damage to the building. The building, which was constructed using reinforced brick and concrete, sustained extensive cracking and was evacuated immediately following the earthquake, being deemed unsafe for occupation. Photograph taken 6 February 2017 by Ulrich Lange (Bochum, Germany); shared via Wiki Commons.

## Stop 2: The Humps Fault fence offset

The Kaikōura earthquake originated on The Humps Fault, which is the southwestern-most surface rupture of the Kaikōura earthquake. It strikes east to northeast and extends for ~36 km from a tip on the western margin of the Emu Plains to its junction with the Leader Fault at the base of the Mount Stewart Range in the east (Figure 2). In general, the western section of The Humps fault (Figure 2) dips steeply to the south, with dips of 71° S and 80° S measured from the surface trace (see Figure 2 inset stereonet for The Humps Fault). These observations are comparable with the dip angle of 80° S estimated from the line of best fit on the fault-normal profile of aftershocks and to the dip of  $80 \pm 5^\circ$  estimated by assuming a constant dip between the surface trace and the location of the main shock at  $14 \pm 2$  km (Figure 3 section A-A'). Prior to the Kaikōura earthquake, insufficient information was available to define the active fault length or its sense of slip. Barrell and Townsend (2012) mapped The Humps fault as “definitely active” (~2 km) and “likely active” (~13 km) east of the Waiiau township (Figure 2). The Emu plains, which are part of the Culverden Basin, vary in altitude above the modern rivers and are inferred to be mainly 71 kyr or younger in age (i.e. Q2 and Q4 of Rattenbury et al., 2006). Pre-earthquake scarp heights of up to ~7m have been recorded on these surfaces and indicate one or more surface-rupturing earthquakes on The Humps Fault younger than ~18 thousand years in age.

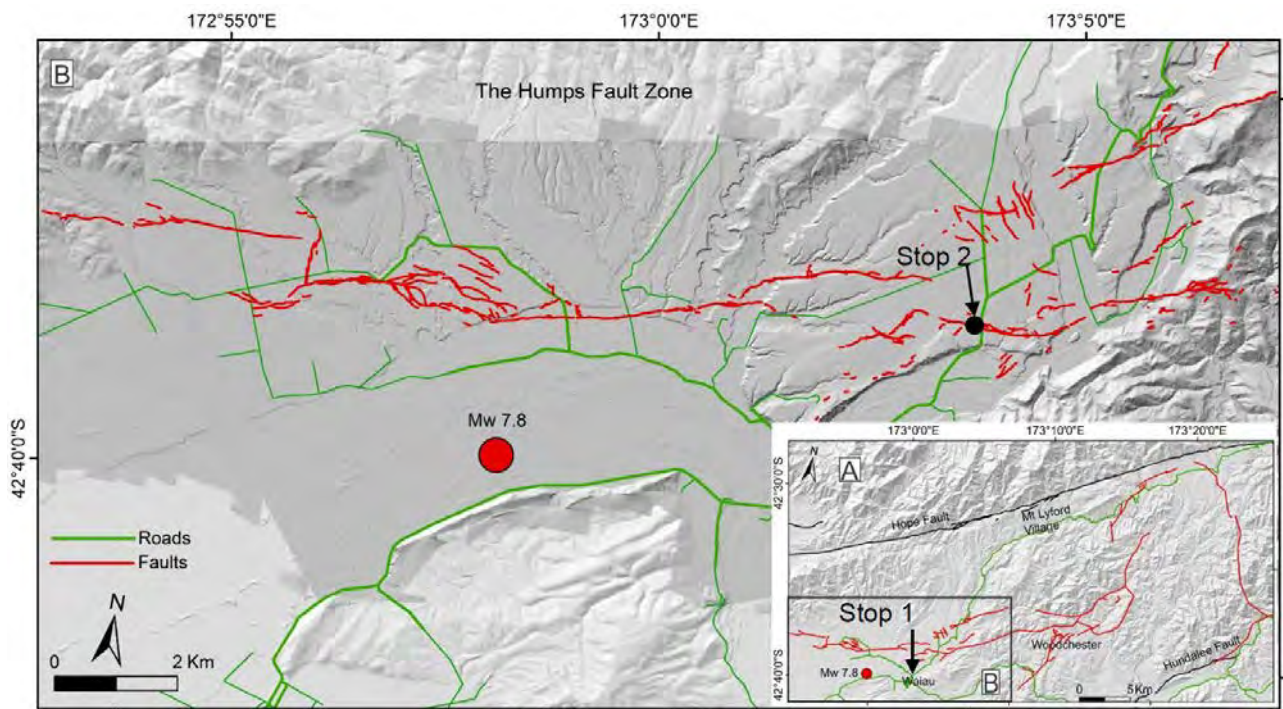


Figure 5. Overview of the Kaikōura earthquake southern fault ruptures (A) and the Humps Fault Zone (B). The epicentre of the Kaikōura earthquake is shown by the red circle; the rupture initiated as a 80° S dipping dextral reverse fault at 14.2 km depth and mainly propagated to the east.

Surface ruptures of the ground surface (e.g. red lines on Figure 5) were primarily mapped using cracks, fissures and displacements of cultural features (e.g., roads, farm tracks, fences and tree lines). The Humps Fault on the Emu Plains is primarily right-lateral. The displaced fence on the Dalmer property provides a good example of the displacements observed along many of the 2016 surface ruptures (see Stop 2 on Figure 5 for location; see Figure 6 for photo of displaced fence). At this locality the fence displays about a metre of right lateral displacement and approximately half a metre of down throw to the north. Along The Humps Fault right-lateral strike displacement, vertical displacement and net displacement reach values of up to  $4 \pm 0.3$  m,  $3.5 \pm 0.5$  m and  $3.9 \pm 0.3$  m, respectively. Displacement measurements across the alluvial plains display significant variation in both horizontal and vertical displacement. Many of the strike-slip displacement lows are located at steps or branch-points along the fault trace indicating that some of the fluctuations in displacement may reflect fault segmentation. One possible explanation for the coincidence

of displacement lows and segment boundaries is that these are sites of elevated off-fault deformation, which is not well sampled by our displacement measurements.



Figure 6. Photograph (looking north) of displaced fence on The Humps Fault, Dalmer Property, near Waiiau (Photograph Kate Pedley).

### Stop 3: Leader Fault and Waiau Wall

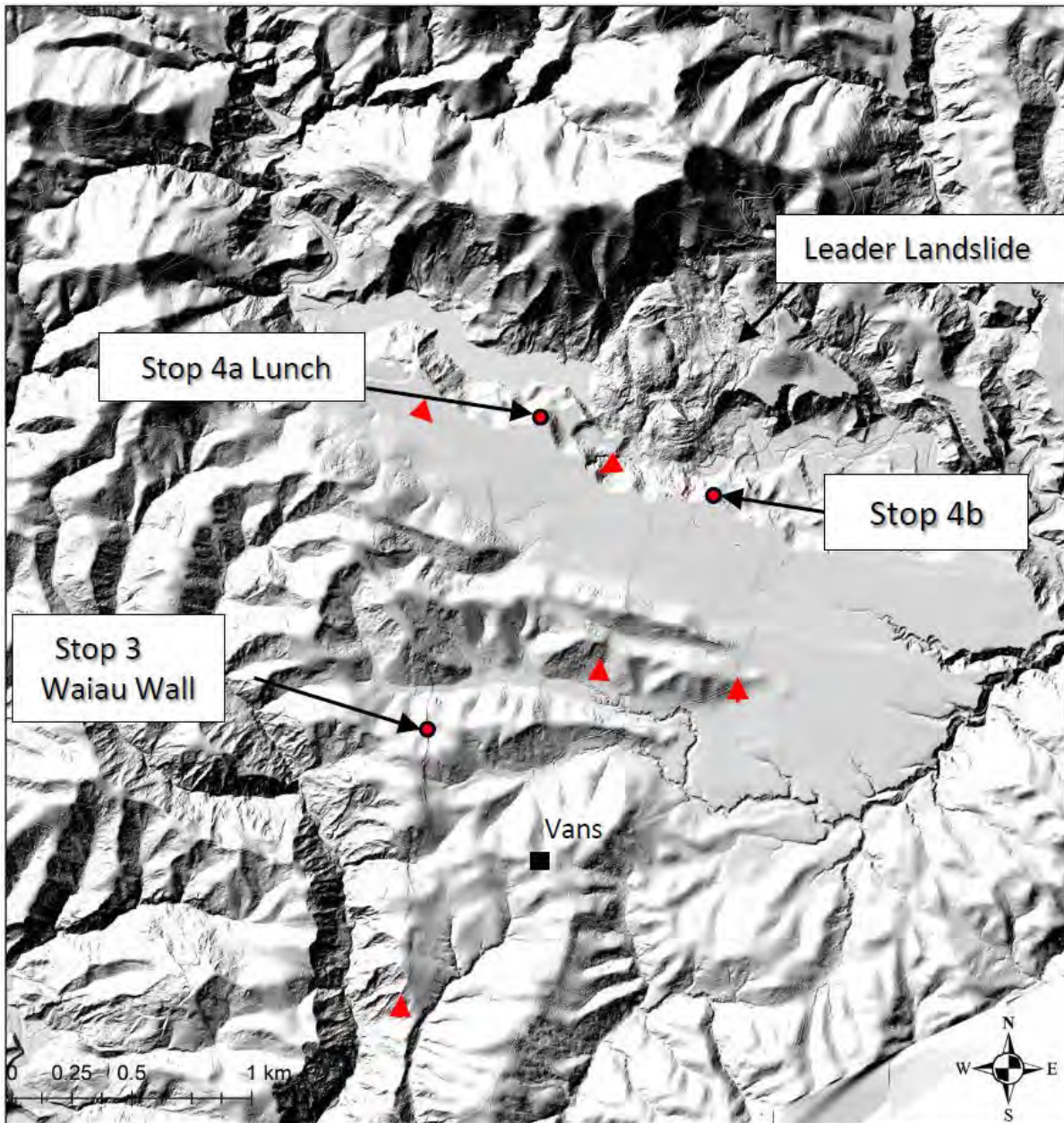


Figure 7. Hill shaded LiDAR map showing the topography of Woodchester Station and Stops 3 & 4. Red triangles indicate the locations of surface ruptures produced in the 2016 Kaikōura earthquake.

The Waiau wall fault surface rupture is located on the Leader Fault which has an overall strike of NNE and exhibits primarily left-lateral reverse displacement with throw up to the west (Figure 2). The fault extends for ~28 km along strike from a tip in the south to its intersection with the Conway-Charwell fault in the north (Figure 2). A complex array of mapped traces ruptured during the earthquake, forming a zone of up to ~3.5 km wide, with strike varying through 180°, and dips from 80° E to 25° W (Figure 2 Leader Fault inset stereonet). Along the Leader Fault no active fault scarps were identified prior to the earthquake. Paleoseismic studies after the earthquake reveal that it probably ruptured at least once in the last 1000 years, although the precise timing of this event remains poorly constrained.

During the Kaikōura earthquake the Leader Fault primarily accommodated left-lateral reverse displacement, with vertical and horizontal components ranging up to 3.5 m and 3 m (including uncertainties), respectively (Figure 8). Given that landsliding is common along the Leader Fault (Dellow et al., 2017; Massey et al., 2018), it is possible that vertical displacement was locally increased by slope failure. The Waiau wall site (Figure 3C) is one locality where the vertical displacement on the fault is significantly above background values. Based on the elevated displacements at the Waiau Wall site (Figure 7), it is possible that some vertical displacement here reflects gravitational rather than tectonic processes.

When the Waiau wall was freshly exposed it was possible to observe many striations on the fault surface (Figure 8C), which are interpreted to record the slip direction of the fault during the earthquake. Interestingly, the orientations of these slickenside striations were more dip slip on the lower two metres of the of the fault surface at the Waiau Wall. Curvature of the striations down the fault plane suggests that fault slip was initially mostly strike slip and then a mix of dip slip and strike slip. The reason for the change in slip direction at the Waiau wall locality is presently unclear, although further north on the Kekerengu Fault a similar phenomenon has been observed where it is attributed to earthquake rupture direction (Kearse et al., 2019).



Figure 8. The Waiau wall on Woodchester Station from different perspectives. (A) 26/11/16. Days after the earthquake, with most of the fault having formed nearly vertical faces. (B) 6/12/2016. ~1 month after the earthquake. Some anthropogenic modification of the fault scarp begins. Not much has changed. (C) 8/9/2017. Significant ponding along fault scarp; nearly all vertical faces have been degraded; some have soil forming overcolluvial wedges. (D) 6/12/2016. Sinistral-oblique slickensides exposed on the scarp; all have now been degraded and cannot be observed. All photographs by Kate Pedley.

## Stop 4: Leader landslide and Woodchester Station

The primary purpose of this stop is to examine and discuss the Leader landslide. The Leader landslide was triggered by shaking during the Kaikōura Earthquake. It is located on the eastern end of The Humps Fault. The Leader Landslide is one of at least 10,000 landslides of varying size that were triggered by the earthquake (Dellow et al., 2017; Massey et al., 2018). Of these landslides about 50 collapsed into river valleys and produced large dams which impeded the drainage and formed lakes (Figure 9; Figure 10). The Leader landslide material mainly comprises low permeability Late Miocene Greta Siltstone Formation, which dammed the Leader River forming Lake Rebekah. Unlike many other landslide dams the water in Lake Rebekah has not yet fully breached the dam, although without continued human intervention the lake will almost certainly drain in the coming years to decades.

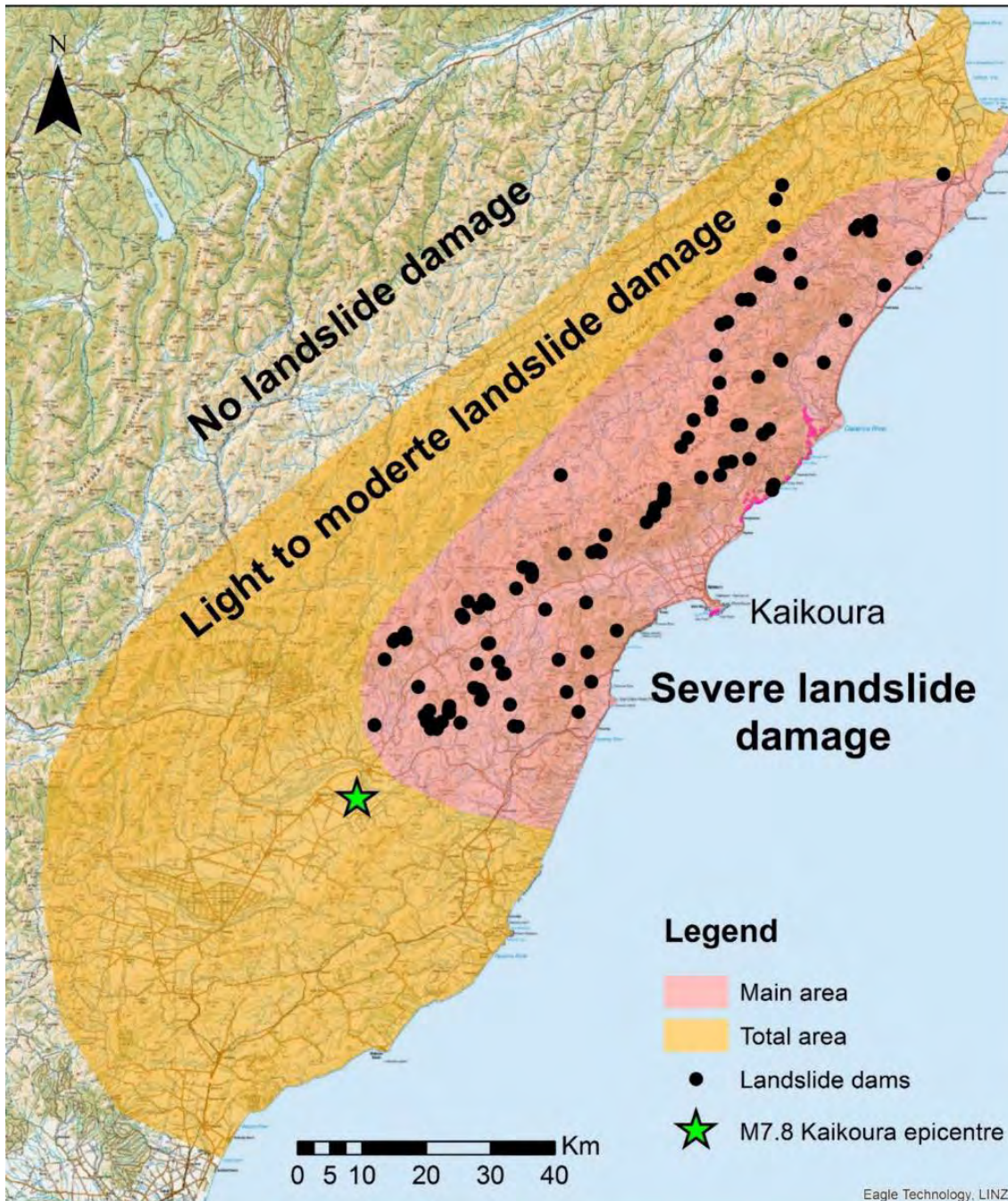


Figure 9. Map showing the regions of no landslides, light to moderate landslides and severe landsliding associated with the Kaikōura earthquake. The black dots show the locations of landslide-dammed drainages produced during the earthquake. The Leader landslide is located about 18 km northeast of the earthquake epicentre. Diagram from Dellow et al. (2017).



Figure 10. Photograph showing aerial view of the Leader landslide and the eastern end of Lake Rebekah. Photograph by Kate Pedley looking north along The Humps Fault.

## Landowner response and recovery

Rebekah Kelly's family, the Gardiners, have operated Woodchester Station for several generations. Rebekah and her husband, David Kelly, took over ownership of the farm in 2014 and had significantly upgraded the farm with new fences and infrastructure. As a result of the earthquake, they have had to reconstruct the fences and significantly upgrade the 6 km long entrance road into the homestead. This was in response to the obvious ground deformation but also to facilitate transport of a temporary farm building into the station for accommodation during repairs. The fault ruptured directly beneath their shearers' quarters and shearing shed; this forced the Kelly's to drive their sheep two days off their property to the neighbouring station for summer shearing. Water pipes for stock were heavily damaged or completely broken in fault shear zones. The Kelly's recognised the need to diversify their farm activities having come out of a three-year drought, and so introduced beekeeping to supplement 'beef and sheep' operations. They also grow winter crops along the Leader River south terraces (most of which had significant fault rupture that had to be smoothed for winter planting) and are keen to develop tourism opportunities on the property. This includes 'glamping'-style accommodation in a Mongolian yurt and geology tours to the Wall and landslide dam. Family and friends are making use of the newly-formed Lake Rebekah for camping, boating and swimming.

## References

- Barnes, P.M., and J.C. Audru (1999). Quaternary faulting in the offshore Flaxbourne and Wairarapa Basins, southern Cook Strait, New Zealand. *New Zealand Journal of Geology and Geophysics* 42: 349–367.
- Barrell, D.J.A., and D.B. Townsend (2012). General distribution and characteristics of active faults and folds in the Hurunui District, North Canterbury. GNS Science Consultancy Report 2012/113, 45p.
- Bastin SH, Ogden M, Wotherspoon LM, van Ballegooy S, Green RA and Stringer M (2018). “Geomorphological influences on the distribution of liquefaction in the Wairau Plains, New Zealand, following the 2016 Kaikōura earthquake”. *Bulletin of the Seismological Society of America*, 108(3B): 1683–1694. doi: 10.1785/0120170248.
- Beanland, S., K. R. Berryman, and G. H. Blick (1989). Geological investigations of the 1987 Edgecumbe earthquake, New Zealand. *New Zealand Journal of Geology and Geophysics* 32: 73–91.
- Beavan, J., and J. Haines (2001). Contemporary horizontal velocity and strain-rate fields of the Pacific-Australian plate boundary zone through New Zealand. *J. Geophys. Res.* 106: 741–770.
- Beavan R.J., P. Tregoning, M. Bevis, T. Kato, and C. Meertens (2002). Motion and rigidity of the Pacific Plate and implications for plate boundary deformation. *J. Geophys. Res.* 107(B10). doi:10.1029/2001JB000282.
- Beavan, J., M. Motagh, E. J. Fielding, N. Donnelly, N., and D. Collett (2012). Fault slip models of the 2010–2011 Canterbury, New Zealand, earthquakes from geodetic data and observations of postseismic ground deformation. *New Zealand Journal of Geology and Geophysics* 55: 207–221.
- Cesca, S., Y. Zhang, V. Mouslopoulou, R. Wang, J. Saul, M. Savage, S. Heimann, S.-K. Kufner, O. Oncken, and T. Dahm (2017). Complex rupture process of the Mw 7.8, 201k, Kaikoura earthquake, New Zealand and its aftershock sequence. *Earth Planet. Sci. Lett.* 478: 110–120.
- Clark, K., E. Nissen, J. Howarth, I. Hamling, J. Mountjoy, W. Ries, K. Jones, S. Goldstein, U. Cochran, P. Villamor, S. Hreinsdóttir, N. Litchfield, K. Berryman, and D. Strong (2017). Highly variable coastal deformation in the 2016 Mw7.8 Kaikōura earthquake reflects rupture complexity along a transpressional plate boundary. *Earth Planet. Sci. Lett.* 474: 334–344. <https://doi.org/10.1016/j.epsl.2017.06.048>.
- Downes, G.L., and D.J. Dowrick (2015). Atlas of isoseismal maps of New Zealand earthquakes, 1843–2003, 2<sup>nd</sup> Edition. Institute of Geological & Nuclear Sciences monograph 25 (issued as a CD). Lower Hutt: Institute of Geological & Nuclear Sciences.
- Eberhart-Phillips D, and S. Bannister (2010). 3-D imaging of Marlborough, New Zealand, subducted plate and strike-slip fault systems, *Geophys. J. Int.* 182: 73–96. doi:10.1111/j.1365-246X.2010.04621.x.
- Eberhart-Phillips, D., M. Reyners, S. Bannister, M. Chadwick and S. Ellis (2010). Establishing a versatile 3-D seismic velocity for New Zealand. *Seismological Research Letters*, doi:10.1785/gssrl.81.6.992.
- Eberhart-Phillips, D., and M. Reyners (2012). Imaging the Hikurangi Plate interface region, with improved local- earthquake tomography, *Geophys. J. Int.* 190 (2): 1221–1242.
- Forsyth, P.J., D.J.A Barrell, and R. Jongens (2008). *Geology of the Christchurch Area: Institute of Geological and Nuclear Sciences Geological Map 16: Lower Hutt, New Zealand*, GNS Science, 1 sheet + 67 p., scale 1:250,000.
- Hamling, I., S. Hreinsdóttir, K. Clark, J. Elliott, C. Liang, E.J. Fielding, N. Litchfield, P. Villamor, L. Wallace, T.J. Wright, E. D’Anastasio, S. Bannister, D. Burbridge, P. Denys, P. Gentle, J. Howarth, C. Mueller, N. Palmer, C. Pearson, W. Power, P. Barnes, D. Barrell, R. Van Dissen, R. Langridge, T. Little, A. Nicol, J. Pettinga, J. Rowland and M. Stirling (2017). Complex multi-fault rupture during the 2016 Mw 7.8 Kaikōura earthquake, New Zealand. *Science* 356 (6334): eeam7194. doi: 10.1126/science.aam7194
- J. Ristau, S. Bannister, A. Christophersen, K. Clark, W. Power, D. Rhoades, C. Massey, I. Hamling, L. Wallace, J. Mountjoy, Y. Kaneko, R. Benites, C. Van Houtte, S. Dellow, L. Wotherspoon, K. Elwood, and K. Gledhill (2017). The 2016 Kaikōura (New Zealand) Earthquake: Preliminary seismological report, *Seismol. Res. Lett.* 88 (3), 727–739.
- Kearse, J., Kaneko, Y., Little, T., Van Dissen, R. J. (2019). Curved slickenlines preserve the direction of rupture propagation. *Geology*, 47 (9), 838–842. <https://doi.org/10.1130/G46563.1>
- Langridge, R.M., Ries, W.F., Litchfield, N.J., Villamor, P., Van Dissen, R.J., Barrell, D.J.A., Rattenbury, M.S., Heron, D.W., Haubrock, S., Townsend, D.B., Lee, J.M., Berryman, K.R., Nicol, A., Cox, S.C., Stirling, M. (2016). The New Zealand Active Faults Database. *New Zealand Journal of Geology and*

- Geophysics 59: 86–96. doi: 10.1080/00288306.2015.1112818.
- Litchfield N.J., P. Villamor, R. Van Dissen, A. Nicol, P. Barnes, D. Barrell, J. Pettinga, R. Langridge, T. Little, J. Mountjoy, W.F. Ries, J. Rowland, C. Fenton, M.W. Stirling, J. Kearse, U.A. Cochran, K.J. Clark, M. Hemphill-Haley, N. Khajavi, K. Jones, G. Archibald, P. Upton, C. Asher, A. Benson, S.C. Cox, C. Gasston, D. Hale, B. Hall, A.E. Hatem, D.W. Heron, J. Howarth, T.J. Kane, G. Lamarche, S. Lawson, B. Lukovic, S.T. McColl, C. Madugo, J. Manousakis, D. Noble, K. Pedley, K. Sauer, T. Stahl, D.T. Strong, D.B. Townsend, V. Toy, J. Williams, S. Woelz, and R. Zinke (2018). Surface Fault Rupture from the Mw 7.8 2016 Kaikōura Earthquake, New Zealand, and Insights into Factors Controlling Multi-Fault Ruptures. *Bull. Seismol. Soc. Am.* 108(3B): 1496–1520. doi: 10.1785/0120170300.
- Massey C., Townsend D., Rathje E., Allstadt K., Kaneko Y., Lukovic B., Bradley B., Wartman J., Horspool N., Hamling I., Carey J., Cox S., Davidson J., Dellow S., Holden C., Jibson R., Jones K., Kaiser A., Little C., Lyndsell B., McColl S., Morgenstern R., Petley D.N., Rengers F., Rhoades D., Rosser B., Strong D., Singeisen C., Villeneuve M. (2018). Landslides triggered by the Mw 7.8 14 November 2016 Kaikōura earthquake, New Zealand. *Bulletin of the Seismological Society of America* 108(3B): 1630–1648. doi: 10.1785/0120170305.
- Mouslopoulou, V., Saltogianni, V., Nicol, A., Oncken, O., Begg, J., Babeyko, A., Cesca, S., Moreno, M. (2019). Breaking a subduction-termination from top to bottom: the large 2016 Kaikōura Earthquake, New Zealand. *Earth and Planetary Science Letters* 506: 1–10.
- Nicol, A., B.V. Alloway, and P.J. Tonkin (1994). Rates of deformation, uplift and landscape development associated with active folding in the Waipara area of North Canterbury, New Zealand. *Tectonics* 13: 1321–1344.
- Nicol, A., Van Dissen, R., Stirling, M., Gerstenberger, M. (2016). Completeness of the paleoseismic active fault record in New Zealand. *Seismological Research Letters* 86 (6): 1299–1310. doi:10.1785/0220160088.
- Nicol A, Khajavi N, Pettinga J, Fenton C, Stahl T, Bannister S, Pedley K, Hyland-Brook N, Bushell T, Hamling I, Ristau J, Noble D and McColl ST (2018). Preliminary geometry, displacement, and kinematics of fault ruptures in the epicentral region of the 2016 Mw 7.8 Kaikōura, New Zealand, earthquake. *Bulletin of the Seismological Society of America* 108(3B): 1521–1539. doi: 10.1785/0120170329.
- Pettinga, J. R., M. D. Yetton, R. J. Van Dissen, and G. Downes (2001). Earthquake source identification and characterisation for the Canterbury Region, South Island, New Zealand, *Bull. New Zealand Soc. Earthq. Eng.* 34, 282–317.
- Rattenbury, M. S., D. B. Townsend, and M. R. Johnston 724 (2006). *Geology of the Kaikōura area*. Institute of Geological & Nuclear Sciences 1:250 000 geological map 13. 1 sheet + 70 p. Lower Hutt, New Zealand. GNS Science.
- Stirling, M. W., G. McVerry, M. Gerstenberger, N. Litchfield, R. Van Dissen, K. Berryman, P. Barnes, L. Wallace, B. Bradley, P. Villamor, R. Langridge, G. Lamarche, S. Nodder, M. Reyners, D. Rhoades, W. Smith, A. Nicol, J. Pettinga, K. Clark, and K. Jacobs (2012). National seismic hazard model for New Zealand: 2010 update, *Bull. Seismol. Soc. Am.* 102: 1514–1542.
- Stirling, M.W., N.J. Litchfield, P. Villamor, R.J. Van Dissen, A. Nicol, J. Pettinga, P. Barnes, R.M. Langridge, T. Little, D.J.A. Barrell, J. Mountjoy, W.F. Ries, J. Rowland, C. Fenton, I. Hamling, C. Asher, A. Barrier, A. Benson, A. Bischoff, J. Borella, R. Carne, U.A. Cochran, M. Cockroft, S.C. Cox, G. Duke, F. Fenton, C. Gasston, C. Grimshaw, D. Hale, B. Hall, K.X. Hao, A. Hatem, M. Hemphill-Haley, D.W. Heron, J. Howarth, Z. Juniper, T. Kane, J. Kearse, N. Khajavi, G. Lamarche, S. Lawson, B. Lukovic, C. Madugo, I. Manousakis, S. McColl, D. Noble, K. Pedley, K. Sauer, T. Stahl, D.T. Strong, D.B. Townsend, M. Villeneuve, A. Wandres, J. Williams, S. Woelz, and R. Zinke (2017). The Mw 7.8 Kaikōura earthquake: Surface rupture, and seismic hazard context, *Bull. New Zeal. Soc. Earthquake Eng.* 50: 73–84.
- Van Dissen R., Stahl, T., King, A., Pettinga, J.R., Fenton, C., Little, T.A., Litchfield, N.J., Stirling, M.W., Langridge, R.M., Nicol, A., Kearse, J., Barrell, D.A., Villamor, P. (2018). Impacts of surface fault rupture on residential structures during the 2016 Mw 7.8 Kaikōura Earthquake, New Zealand. *Bulletin of the New Zealand Society for Earthquake Engineering* 52(1): 1–22.
- Waldhauser, F., and W.L. Ellsworth (2000). A Double-Difference Earthquake Location Algorithm: Method and Application to the Northern Hayward Fault, California, *Bull. Seismol. Soc. Am.* 90: 1353–1368.

- Wallace, L.M., P. Barnes, J. Beavan, R. Van Dissen, N. Litchfield, J. Mountjoy, G. Lamarche, and N. Pondard (2012). The kinematics of a transition from subduction to strike-slip: an example from the central New Zealand plate boundary, *J. Geophys. Res.* 117: B02405. doi: 10.1029/2011JB008640.
- Wang, T., S., Wei, X., Shia, Q. Qiu, L. Lia, D. Peng, R.J. Weldon, S. Barbot (2017). The 2016 Kaikōura earthquake: Simultaneous rupture of the subduction interface and overlying faults, *Earth and Planet. Sci. Lett.* 482: 44–51
- Williams, C.A., D. Eberhart-Phillips, S. Bannister, D.H.N. Barker, S. Henrys, M. Reyners, and R. Sutherland (2013). Revised interface geometry for the Hikurangi Subduction Zone, New Zealand, *Seismol. Res. Lett.* 84: 1066–1073.

# FIELD TRIP 4: PETROLEUM EXPLORATION AND PRODUCTION IN NORTH CANTERBURY

Thursday 26 November 2020

Leaders: Mac Beggs and Andy Nicol, University of Canterbury

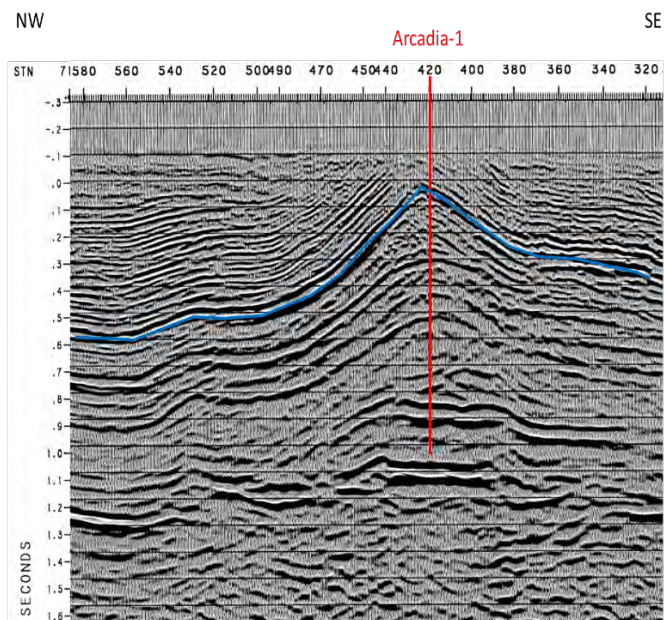
Assistance in absentia from Nick Jackson and Bill Leask, Elemental Petroleum Consultants.



Limestone ridges, Waipara



Kate-1 drilling, 2008



Seismic line IP256-99-107 tie to Arcadia-1

## Trip Summary

Unbeknown to almost everyone, the only active petroleum production in New Zealand outside of Taranaki Basin is located in North Canterbury—a very modest gas development at Hanmer Springs. The occurrence of thermogenic natural gas in conjunction with geothermal water at Hanmer Springs is not well understood. The gas production system at Hanmer Springs will be visited and described, and its geological setting discussed.

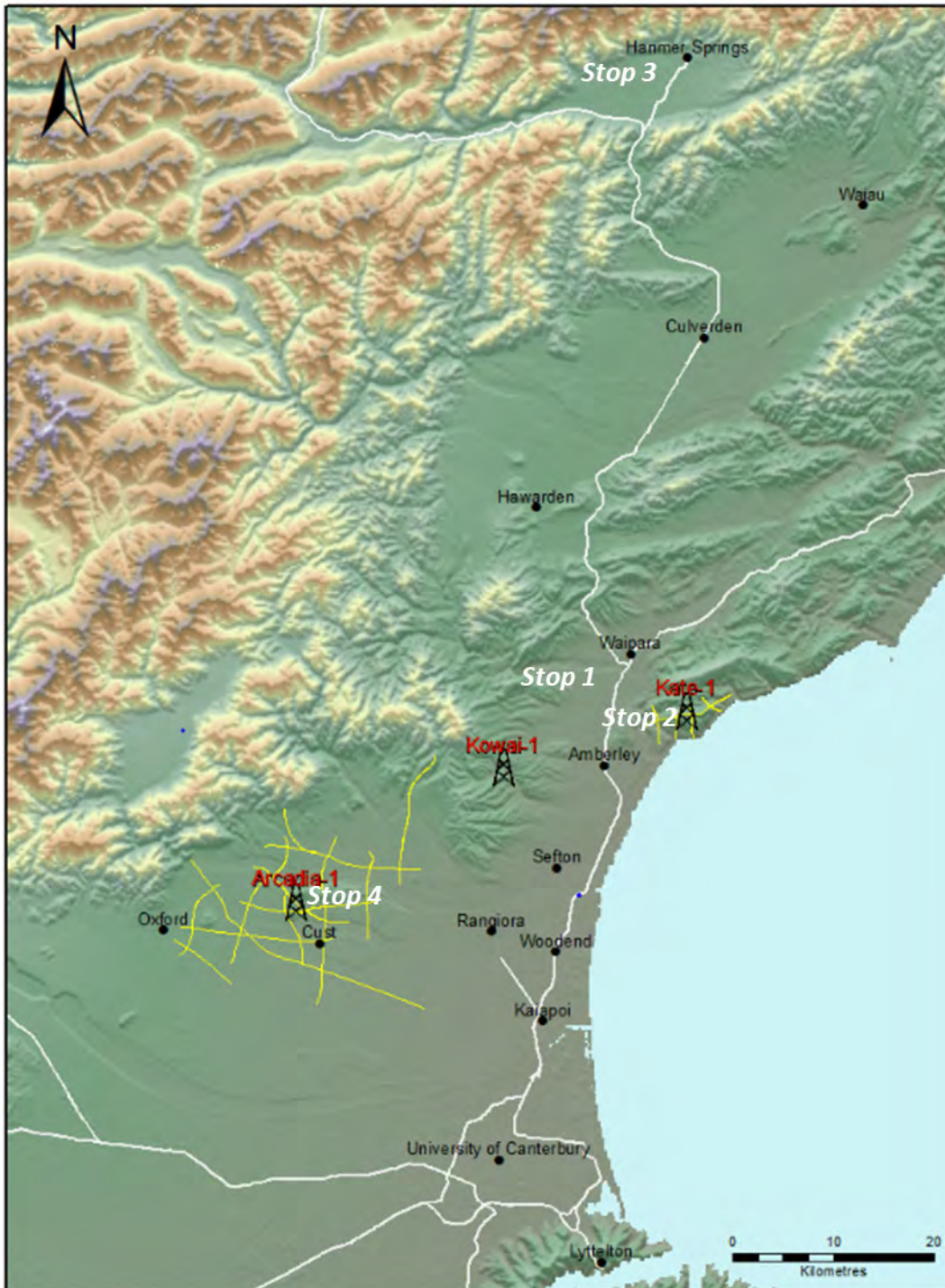


Figure 1. Route map with well and seismic line locations.

On the way to Hanmer Springs, the regional geological setting of North Canterbury will be introduced with stops to showcase the stratigraphy and structure, with an emphasis on the active anticlines in Tertiary strata which have attracted petroleum exploration attention from time to time, culminating in exploration wells Kowai-1 (1978), Arcadia-1 (2000), and Kate-1 (2008). We will visit the Kate-1 well site on the Kate anticline SE of Waipara. On the return from Hanmer Springs we will visit the Cust anticline, west of Rangiora, the site of Arcadia-1.

## North Canterbury stratigraphy and deformation

The field trip traverses the NW part of the Canterbury Basin which extends from an offshore axis east of the Canterbury Bight.

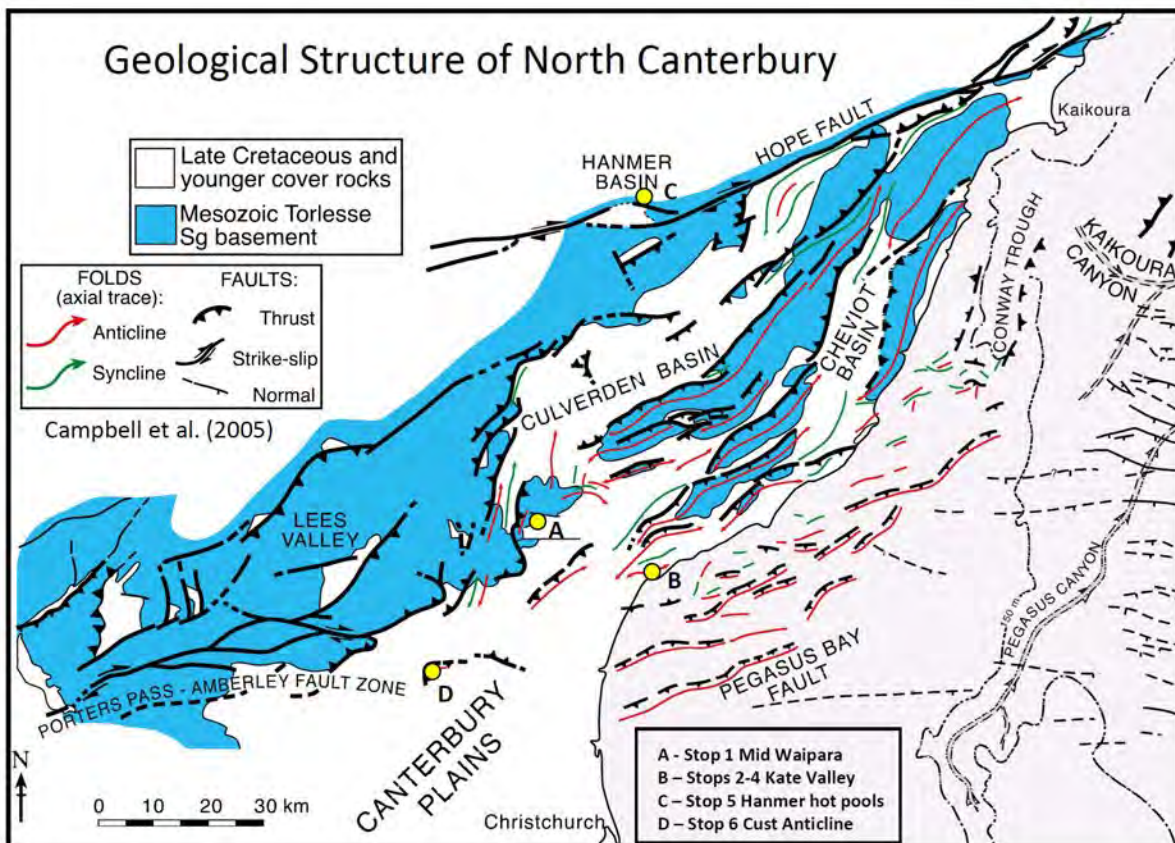


Figure 2. Regional structure map of North Canterbury showing the four main locations to be visited.

Like other basins in Zealandia the Canterbury Basin initiated as an intra-continental rift during the Late Cretaceous (late Albian,  $\sim 105 \pm 5$  Ma) (Field and Browne, 1989; Strogon et al., 2017; Barrier, 2019). Following initial rifting and early post-rift sedimentation, subsequent Paleogene sedimentation became progressively finer-grained and more calcareous with increasing water depths, which culminated in maximum drowning in the early Oligocene (Field and Browne, 1989; King et al., 1999; Landis et al., 2008). After the early Oligocene maximum drowning water depths shallowed with many onshore areas in the Canterbury Basin becoming emergent in the Pliocene-Pleistocene. Offshore south of Banks Peninsula basin strata reach thicknesses in excess of 5 km with 2–3 km of Cretaceous strata deposited in grabens, while onshore and north of the peninsula the entire basin succession generally ranges in thickness from 300–1200 m (Field and Browne, 1989). The thickest parts of the succession primarily occur in half grabens where latest Cretaceous thickening of the Broken River coal measures is observed (Field and Browne, 1989; Nicol, 1993; GeoSphere, 2003). In Figure 3 we show Late Cretaceous half grabens on a regional north-south cross section as depicted in PR3165 (GeoSphere, 2003). This stratigraphic cross section projects a series of outcrop sections onto a south to north line and suggests a boundary between the northern Canterbury Basin platform, with latest Cretaceous extensional depocentres as also observed in Pegasus Bay offshore

(Barnes, 1996), and the southward onlap of the Marlborough/East Coast basin margin onto the Hurunui High.

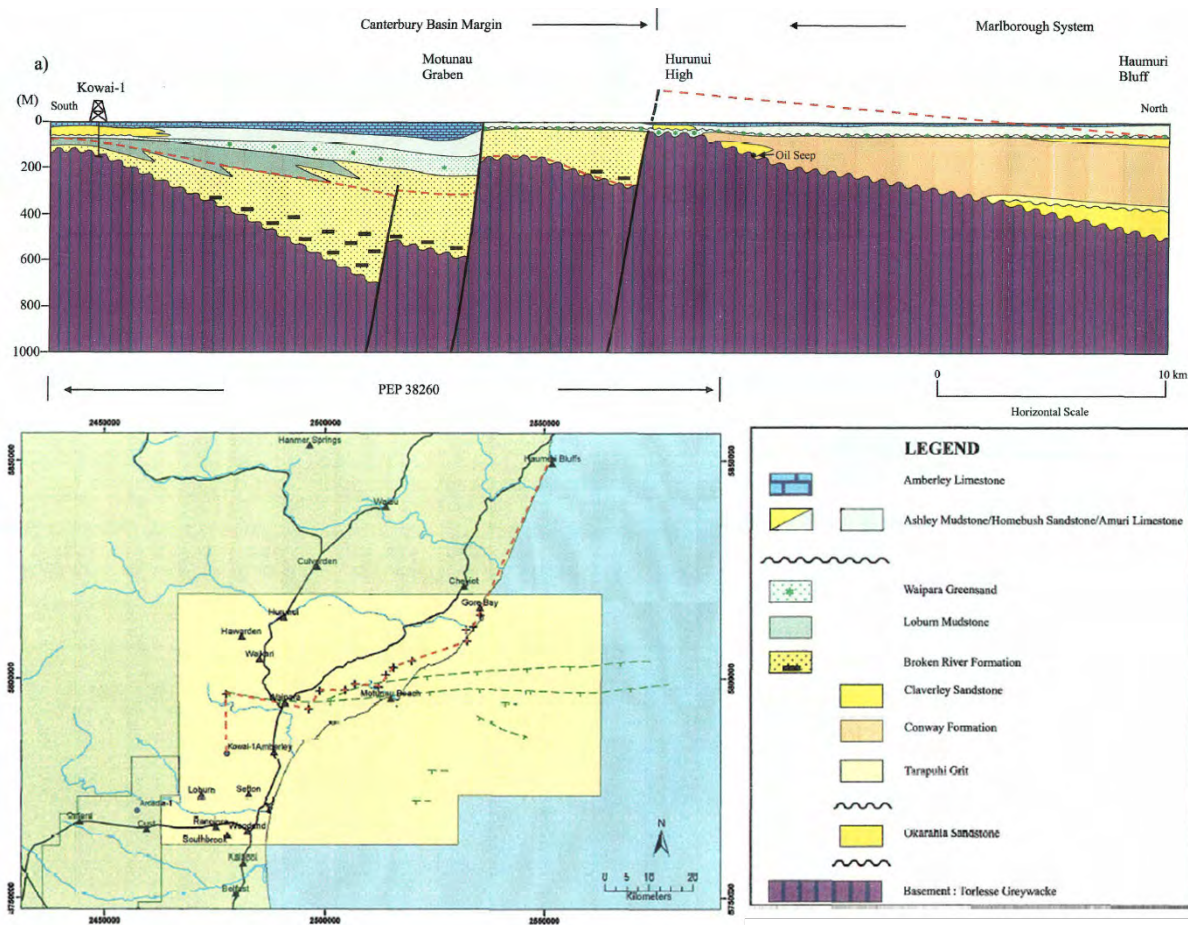


Figure 3. Stratigraphic cross section of late Cretaceous to Oligocene sequence on the northern margin of Canterbury Basin.

The Eocene to Oligocene Amuri Limestone, deposited when the whole region (if not all of Zealandia) was drowned, constitutes an important stratigraphic marker, with considerable lateral variability in both the underlying Eyre Group and overlying Motunau Group giving rise to numerous and often discontinuous local formations.

Generally, the Broken River Formation is latest Cretaceous terrestrial facies with thin (<2 m thick) and minor sub-bituminous rank coal seams, which may thicken or increase in rank in the half grabens. The Broken River coal measures pass upwards into marginal marine Loburn Formation in the Waipara area where the Paleocene is relatively thick the overlying Eocene is shelfal Ashley Mudstone (Browne and Field, 1985; Field and Browne, 1989). Further inland, the equivalent interval includes shelfal sands such as the Homebush. Basaltic volcanics are intercalated with both early and late Cenozoic units locally across North Canterbury.

The Miocene Motunau Group is represented by mainly coarse terrestrial facies in the west, and marine equivalents closer to the coast including various transgressive sandstones passing upward into the Tokama Siltstone and Mount Brown Limestone in the Waipara area (Wilson, 1963; Browne and Field, 1985; Field and Browne, 1989). The Kowai Formation comprises alluvial gravels passing into marginal marine equivalents close to the coast.

The increase in plate convergence rates and possible initiation of the Alpine Fault during the Oligocene and Early Miocene triggered uplift, erosion, and marine regression throughout the majority of the onshore

Zealandia, including the Canterbury Basin (Mortimer et al., 2014; Barrier et al., 2019). In the Canterbury Basin Miocene to Recent strata record an increase in sediment supply from topography created to the west of the basin by uplift in the central South Island that is manifest today as the Southern Alps (Browne and Naish, 2003; Barrier et al., 2019). This increase in sediment supply was initially recorded in the offshore basin where the shelf break prograded towards the deep water mainly from the mid Miocene, while onshore in North Canterbury deposition of the Kowai Gravels was the main manifestation of increased sedimentation and uplift of the Southern Alps.

The present topography and outcrop patterns of Cretaceous and Cenozoic strata mainly reflect Late Pleistocene shortening and transpression. The Kate-1 well is located on the Kate anticline, which is one of many northeast-trending structures that form part of a fold and oblique reverse fault belt (e.g., Nicol et al., 1994; Barnes, 1996; Vanderleest et al., 2017). These faults typically separate hanging-wall anticlines and footwall synclines that are manifest as topographic basins and ranges. Late Cretaceous to Cenozoic strata often occupy the basins, while the ranges are commonly cored by steeply bedded and complexly deformed Torlesse basement (e.g., Warren, 1995; Rattenbury et al., 2006; Forsyth et al., 2008). Many of the faults have active traces which, in combination with ongoing earthquake activity, suggest that the faults and folds are actively growing (e.g., Pettinga et al., 2001; Nicol et al., 1994, 2018).

## Hanmer

Hanmer Basin is a rhomb-shaped topographic depression in North Canterbury, measuring 15 km east-west by 7 km north-south. Active traces of the dextral strike-slip Hope Fault are present on the northern side of the western part of the basin, are absent from the central area, and reappear on the southern side of the eastern part of the basin. This basin formed at a releasing bend between the right-stepping western Hope River segment to the west and the more linear Conway segment to the east (Rattenbury et al 2006). The Hanmer Springs are close to the Hanmer Fault, which is mapped as a series of discontinuous active traces along the northern margin of the basin, associated with a 100–200 m wide zone of ground warping (Wood et al., 1994).

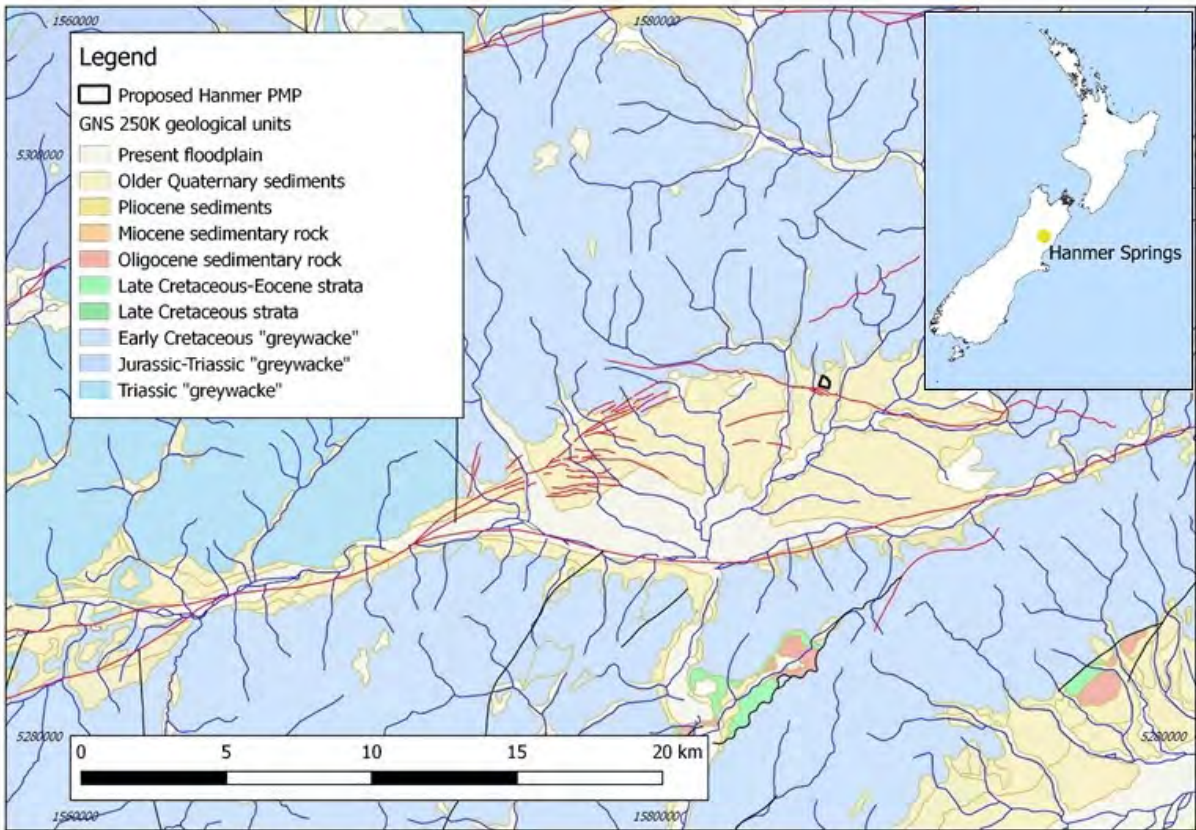


Figure 4. Geology of Hanmer area, from QMAP, adapted for HSTPS by Elemental Petroleum Consultants.

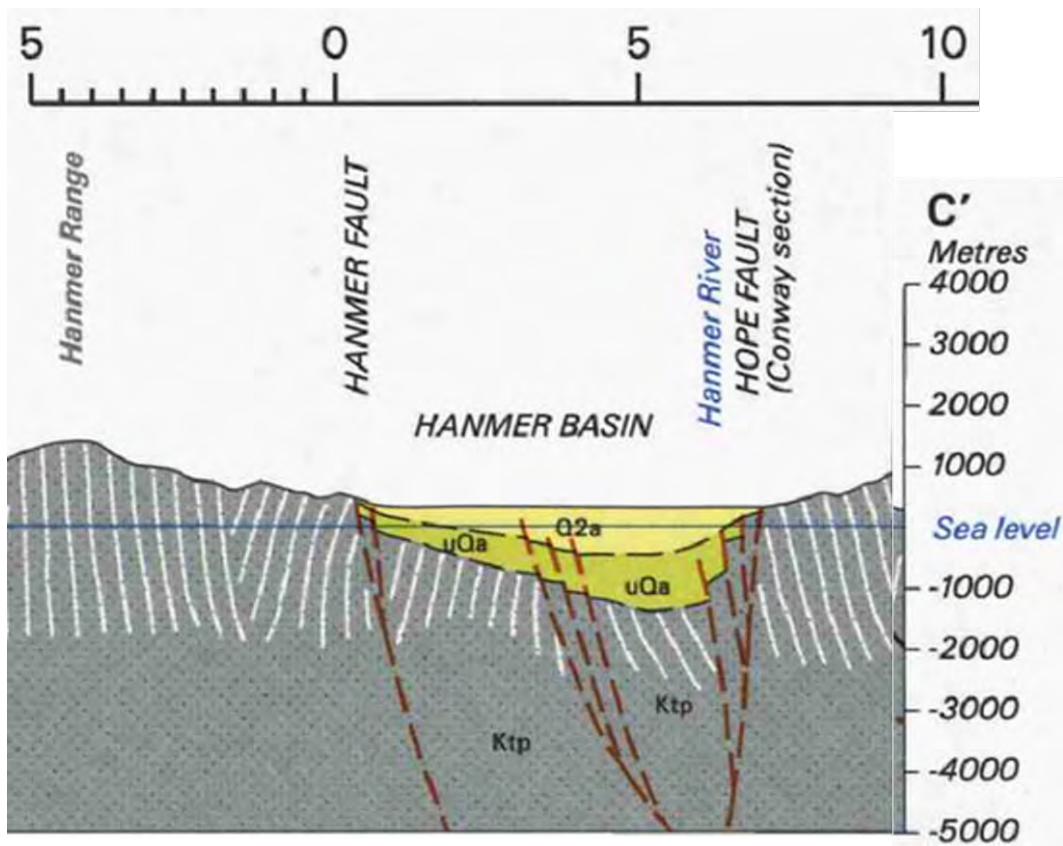


Figure 5. Cross section through Hanmer Springs NW-SE, from QMAP Kaikoura.

The basin is filled with Pleistocene–Holocene sediments up to 1000 m thick. Wells and outcrops indicate these sediments are dominated by alluvial gravels, with subordinate sand, silt and peat. Wood et al (1994) identified four seismic sequences in the sedimentary succession, but all appear to represent alluvial fan systems.

At Hanmer Springs, the top of greywacke basement is at approximately 60 m depth. The sediments above basement are mainly gravel, with several thin sand and silt units (ECAN bore log data). The producing intervals of the water wells either straddle the gravel/bedrock interface, or lie totally within the bedrock (for example, N32/0319 is an uncased open-hole from 224 to 516 m).

The basement rock is Pahau Terrane (Early Cretaceous) age, comprising indurated fine sandstone with subordinate argillite interbeds. Drillers' logs are available for most of the wells (Brown 1973; ECAN bore log data), but as no core was drilled, descriptions are brief, and do not indicate any significant lithology variations.

Several faulted inliers of Paleogene–Late Cretaceous strata occur in the North Canterbury region within 3 km of the south edge of the Hanmer Basin (Figure 1; Rattenbury et al 2006). It is possible that a similarly-aged inlier may be concealed at depth in the basin, either outside the extent of the existing seismic coverage or not recognised within it.

Six seismic reflection lines were acquired in 1989 and 1991 for scientific research (Figure 5), using Mini-Sosie wackers as an energy source (Wood et al., 1994). Wood et al. (1994) carried out a basic seismic interpretation using hardcopies of the profiles (in the era before workstations). The raw shot data are still held by GNS Science, but no stacked data can be found (R.A. Wood, pers. comm. to Elemental, 2016).

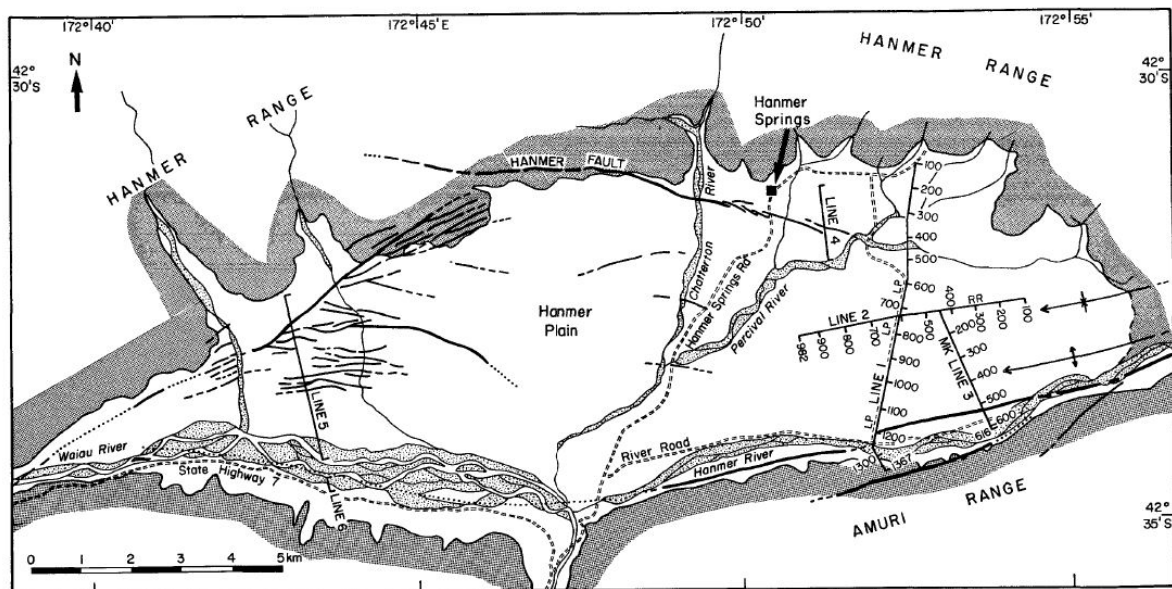


Figure 6. Seismic lines in Hanmer Basin (Wood et al, 1994)

## Petroleum Exploration history of North Canterbury

The earliest industry attention to the petroleum potential of North Canterbury was a programme of regional geological and geophysical mapping commenced by the consortium of BP Shell and Todd in the late 1950's. This work, initiated by Todd Brothers who held a concession over much of Canterbury that was incorporated into the BP-operated joint venture, is synthesised in PR 319 (Haw, 1961). A suite of structural prospects were identified in PR 260 (Hazard, 1971, for Antipodes Oil Co.)

The first exploration well in the district, Kowai-1, was drilled on one of these prospects by the newly formed

state oil company, Petrocorp, in 1978. Katz (1982) demonstrated that this well was not crestal and hence does not entirely condemn the prospect or region, as others had concluded.

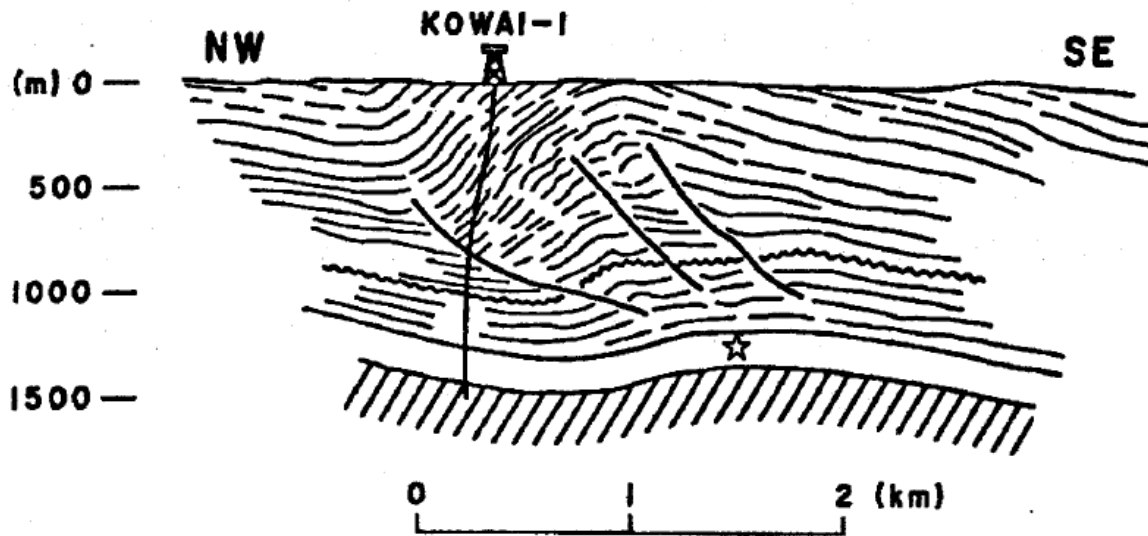


Figure 7. Katz's (1982) interpretation of the relationship between the Kowai-1 dry well and its target structure, the crest of which (at Broken River Formation level) is to the SE as indicated by the star.

Indo Pacific Energy held a large exploration permit (PEP38256) over much of the onshore Canterbury Basin from 1997, shooting 8 seismic lines in the North Canterbury part of the permit in 1998 and 1999. One of two wells they drilled in 2000, Arcadia-1, tested the Cust Anticline, another of the surface anticlines noted (as the Mairaki Downs structure) by Hazzard in PR 260 (1971). See Stop 4 content below.

In 2004, Green Gate Ltd was granted PEP 38260 covering an area between Rangiora/Woodend in the south, and Cheviot in the north, and extending offshore. The stimulus for this venture was a report of light oil seepage in excavations for the regional Kate Valley landfill, which was then being developed on the north flank of a surface anticline mapped by Wilson (1964) A grid of seismic lines was shot over the Kate Anticline, and the Kate-1 well was drilled in 2008. See Stop 2 content below.

PEP 38256 expired in 2007 and PEP 38260 in 2009. The only active petroleum permit in North Canterbury is PMP 60215 at Hanmer Springs, granted for a period of 40 years from November 30, 2016.

In 2018 the Crown Minerals Act was amended to prohibit any new petroleum exploration permits except in the onshore Taranaki region.

## Stop 1: Waipara District overview—mid-Waipara section

The stratigraphic sequence in the middle Waipara-Weka Pass area offers a near complete Cretaceous-Cenozoic section (~80-70 Ma to present) (Figure 7). Much of the stratigraphy from the Torlesse rocks of the Doctors Range in the west to the Mt Brown Formation, which forms prominent limestone dip slopes in the east, can be observed from the panorama view at stop 1. The Broken River Formation resting on Torlesse Mesozoic basement rocks comprises interbedded clean sandstones and sub-bituminous rank coal beds, which are the most promising petroleum source rocks in the succession.

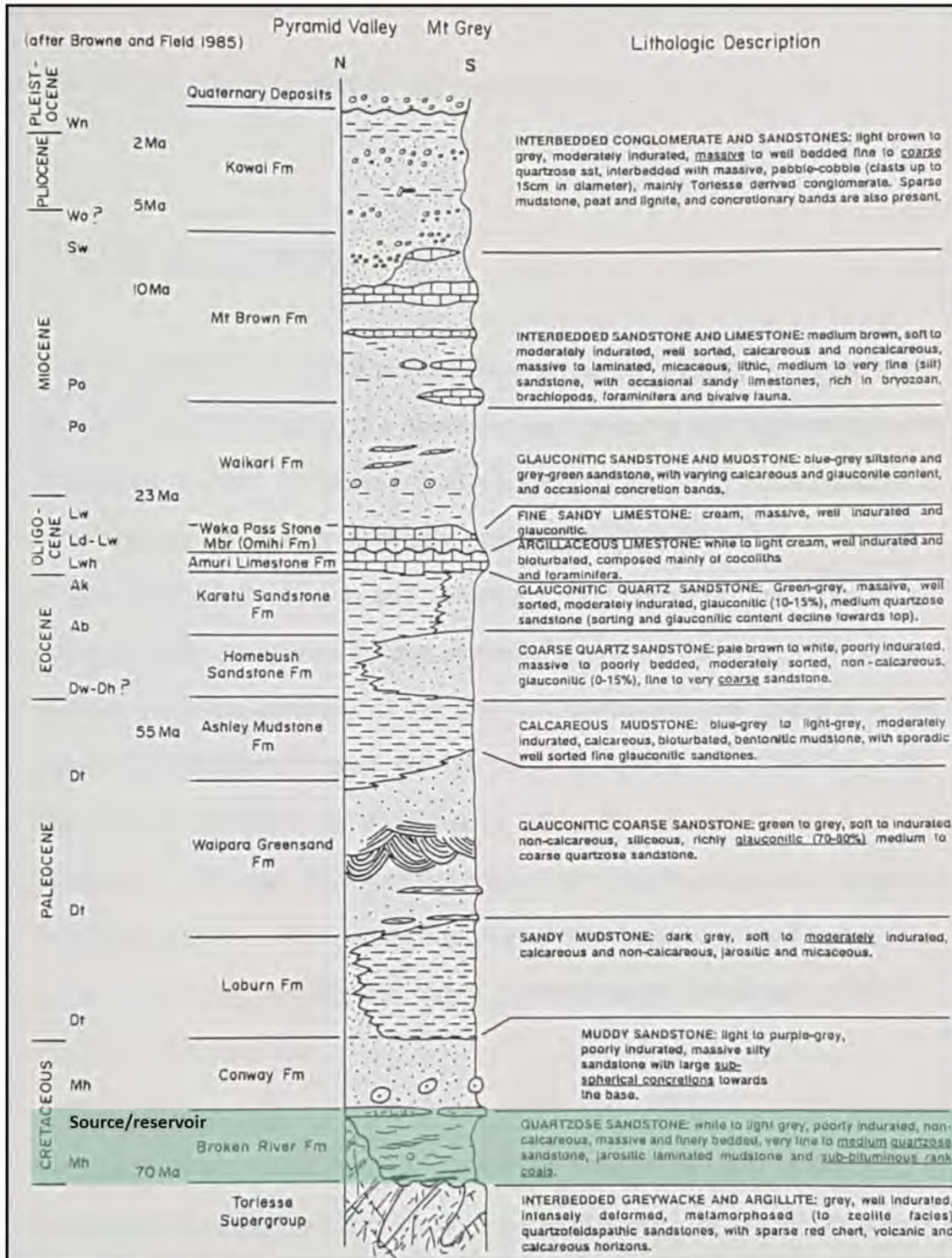


Figure 8. Generalised stratigraphic column for the Waipara area (from Nicol 1991).

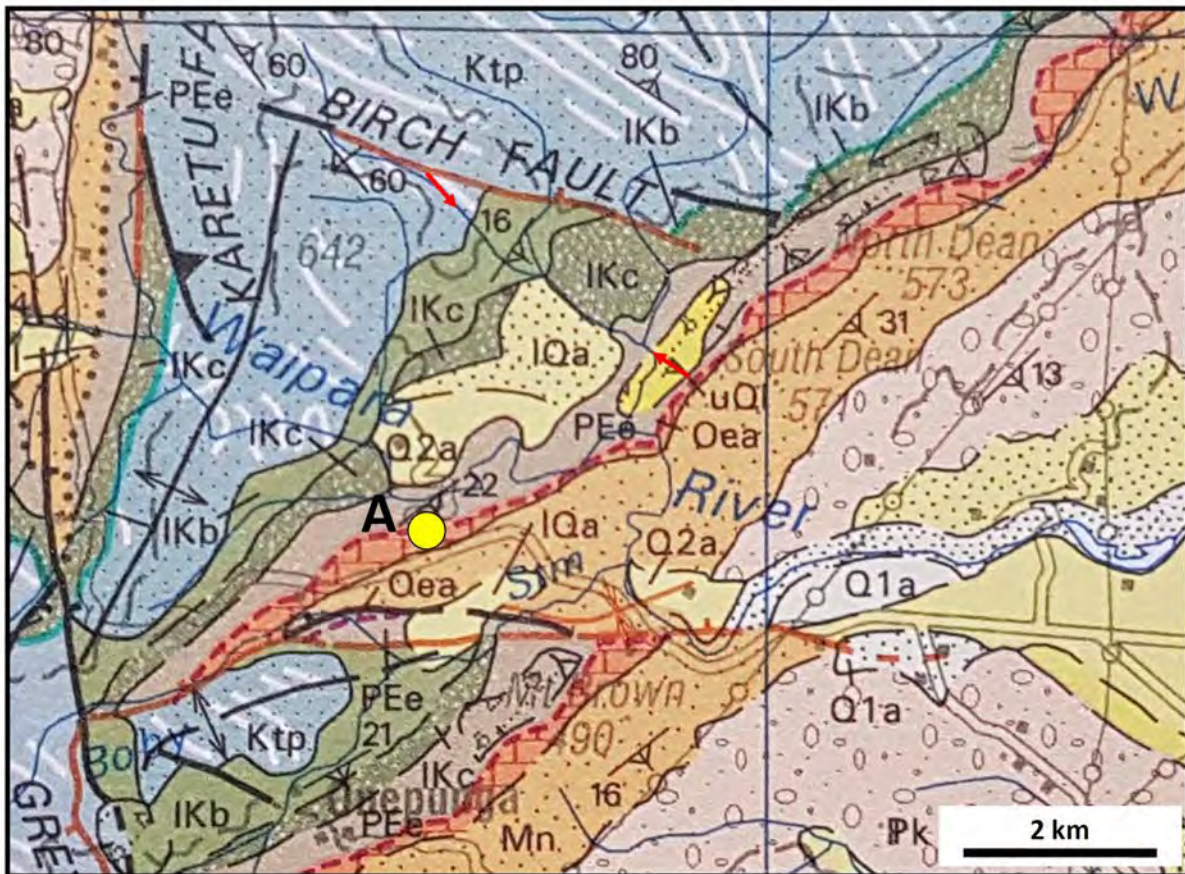


Figure 9. Geological map of the Mid Waipara area from QMAP Christchurch (Forsyth et al., 2008). Stop location indicated by the letter "A" and yellow filled circle. Birch Hollow stream (shown by red arrows) exposures strata in the thickest part of the graben.

The Mid Waipara area is one of the few places in the onshore Canterbury Basin where a Cretaceous half-graben can be observed. The Birch Hollow half graben is bounded to the north by the Birch Fault, which was active in the Late Cretaceous and has accumulated slip in the Quaternary (Nicol, 1993). The strata in the half graben comprise up to 100 m thickness of basal conglomerates, 250 m of quartz sandstone and occasional thin (<1 m thick) coal seams and 250 m of silty sandstones with large spherical concretions (Conway Formation).



Access to this stop is provided by roads servicing the Kate Valley Landfill, a facility developed since 2004, servicing Canterbury district councils from Ashburton to Hurunui (including Christchurch city). Interest in the petroleum prospectivity of the Kate anticline was stimulated by the report of light oil seepages during early excavations for the landfill, and a private company (Green Gate Ltd) was formed to secure an exploration permit (PEP 38260) and undertake investigations culminating in a small local grid of seismic lines, and the drilling of Kate-1 in 2008 (PR3929).

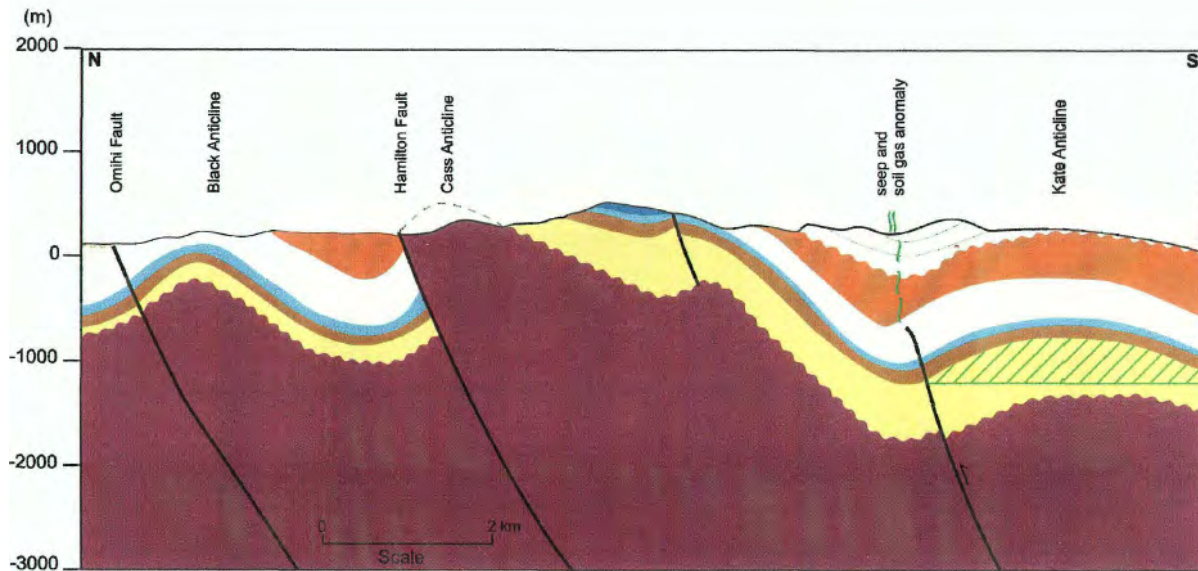


Figure 11. Green Gate’s interpretation of the Kate Anticline prospect prior to acquisition of seismic to confirm the structure. PR 3165.

The landfill is situated in the Teviotdale Syncline to the north of the Kate Anticline, and the Kate-1 well site is just across its southern boundary. There are excellent exposures of the Pliocene Greenwood formation (local synonym of Kowai formation) in the landfill excavations.



Figure 12. Southern flank of Kate Valley landfill exposing Greenwood (Kowai) Formation. November 2020. Kate-1 well location was in the valley below the plantation, mid-right (out of sight behind ridge).

Kate-1 drilled to Torlesse greywacke basement at a depth of 1057m. The Miocene (Tokama Formation) was thicker than expected and hence the Oligocene limestone somewhat deeper, and older formations thinner than expected. Nevertheless, the Broken River objective was well developed comprising 73m of highly porous sandstone, with sharp basal (on greywacke) and upper (beneath Conway Formation) boundaries. The well is not crestal (as intended) but recorded northward dips of about 25o. Although it could be argued that there may still be untested prospectivity in the Kate anticline crest (as for Kowai-1), the absence of any meaningful indications of hydrocarbons in the excellent potential reservoir, as well as of a plausible migration pathway from source kitchens which would be at a considerable lateral distance, dissuaded further exploration of the structure.

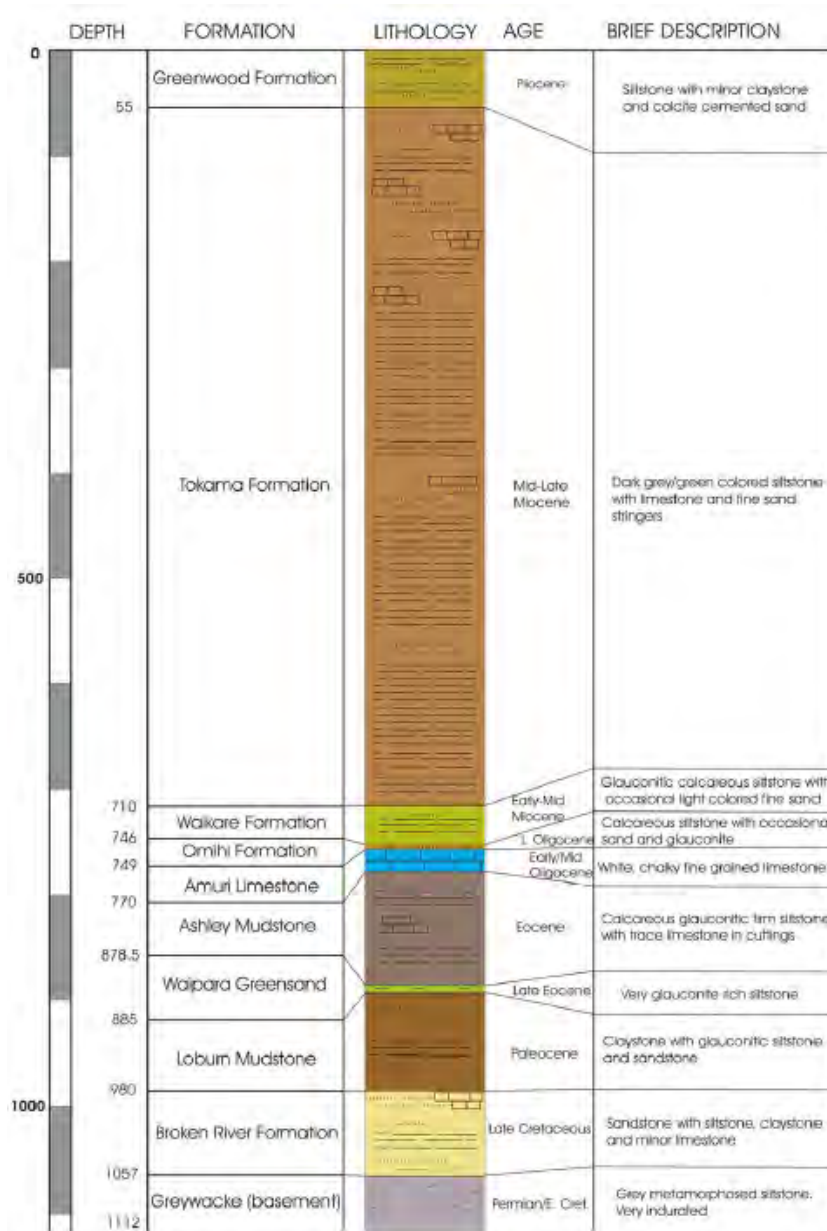


Figure 13. Kate-1 lithological and stratigraphic sequence.

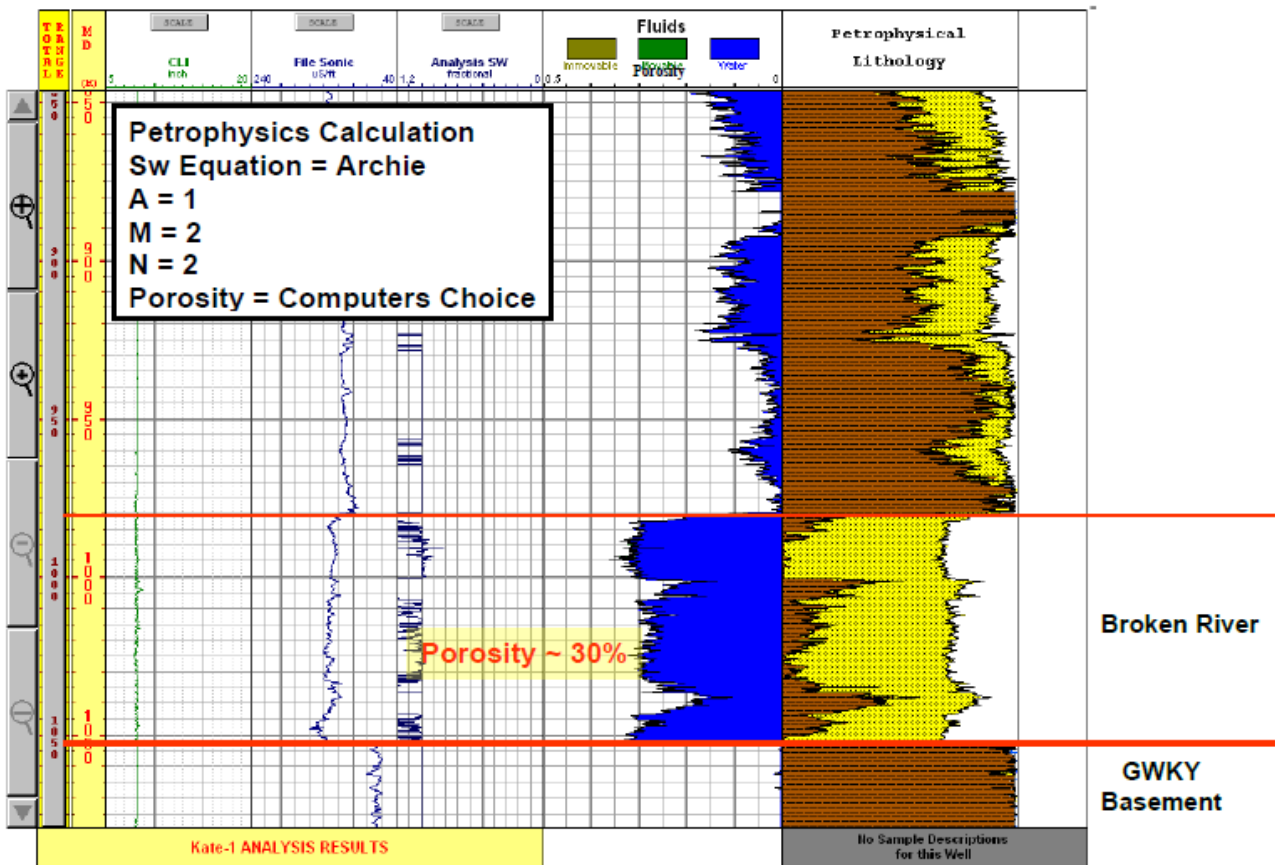


Figure 14. Petrophysics of the Broken River sandstone, Kate-1.

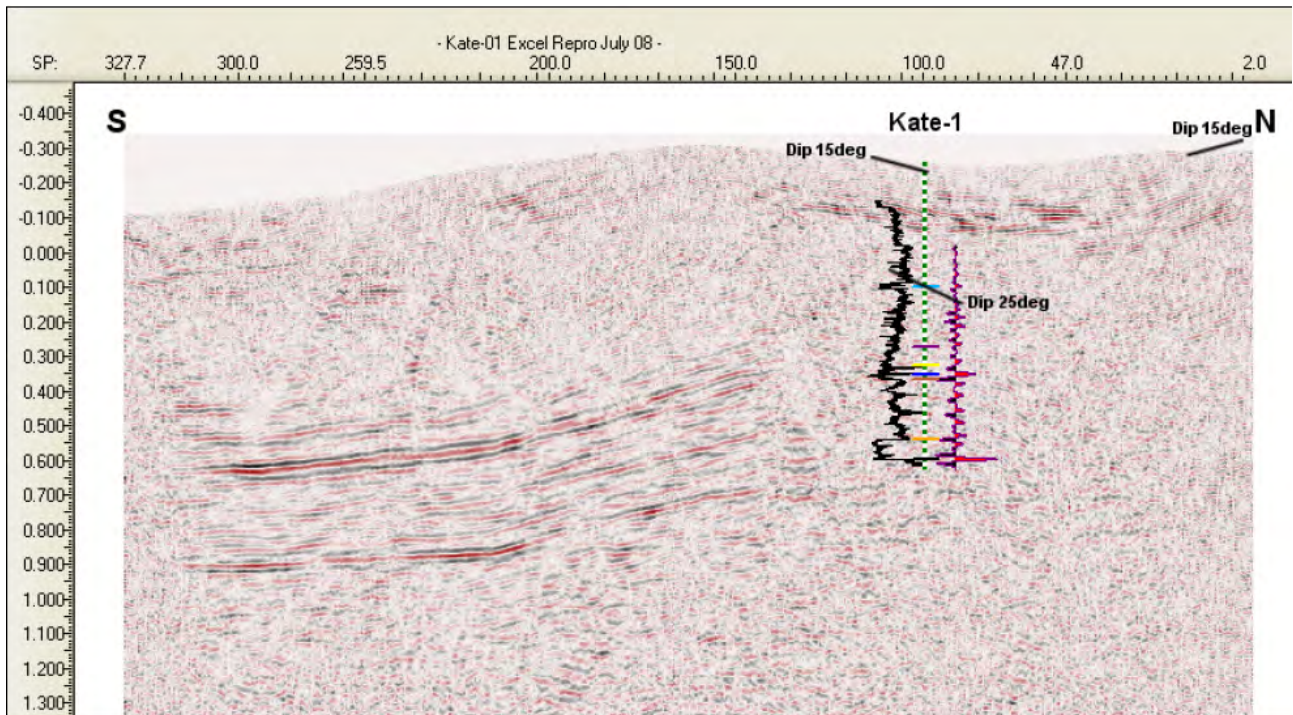


Figure 15. Seismic line tie to Kate-1

### ***Landfill gas to electricity***

Organic matter in the municipal waste that is disposed of in the Kate Valley landfill continuously generates significant volumes of gas (methane and CO<sub>2</sub>): recently about 2700 m<sup>3</sup>/hour. This is collected by a network of wells and used as fuel for four 1MW electricity generators at the site. The electricity is supplied into the national grid via high voltage power lines to a substation at Waipara.

Any gas production surplus to the capacity of the generation facilities is flared. There is a possibility to expand generation to as much as 10MW as gas output grows further.

### Stop 3: Hanmer Springs Thermal Pools and Spa (HSTPS)

The following is largely extracted from reports done for HSTPS by Elemental Consultant (Nick Jackson and Bill Leask) in support of the application for a Petroleum Mining Permit.

Hot springs at Hanmer were first reported by European settlers in April 1859, and soon became a popular tourist destination (Brown 1973). By 1910, the natural flow from the springs was inadequate for the demand, and three wells were drilled in the immediate vicinity of the springs in 1911-1912 to augment the supply. Further wells were drilled in 1936, 1962, 1975 and 2010.

The hot pools are currently supplied with water produced at a temperature of about 58°C, from the two most recent wells. Gas is produced along with the thermal water.

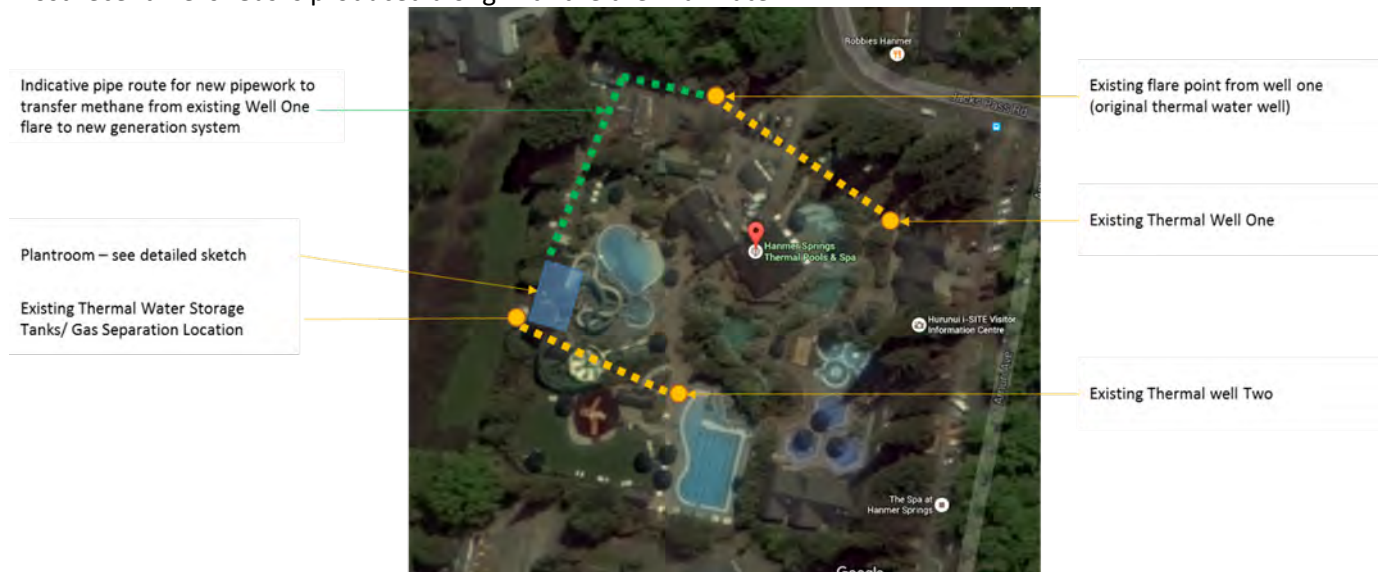


Figure 16. Well locations and associated facilities within the Hanmer Springs complex.

In 1975, thermal well N32/0054 (“Two”) was drilled under supervision of the Ministry of Works & Development to 84.8 m depth, but plugged back to 76 m. The ECAN database summarises this as a 250 mm well drilled to 76 m, but their detailed records state that the well was originally drilled to 96 m, then plugged back to 76 m. The top of the plug was tagged at 69.4 m, and casing was run to 58.9 m. The open-hole section is in gravels to 61.3 m, then bedrock to TD.

In 2010, thermal well N32/0319 (“One”) was drilled to 516 m depth. The ECAN database records a 200 mm diameter bore cased to 224 m with open hole from 224 to 516 m. It achieved a maximum yield of 20 L/s, with maximum drawdown of 12.7 m. The temperature of the produced water is 58 °C. The top of greywacke was intersected at 57 m.

Gas was previously vented or flared, but since 2018 HSTPS has established facilities to produce it for electricity generation subject to New Zealand’s smallest Petroleum Mining Permit (PMP 60215). The water and gas are co-produced from fracture zones within the greywacke bedrock. Calorific values of 35.1 to 38.8 MJ/sm<sup>3</sup> have been determined for the gas.

Gas composition (Table 1) has been analysed several times since 1921 (Brown 1973).

Table 1. Gas analyses of Hanmer Springs water wells. It is likely that all analyses in Table 1 were from N32/0102 (Thermal well Two)

Date	CH <sub>4</sub>	C <sub>2+</sub>	He + Ar	H <sub>2</sub>	CO <sub>2</sub>	O <sub>2</sub>	N <sub>2</sub>
5/5/2009	74.8	11.64	-	-	9.1	-	4.38
1/10/2005	89.21	2.08E-04	0.232	<0.01	0.004	0.008	10.54
23/9/1999	74.1	-	0.317	0.030	0.058	4.19	21.3
2/2/1990	89.4	0.077	-	-	0.11	-	10.0
Ross 1967	72.0	13.2	2.5	3.8	0.1	0.2	8.2
1921	92.31	-	-	-	0.06	0.5	7.13

Lyon and Giggenbach (1994) measured stable isotope ratios of methane in the gas. Three samples yielded values averaging -36.5 ppk  $\delta^{13}\text{C}$  and -157 ppk  $\delta^2\text{H}$ . Using published domains, these data plot in the dry thermogenic gas domain. Lyon & Giggenbach commented that methane from Hanmer Springs has a thermogenic composition resembling those of gases from greywackes of the axial ranges of the North Island. Ratios of  $^3\text{He}/^4\text{He}$  for the Hanmer gas, and indeed for most of the South Island gases, are generally above crustal values ( $> 0.1\text{RA}$ ) and indicate a contribution of mantle fluids.

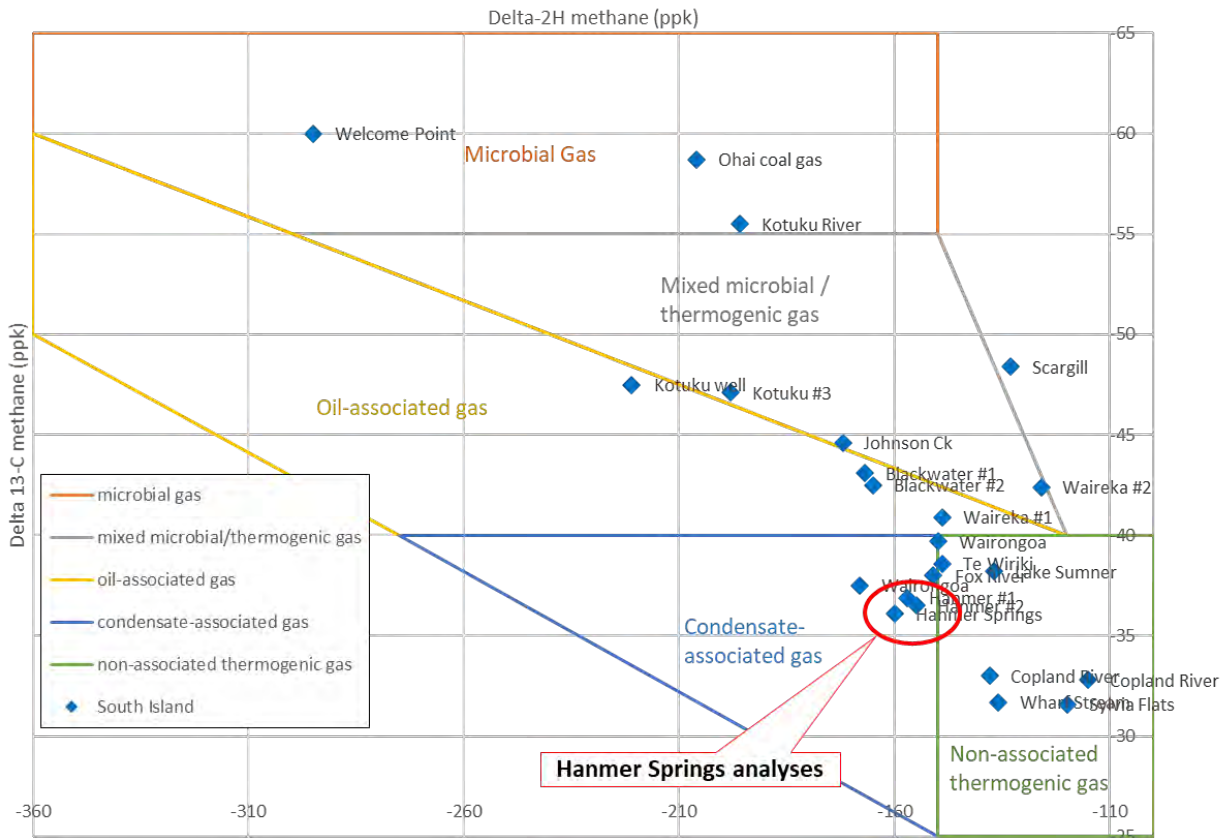


Figure 17. (from Elemental, for HSTPS). Stable isotopes for methane from South Island natural gas samples (Lyon and Giggenbach, 1994) plotted on fields established by Laughrey and Baldassare (1998).

Potential sources of gas at Hanmer Springs are:

- 1) Biogenic hydrocarbon from decomposition of organic material in the alluvial succession;
- 2) Thermogenic hydrocarbon from Paleogene-Late Cretaceous strata incorporated in the Hope Fault crush-zone. The gas composition is suggestive of source kerogen at fairly advanced maturity (e.g., medium or low volatile bituminous coals, Suggate rank 14-16, Ro about 1.5, based on Sykes and Zink, 2013).
- 3) Thermogenic hydrocarbon from organic-rich strata within the Pahau Terrane. Compilation of Torlesse geochemical data by Suggate (1990) outlined a zone of relatively un-metamorphosed rock within the North Canterbury region (i.e., the organic material had not been destroyed by metamorphism); coaly fragments were of high-volatile A bituminous to medium-volatile bituminous coal rank, potentially capable of generating late-stage thermogenic hydrocarbons consistent with Hanmer gas composition.
- 4) Thermogenic hydrocarbon generated on the subduction interface, but the farthest southwest extent of the Hikurangi slab barely reaches the Hanmer area (e.g., figure 6 in Furlong and Kamp, 2009).

The isotopic analyses of Lyon and Giggenbach (1994) (Figure 17) favour a deep thermogenic source within the Hope Fault crush zone. Apparent maturity would suggest the source rock has been buried to several km depth.

### ***Dynamic effects***

In March 2018, workover on thermal well One was carried out to replace the submersible pump. While the pump was out of the well, wireline logging was carried out. Western Energy Services (WES) ran a drifting tool to check well depth and lack of obstructions. This revealed that the well, which had been drilled to 516 m, was now blocked at 335.5 m, probably as a result of the November 2016 Kaikoura Earthquake. Well Drillers Wanganui (WDW) ran a borehole video camera downhole to record the wellbore condition and rockmass features. WES then ran a pressure-temperature-spinner tool down in a series of passes at different speeds to evaluate temperature variation and any zones of water influx.

Temperature logging shows a peak at 115 m, about halfway down the cased hole section. This is approximately 40 m below the top of the bedrock. A second jump in temperature occurs at 223.9 m, at the 8" casing shoe. The character of the temperature log and observations of the video suggest that water is flowing from the well into the annulus (i.e. from below the casing shoe).

PMP	Application		Casing Data				Wellhead Data	
Field	Hanmer Springs		Casing Size	Grade	Coupling	Comment	Type	
Well	N32/0319		12"					
	From	To	10"					
12"	0	166.5	8"					
10"	0	210						
8"	0	224						

Depth (m)	MD (m)	Inc	Component / Formation			
0	0.00					Ground level (GL)
20						
40						
60	60.00					Top of Pahau Terrane
80						
100						
120						
140						
160	166.50					12" shoe
180						
200						
220	210.00					10" shoe
240	224.00					8" shoe
260						
280						open-hole, unscreened
300						
320						
340						
360						
380						
400						
420						
440						
460						
480						
500						
520	516.00					7-7/8" (200 mm) TD

Revision	A	Date			Checked By	
----------	---	------	--	--	------------	--

Figure 18. Well schematic for the main production well at Hanmer Springs.

The largest jump in temperature occurs at 318 m, and although this is 17 m above the Total Depth at 335.5m, there is evidence for water and gas influx at the base of the well. Intervals with natural gas bubbling occur throughout the open-hole section of the well. In addition, slits in welded casing joints as high as 110 m also show very small gas bubbles entering the wellbore.

Flow rates of the gas are in proportion to the volume of water pumped (which varies according to seasonal demand). From the current production bores, a volume of 350 m<sup>3</sup> gas per day has been estimated (DETA Consulting 2015 report for HSTPS). In 2019, a total of 117,425 m<sup>3</sup> (1.26 million cubic feet) was produced, deriving a royalty payment to the Crown of \$1211.34. Over the 40-year term of the permit, about 5 million m<sup>3</sup> (55 mmscf) of gas is expected to be utilised.

The facilities include a gas/water separator, with the hot water used as previously for the hot pools. The processed gas is piped to an 80kW gas engine. The electricity produced offsets approximately 25% of HSTPS's requirements.

Although the producing intervals of older wells straddle the gravel/bedrock interface, the most recent well, N32/0319 (thermal well 1) produces significantly larger volumes of both water and gas than its

predecessors totally from within the bedrock. The fracture systems within the Pahau Terrane bedrock are therefore the main reservoir for both water and gas.

Permeable fracture systems commonly occur at the intersection of major fracture sets. The Hanmer Fault itself, with an ESE strike, is slightly oblique to the ENE trend of the Hope Fault segments (Figure 3; Figure 5). In addition, a significant defect orientation is indicated by inactive faults within the Pahau Terrane bedrock and stream alignments, and suggests a fracture set parallel to bedding. We can only speculate that these systems intersect in the Hanmer Springs area and provide a conduit for water and gas to the surface.

There are substantial structural uncertainties that could affect reserves, and these cannot be quantified given the limited amount of subsurface data. An additional uncertainty is the impact of future severe earthquakes in the area. Brown (1973) suggested that the hot spring activity may have been initiated by large earthquakes in 1848 and/or 1855. He cited Alexander Mackay's description of the springs in 1888 after the Glynn Wye earthquake on the Hope Fault: "The wells emitted more gas and, it may be, had for a few days a greater escaping volume of water; they very soon returned to their normal condition, and at the time of my visit were said to be slightly colder than usual."

During the February 2011 Christchurch earthquakes, the noise of the gas flow was "like a jetplane taking off" (HSTPS pers. comm.). After the November 2016 Kaikoura Earthquake, the water level dropped overnight from 52 m to 67-68 m, then settled at an average depth of 64 m. Water production decreased to approximately 16 L/s. Gas production also increased significantly for a few weeks, before returning to normal.

#### Stop 4: Cust Anticline

This will be a relatively brief stop en route back to Christchurch from Hanmer Springs. As at the Kate anticline, in the Cust district Pliocene strata are structurally elevated and folded forming inliers within Quaternary and modern fluvial deposits.

The Cust anticline is mapped as a southward continuation of Mairaki Downs, where Pliocene Kowai gravels are exposed. The western end of the Mairaki Downs plunges and veers southward, with mid Pleistocene alluvial deposits folded as a gentle ridge with active normal fault traces on either side. The anticline swings back to W-E trend again south of the Cust River bed. Campbell et al (2000) deduced from the geomorphology that the late Pleistocene emergence of the Cust/Mairaki Downs structure diverted the Ashley River from its previous course down the Cust valley, tributary to the Waimakariri.

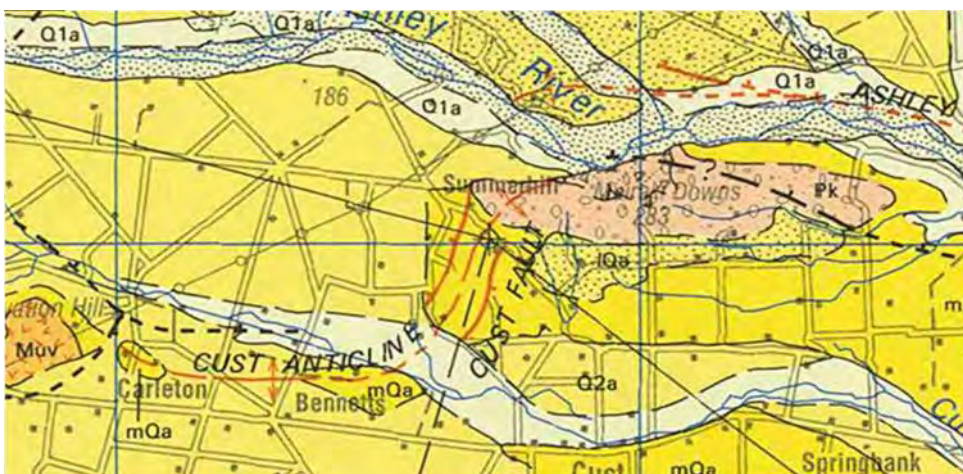


Figure 19. from QMAP (Forsyth et al, 2008). Blue grid lines are 10km apart. Arcadia-1 well location is shown just SE of Summerhill. Bright yellow "mQa" is mid Quaternary alluvium forming the core of the Cust anticline.

Indo Pacific as Operator for PEP 38256 over onshore Canterbury, acquired seismic lines in 1999, with line 107 (PR ) along Summerhill Rd across the anticline axis. This line shows quite a tight and fairly symmetrical

fold with the dip of its flanks diminishing with depth.

In 2000 the petroleum exploration well Arcadia-1 was drilled at the anticlinal crest adjacent to line 107 on the NE side of Summerhill Road.

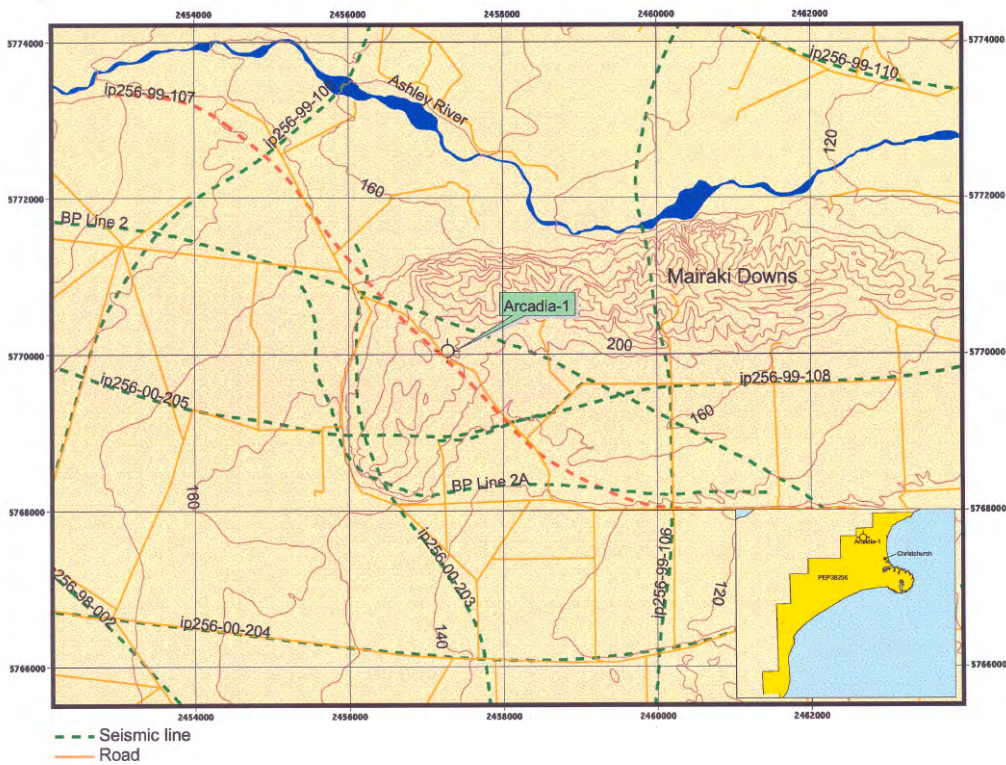


Figure 20. Location of Arcadia-1 exploration well near Cust, and seismic coverage. From PR 2561 (2000).

The sequence encountered below Kowai gravels in the well differed considerably from expectation. The prognosis of relatively thick Miocene similar to that mapped in the Waipara area (Tokama Siltstone with Mount Brown limestone) was disproved, with un-anticipated basalts (correlating to the Miocene basalt (Burnt Hill volcanics) at Starvation Hill several km to the WSW) making up 100m+ between Pliocene alluvial deposits and the Oligocene Amuri Limestone—much shallower than expected at 301.5m depth.

A prominent and reasonably continuous seismic reflector corresponds to the Amuri. The early Cenozoic-late Cretaceous succession was more as expected, but structurally thickened. The Eocene Homebush sandstone exhibited excellent reservoir properties but there were no hydrocarbon indications. Total depth of the well is 1479m, within the Broken River Formation.

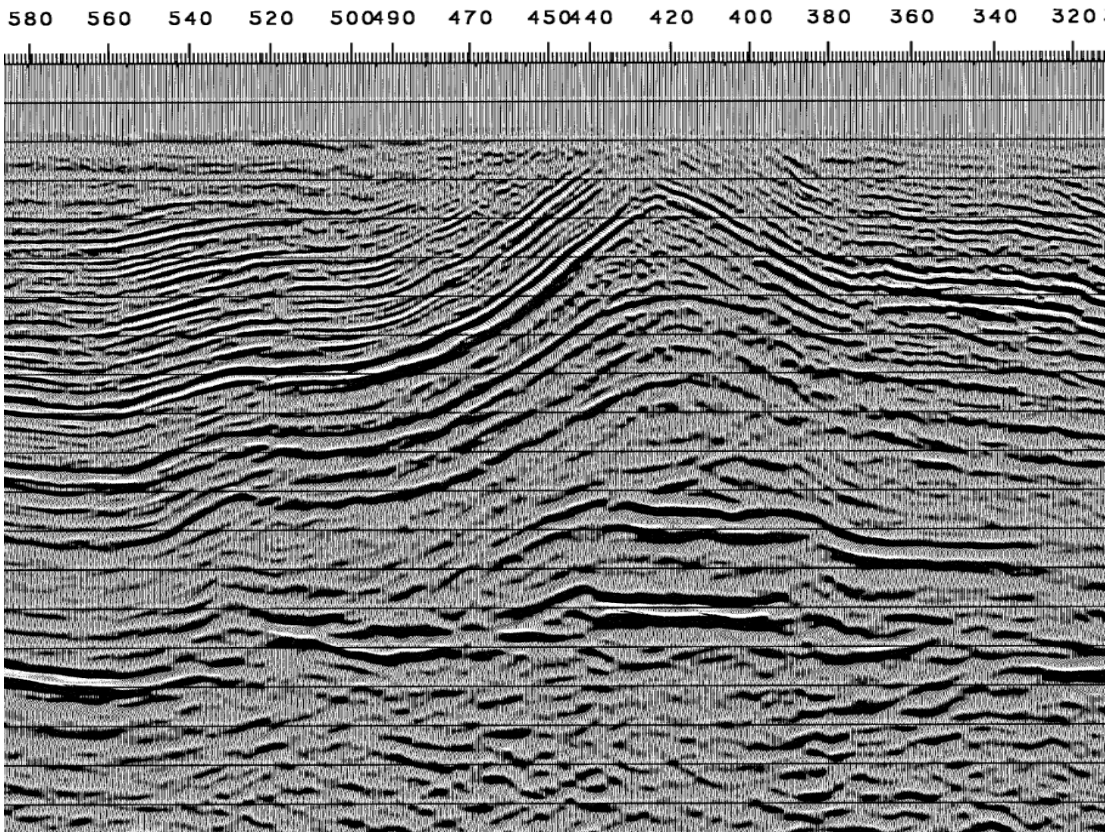


Figure 21. Part of seismic line 107.

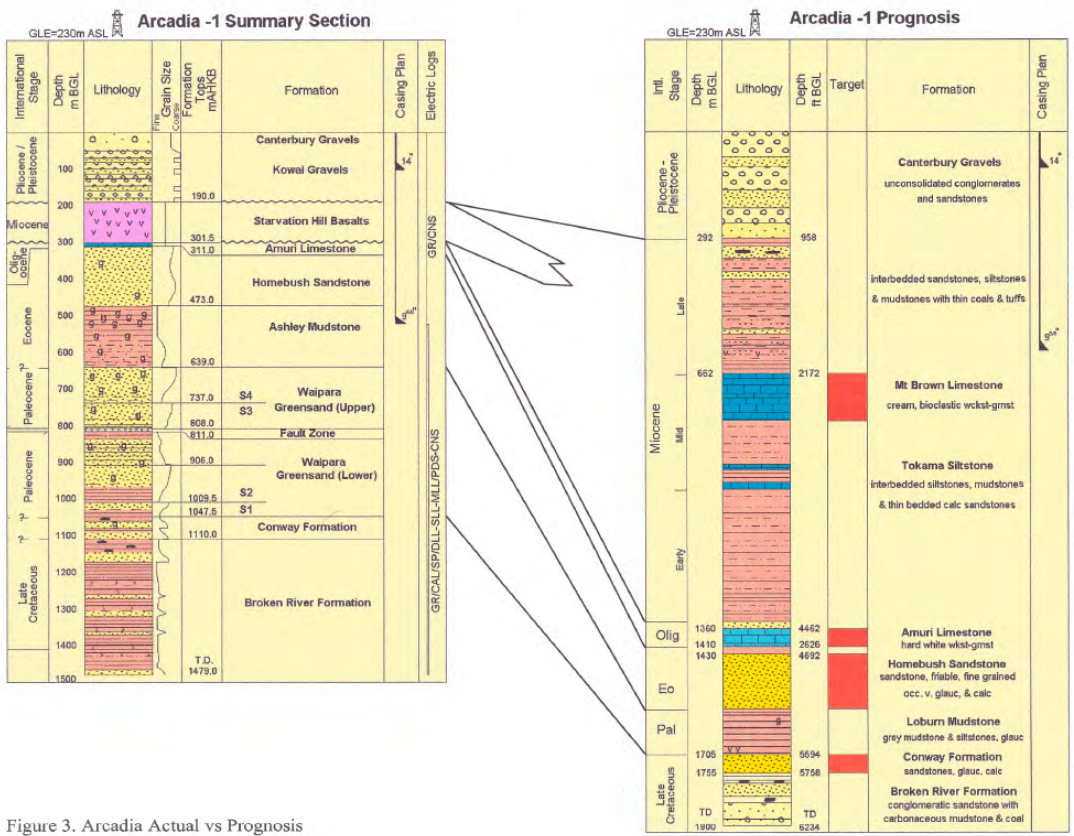


Figure 3. Arcadia Actual vs Prognosis

Figure 22. Stratigraphic sequence in Arcadia-1 compared to prognosis.

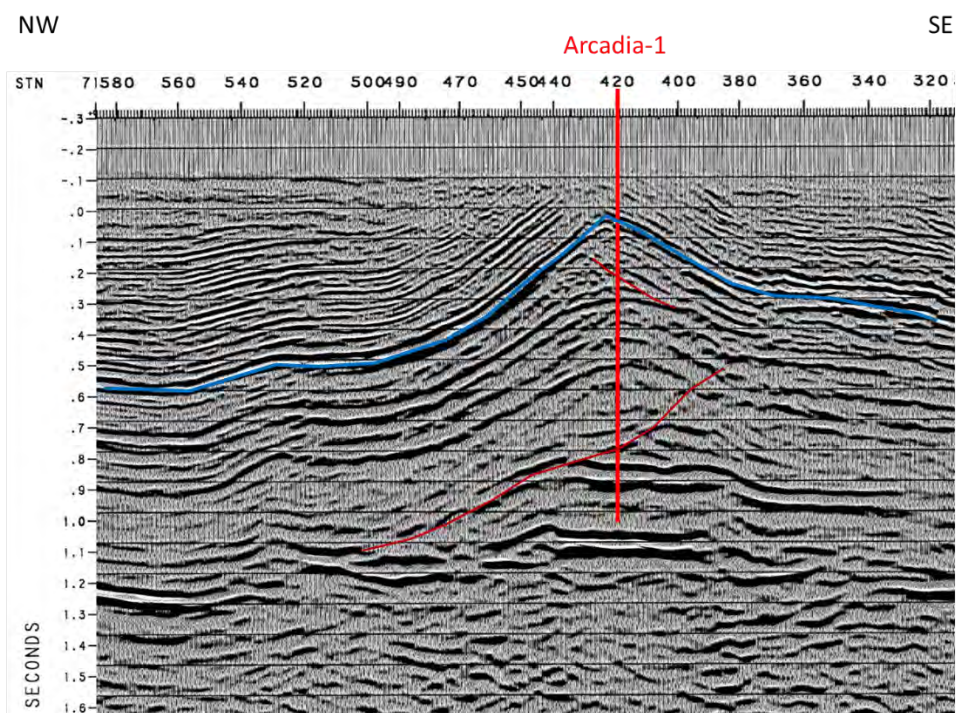


Figure 23. Line 107 with Arcadia-1 well, Amuri reflector (blue), and possible faults (dark red).

## References

- Barnes, P.M. (1996). Active folding of Pleistocene unconformities on the edge of the Australian-Pacific plate boundary zone, offshore North Canterbury, New Zealand. *Tectonics* 15: 623–640.
- Barrier, A., Nicol, A., Browne, G., Bassett, K. (2019). Early Oligocene marine canyon-channel systems: Implications for regional paleogeography in the Canterbury Basin, New Zealand. *Marine Geology* 418. <https://doi.org/10.1016/j.margeo.2019.106037>.
- Brown, L.J. (1973). Thermal water and ground water resources of the Hanmer Basin. New Zealand Geological Survey unpublished report.
- Browne, G.H., Field, B.D. (1985). The lithostratigraphy of Late Cretaceous to early Pleistocene rocks of northern Canterbury, New Zealand. New Zealand Geological Survey record 6, 63p.
- Browne, G.H., Naish, T.R. (2003). Facies development and sequence architecture of a late Quaternary fluvial-marine transition, Canterbury Plains and shelf, New Zealand: implications for forced regressive deposits. *Sedimentary Geology* 158: 57–86.
- Campbell, J. Bennett, D. and Brand, R. (2000). Actively emergent, fault-related fold structures beneath the Canterbury Plains. New Zealand Petroleum Conference Pre-conference Field Trip Guide.
- Field, B.D., Browne, G.H. (1989). Cretaceous and Cenozoic sedimentary basins and geological evolution of the Canterbury Region, South Island, New Zealand. Institute of Geological & Nuclear Sciences Monograph 2, 94p.
- Forsyth, P.J., Barrell, D.J.A., Jongens, R. (2008). Geology of the Christchurch Area: Institute of Geological and Nuclear Sciences Geological Map 16: Lower Hutt, New Zealand, GNS Science, 1 sheet + 67 p., scale 1:250,000.
- Furlong, K.P. and Kamp, P.J.J. (2009). The lithospheric geodynamics of plate boundary transpression in New Zealand: Initiating and emplacing subduction along the Hikurangi margin and the tectonic evolution of the Alpine Fault system. *Tectonophysics* 474: 449–462.
- King, P.R., Naish, T.R., Browne, G.H., Field, B.D., Edbrooke, S.W. (1999). Cretaceous to Recent sedimentary patterns in New Zealand. Institute of Geological and Nuclear Sciences Folio Series 1, 35p.
- Landis, C.A., Campbell, H.J., Begg, J.G., Mildenhall, D.C., Paterson, A.M., Trewick, S.A. (2008). The Waipounamu Erosion Surface: questioning the antiquity of the New Zealand land surface and terrestrial fauna and flora. *Geological Magazine* 145: 173–197.
- Laughrey, C.D., Baldassare, F.J., (1998). Geochemistry and origin of some natural gases in the Plateau

- Province, Central Appalachian Basin, Pennsylvania and Ohio. *Am. Assoc. Petrol. Geol. Bull.* 82: 317–335.
- Lyon G.L., Giggenbach W.F. (1994). The isotopic and chemical composition of natural gases from the South Island, New Zealand. Ministry of Energy 1994 New Zealand Petroleum Conference Proceedings: 361–369.
- Mortimer, N., Rattenbury, M.S., King, P.R., Bland, K.J., Barrell, D.J.A., Bache, F., Begg, J.G., Campbell, H.J., Cox, S.C., Crampton, J.S., Edbrooke, S.W., Forsyth, P.J., Johnston, M.R., Jongens, R., Lee, J.M., Leonard, G.S., Raine, J.I., Skinner, D.N.B., Timm, C., Townsend, D.B., Tulloch, A.J., Turnbull, I.M., Turnbull, R.E. (2014). High-Level Stratigraphic Scheme for New Zealand Rocks. *New Zealand Journal of Geology and Geophysics* 57: 402–419.
- Nicol, A. (1991). Structural styles and kinematics of deformation on the edge of the New Zealand plate boundary zone, mid Waipara region, North Canterbury. Unpublished PhD thesis, lodged in the Library, University of Canterbury, Christchurch, New Zealand.
- Nicol, A. (1993). Haumurian (c. 66–80 Ma) half-graben development and deformation, mid Waipara, North Canterbury, New Zealand. *New Zealand Journal of Geology and Geophysics* 36 (1): 127–130. doi: 10.1080/00288306.1993.9514560
- Nicol, A., Alloway, B.V., Tonkin, P.J. (1994). Rates of deformation, uplift and landscape development associated with active folding in the Waipara area of North Canterbury, New Zealand. *Tectonics* 13: 1321–1344.
- Nicol, A., Khajavi, N., Pettinga, J.R., Fenton, C., Stahl, T., Bannister, S., Pedley, K., Hyland-Brook, N., Bushell, T., Hamling, I., Ristau, J., Noble, D., McColl, S.T. (2018). Preliminary geometry, displacement and kinematics of fault ruptures in the epicentral region of the 2016 MW 7.8 Kaikōura earthquake, New Zealand. *Bulletin of the Seismological Society of America* 108 (3B): 1521–1539. [doi.org/10.1785/0120170329](https://doi.org/10.1785/0120170329).
- Pettinga, J.R., Yetton, M.D., Van Dissen, R.J., Downes, G. (2001). Earthquake source identification and characterisation for the Canterbury Region, South Island, New Zealand, *Bull. New Zealand Soc. Earthq. Eng.* 34: 282–317.
- Rattenbury, M.S., Townsend, D.B., Johnston, M.R. (compilers) (2006). Geology of the Kaikoura area. Institute of Geological & Nuclear Sciences 1:250 000 geological map 13.
- Strogen, D., Seebeck, H., Nicol, A., King, P. (2017). Two-phase Cretaceous-Paleocene rifting in the Taranaki Basin Region, New Zealand; implications for Gondwana breakup. *Journal of the Geological Society* 174 (5): 929–946. <https://doi.org/10.1144/jgs2016-160>.
- Suggate R.P. (1990). Coal ranks in Permian–Lower Cretaceous rocks of New Zealand. *New Zealand Journal of Geology and Geophysics* 33: 163–172.
- Sykes, R., Zink, K-G. (2013). Improved calibration of the absolute thermal maturity of coal-sourced oils and gas condensates using PLS regression. Search and Discovery Article 10480, AAPG.
- Vanderleest, R.A., Fisher, D.M., Oakley, D.O.S., Gardner, T.W. (2017). Growth and seismic hazard of the Montserrat anticline in the North Canterbury fold and thrust belt, South Island, New Zealand. *J. Struct. Geol.* 101: 1–14.
- Warren, G. (1995). Geology of the Parnassus area. Institute of Geological and Nuclear Sciences Geological Map 18: Lower Hutt, New Zealand, GNS Science, 1 sheet + 36 p., scale 1:50,000.
- Wilson, D.D. (1963). Geology of Waipara Subdivision (Amberley and Motunau Sheets S68 and S69). *New Zealand Geological Survey Bulletin* 64.
- Wood, R.A. (1991). Seismic reflection data from the Hanmer Basin, NZ. *Exploration Geophysics* 22: 503–508.
- Wood, R.A., Pettinga, J.R., Bannister, S., Lamarche, G., McMorran, T.J. (1994). Structure of the Hanmer strike-slip basin, Hope Fault, New Zealand. *Geological Society of America Bulletin* 106: 1459–1473.

### ***Petroleum Reports***

- PR 260 (1971). Geological report on PPLs and areas of interest. Antipodes Oil Co Ltd.
- PR 319 (1961). A Geological Reconnaissance of the North Canterbury Region, South Island, New Zealand. D. Haw, BP.
- PR 2424 (1999). PEP 38256 Canterbury Basin seismic survey. Schlumberger Geco-Prakla.

PR 2561 (2000). Arcadia-1 Well Completion Report. PEP 38256. Indo Pacific.  
PR 3165 (2005). Results of Year One exploration work conducted for Green Gate Ltd. GeoSphere.  
PR 3929 (2008). Kate-1 Well Completion Report. GeoSphere.

## Acknowledgements

Management of Kate Valley Landfill, and of Hanmer Springs Thermal Pools and Spa.  
Jarg Pettinga for copy of the 2000 Petroleum Conference field trip guide.  
Nick Jackson and Bill Leask for unpublished work on gas at Hanmer Springs.  
Jessica Fensom for preparation of Figure 1.

# FIELD TRIP 5: BANKS PENINSULA'S BEST BITS: VOLCANOLOGY, RESEARCH AND GEOPARK

Thursday 26 November 2020

Leaders: Sam Hampton<sup>1,2,3</sup> and Darren Gravley<sup>1,2</sup>

<sup>1</sup>School of Earth and Environment / Te Kura Aronukurangi

University of Canterbury / Te Whare Wānanga o Waitaha

[Samuel.hampton@canterbury.ac.nz](mailto:Samuel.hampton@canterbury.ac.nz)

[Darren.gravley@canterbury.ac.nz](mailto:Darren.gravley@canterbury.ac.nz)

<sup>2</sup>Frontiers Abroad Aotearoa

[sam@frontiersabroad.com](mailto:sam@frontiersabroad.com)

[darren@frontiersabroad.com](mailto:darren@frontiersabroad.com)

<sup>3</sup>Te Pātaka o Rākaihautū / Banks Peninsula Geopark Trust

[bankspeninsulageopark@gmail.com](mailto:bankspeninsulageopark@gmail.com)

## Overview

This field trip showcases key sites, findings, lessons, and understandings from the last decade of research being undertaken on Banks Peninsula. Frontiers Abroad Aotearoa in partnership with the School of Earth and Environment, University of Canterbury, have been undertaking detailed geological mapping and using Banks Peninsula as a basis for independent research projects. Detailed geological mapping has focussed on previously overlooked areas on Banks Peninsula, especially in the eastern sector of the Akaroa Volcanic Complex. Through systematic mapping and sampling we are gaining insights into the processes (i.e. eruptive cycles, intrusive events, parasitic cone eruptions) and formation of the volcanic system (i.e. magmatic-volcanic), and volcanic complex development (i.e. geomorphic signatures, reconstructions). Independent research projects use Banks Peninsula as a linking principle, with projects ranging from geological mapping, geochemical, petrological, Mātauranga Māori, Quaternary sequences, geodiversity, geo-education, and Geoparks. This research has provided the foundational understandings and forging of relationships in the formulation and collaborative creation of Te Pātaka o Rākaihautū / Banks Peninsula Geopark. The field trip visit sites that link together elements of this decade of research, presenting new findings and hypotheses, visions and lessons with the Geopark framework, and present future research themes and opportunities.



Figure 1. Geological map of Banks Peninsula with field trip locations. 1: UC Campus, 2: Waikakahi/Birdlings Flat, 3: Wairewa/Little River, 4: Hilltop, 5: Ōnawe, 6: Duvauchelle, 7: Ōtepatotu Reserve, 8: Pigeon Bay overlook, 9: Gebbies Pass, 10: Whakaraupo/Lyttelton.

## Waikakahi / Birdlings Flat

### ***Te Pātaka o Rākaihautū / Banks Peninsula Geopark***

Te Pātaka o Rākaihautū / Banks Peninsula Geopark will engage people in the landscapes and stories of Banks Peninsula. Te Pātaka o Rākaihautū / Banks Peninsula Geopark is a local resident, rūnanga, and community group-initiated concept designed to provide local and place-based educational experiences to a range of target visitors, and provide a mechanism for sustainable growth and development. Banks Peninsula has a unique geology on which has evolved a diverse biosphere, cultural history, concepts of conservation, and land use practices. These features are key to UNESCO Geopark accreditation, which is the ultimate aim of this initiative.

The vision is to create a Geopark of international significance founded on the geological, biological, heritage, and cultural features, and the communities, of Banks Peninsula. Te Pātaka o Rākaihautū / Banks Peninsula Geopark will tell the stories of our landscape, relate human histories and their significance to Aotearoa / New Zealand. The Geopark will promote conservation and sustainable behaviours, provide economic benefit to Banks Peninsula through increased, long-staying, visitor numbers, support and stimulate ongoing scientific research and science communication, and bring together Banks Peninsula's communities by providing a framework for social, economic, cultural, environmental, and educational interaction. Te Pātaka o Rākaihautū / Banks Peninsula Geopark will be a coordinating principle for the numerous and varied initiatives already occurring on Banks Peninsula.

Te Pātaka o Rākaihautū / Banks Peninsula Geopark is designed as an engagement and educational platform: informing locals and visitors about the region's geology, landscape, flora, fauna, archaeology, histories, communities, and organisations. It aims to encourage the local Canterbury population to engage with Banks Peninsula through trails, sign boards, open air learning, field trips, research, experiences, and digital interfaces, as well as attract national and international visitors to Banks Peninsula. Because of what the Geopark model offers, visitors will be immersed in the landscape more than traditional visitors. This results in a stronger connection to place and more time spent experiencing the area.

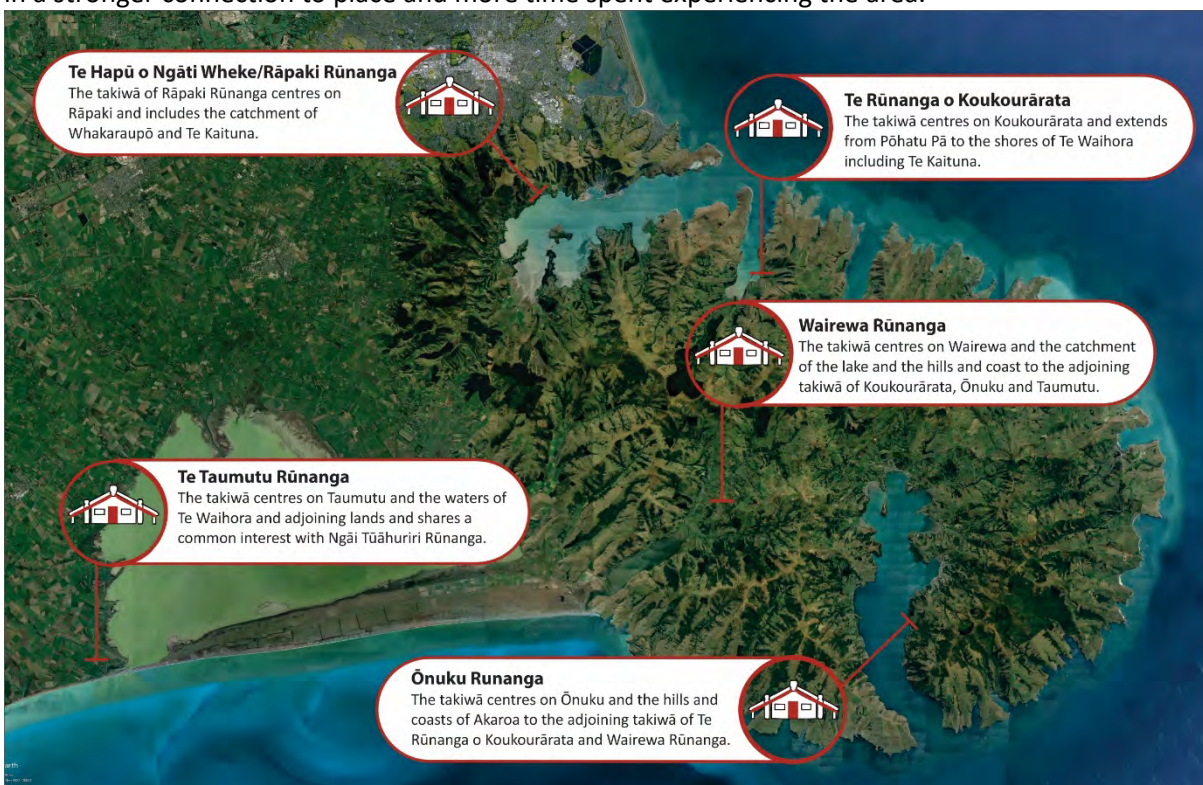


Figure 2. Papatipu rūnanga of Te Pātaka o Rākaihautū / Banks Peninsula. Not represented within this figure is Te Ngāi Tūāhuriri Rūnanga

## Hill top overview

### **Akaroa Volcanic Complex**

Significant stages of volcanism at Banks Peninsula are split into four major volcanic groups: Lyttelton, Mt Herbert, Akaroa, and Diamond Harbour (Figure 3). All volcanic groups were active during the late Miocene, with the main eruptive activity of Akaroa taking place around 9.4–8 Mya (Sewell, 1988, Timm, 2009). Common eruptive products across Banks Peninsula include lava flows, ash beds, dikes, sills, scoria cones, trachytic domes, and lahar deposits (Hampton and Cole, 2009). The Akaroa Volcanic Complex (AVC) was a 1200 km<sup>3</sup> composite volcano that erupted from multiple vents (Sewell, 1988; Hampton and Cole, 2009).

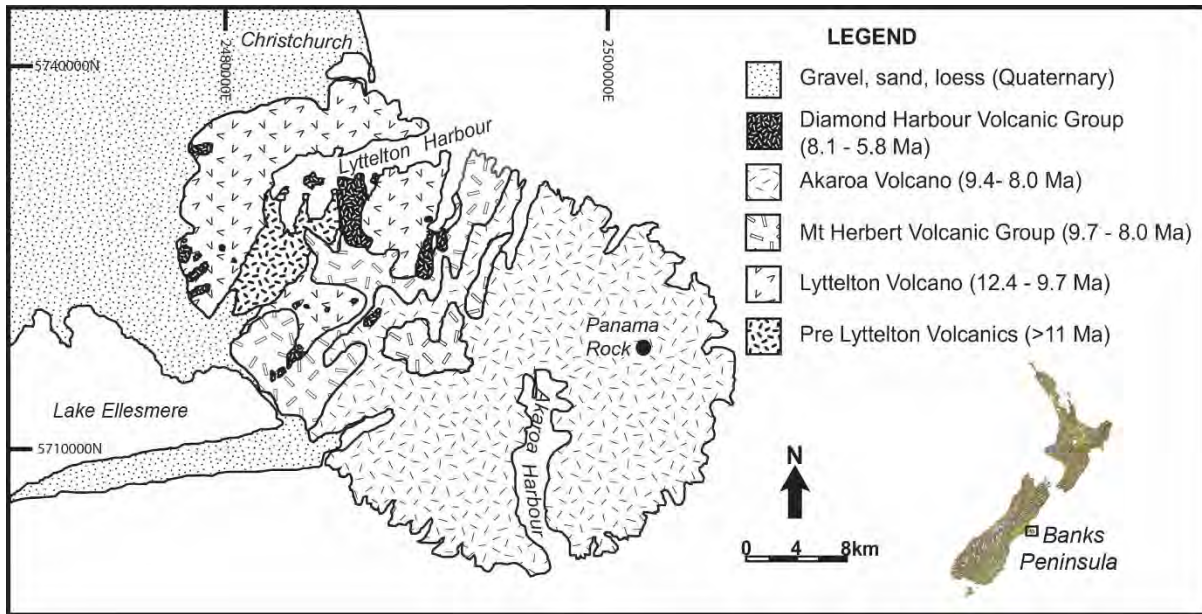


Figure 3. Geological map of Banks Peninsula, illustrating the location and age range of the five main volcanic groups at Banks Peninsula (adapted from Hampton and Cole, 2009).

Field studies have also indicated that not all lava flows are derived from main vent and that flank eruptives can produce high volume lava flows. The distribution of trachytic lava domes, basaltic scoria cones and vents, and dikes of both compositions highlight relationships within the volcanic system. Trachytic intrusions and eruptives occurred throughout the duration of activity at the Akaroa Volcanic Complex. Scoria cones occur throughout the eruptive sequences of Akaroa. It is hypothesised that the concentration of basaltic vents on the outer flanks of Akaroa was tectonically controlled, while the concentration of most trachytic domes within elevations of 400–600 m was caused by the weight of the growing Akaroa Volcanic Complex edifice deflecting trachytic feeder dikes into lateral orientations (Goldman et al., in prep).

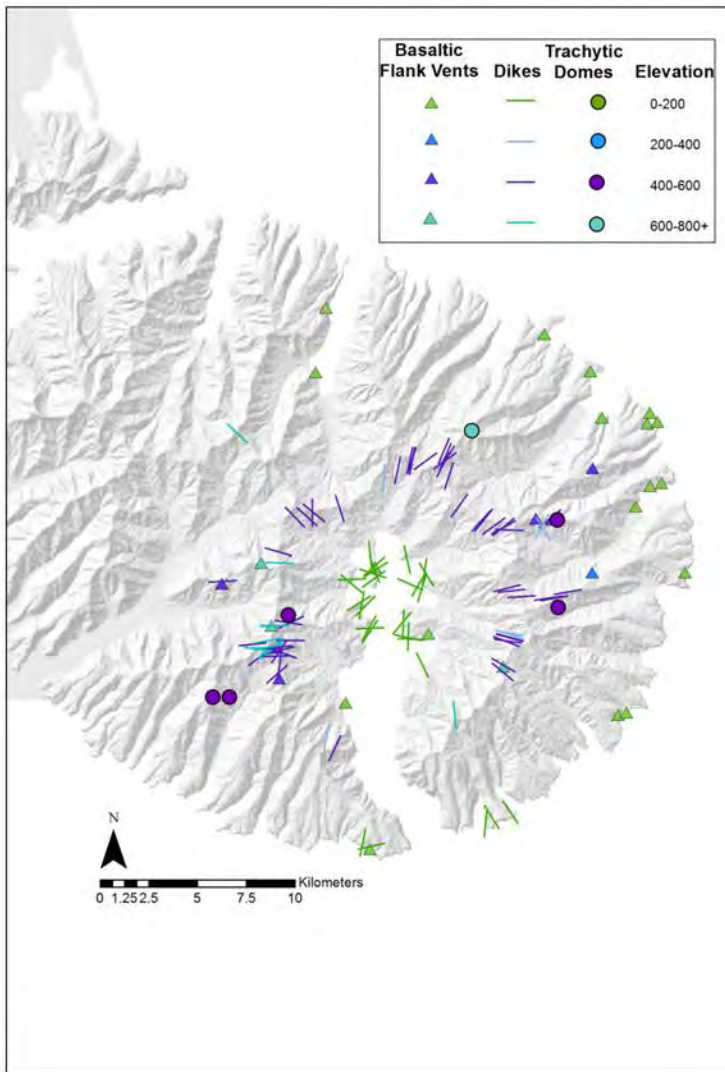


Figure 4. Topographic Distribution of Primary Volcanic Features. Distinct stratification of feature types exist, with basaltic vents generally at the lowest elevations, domes within the 400-600 m contour range, and very few features at all in the upper 200 m of elevation (from Gaddis and Hampton 2014).

***Eruptive Sequences: stratigraphic evidence (Johnson, Hampton and Gravley 2012, Beckham, Hampton, and Gravley 2015, Barran, Hampton and Gravley 2019)***

Collective unpublished Frontiers Abroad undergraduate research projects have noted a repeated compositional pattern from picrite to benmoreite within lava flow transects within Akaroa Volcanic Complex (Johnson, 2012; Crystal, 2013; Patel, 2013; Beckham, 2015). These trends suggest frequent magma recharge events, which injected less-evolved magma into the AVC system, may have triggered eruptions. In several cases, the change from picritic to benmoreitic composition is documented multiple times within a mapped transect (Johnson, 2012; Crystal, 2013; Patel, 2013). This close temporal relationship between evolved and unevolved products may implicate a complex magma storage system that allowed for the evolution of different melts within distinct chambers.

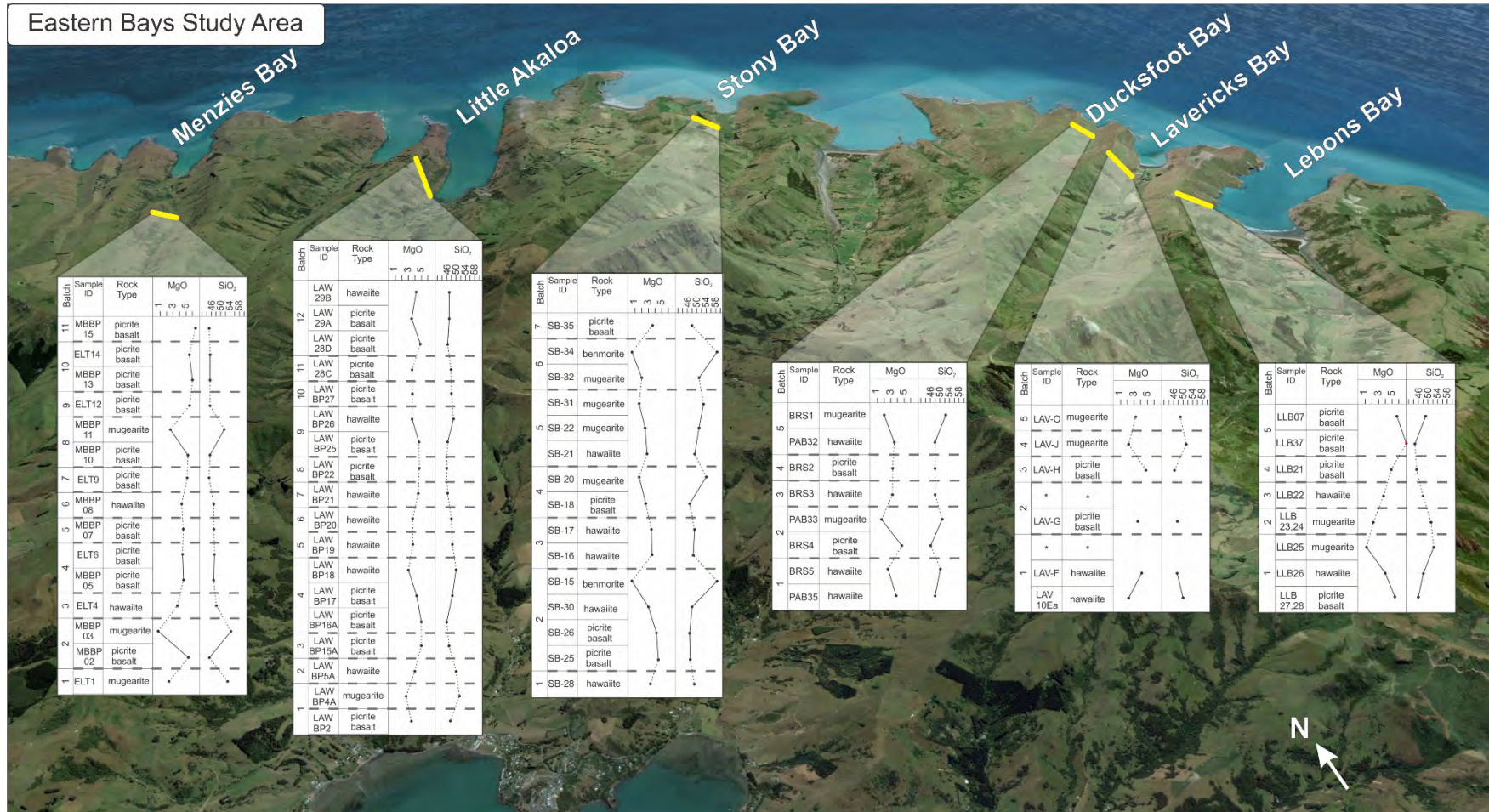


Figure 5. Oblique view of eastern Akaroa Volcanic Complex transects (yellow lines). Geochemical plots for each transect are shown, depicting the SiO<sub>2</sub> and MgO trends observed in stratigraphic sequence. Horizontal dashed lines divide batches, vertical solid lines relate flows within single batches, and vertical dashed lines show unrelated flows between two batches (Beckham, Hampton, and Gravley 2015)

**Petrographic evidence (Beckham, Hampton, and Gravley 2015. Xu and Hampton 2017, and Barran, Hampton and Gravley 2019)**

The history of these events are well recorded in the textures of mineral grains in igneous rocks because as magmas ascend, they crystallise and/or entrain crystals from different depths. Crystal textures provide insight into magma dynamics including ascent, storage, mixing and rejuvenation.

Observed mineral textures include sieved, resorption surface, and melt inclusions. Sieved rim, patchy cores, zoning, swallow-tailed, synneusis, glomero-crysts, broken crystals and crystal clusters were also observed to a lesser extent within the transects. A general petrographic observation is that phenocrysts in most samples, but particularly in the least evolved picrites, experienced multiple magma recharge events and decompression. These suggest a highly dynamic volcanic systems under frequent magma recharge, chamber convection, and decompression events. The complex growth histories preserved in phenocrysts within individual thin sections imply a complex magma system characterised by interconnected magma bodies (i.e. sills and dykes) as opposed to a large unitary magma chamber. This complex magma architecture hypothesis is also supported by a recent PhD textural/geochemical study (Bertolett, 2019) on erupted plutonic lithics from Akaroa.

	TEXTURE	INTERPRETATION
	Sieved	Intermediate decompression
	Sieved Rim	Magma recharge (primitive) and mixing
	Patchy Core	Slow decompression
	Melt Inclusions	Rapid crystal growth with decompression, undercooled
	Zoning	Chamber convection
	Resorption Surface	Magma recharge
	Swallow-tailed	Fast decompression
	Synneusis	Chamber convection
	Glomero-crysts	Suturing of spatially closer resorbed crystals under relative equilibrium condition
	Broken Crystal	Decompression related forceful aerial eruption
	Crystal Cluster	Chamber convection or syn-eruptive event

Figure 6. Petrographic guide with schematic representation of observed plagioclase textures and their interpretation. The classification is based on plagioclase textural analysis in Viccaro et al. (2010), Giacomoni et al. (2014), Renjith (2014) (from Beckham, Hampton, and Gravley 2015).

## Interpretive Models of the Akaroa Volcanic Complex

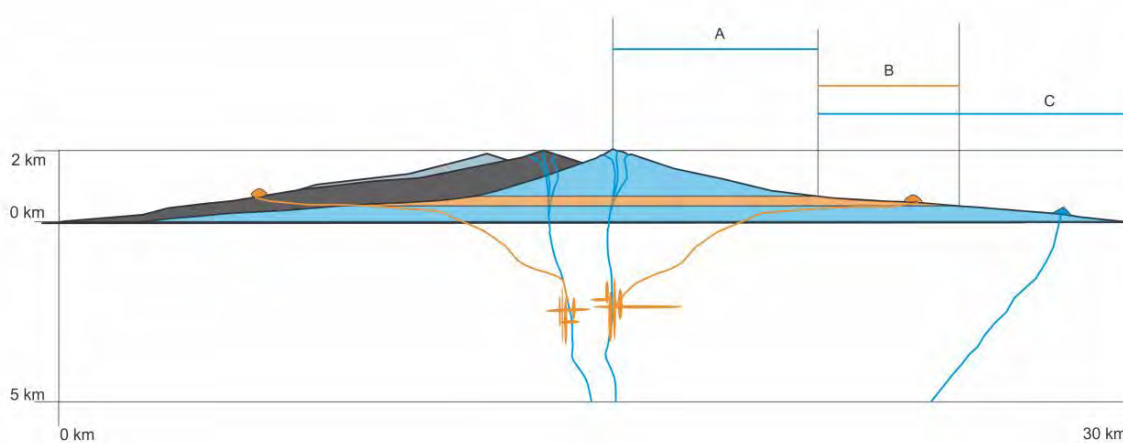


Figure 7. Interpretive Model of Compositional Vertical Stratification. Load stress related to edifice height relates closely with the compositional stratification identified from this study. Basaltic vents primarily span ranges of 0-200m, then basaltic dikes appear in the topographies above 600m (A). Trachytic domes and dikes exist in a small middle zone, between 400 and 700 m (B). Basaltic vents are theorized to stem directly up from deeper magma reservoirs (from Gaddis and Hampton 2014).

Schematic Magmatic System	Lithic Type Samples	Analytical Properties		Interpreted Relationships / Processes
	<p>GR 14</p>	<p>Whole Rock SiO<sub>2</sub> wt.%: 55                      Plag. %: 93 %                      CPO: Weak                      An#: 24                      Interstitial Material %: 6 %</p>	<p>Interstitial Material SiO<sub>2</sub> wt.%: 63                      Mafic Enriched Domain %: N/A                      Mafic Enriched Domain SiO<sub>2</sub> wt.%: N/A</p>	<p><b>Mush:</b> Crystal accumulation of more evolved phases in a comparatively felsic magma                      Compaction: Weak compaction aligning crystals                      Interstitial Material: Continuous and homogenous distribution of felsic residual melt, preserved as interstitial material crystallizing around phenocrysts                      Mafic Enriched Domains: None present</p>
	<p>GR 20</p>	<p>Whole Rock SiO<sub>2</sub> wt.%: 47                      Plag. %: 80 %                      CPO: Moderate                      An#: 30                      Interstitial Material %: 3 %</p>	<p>Interstitial Material SiO<sub>2</sub> wt.%: 59                      Mafic Enriched Domain %: Trace                      Mafic Enriched Domain SiO<sub>2</sub> wt.%: N/A</p>	<p><b>Mush:</b> Crystal accumulation and settling/sorting in a semi-evolved magma                      Compaction: Moderate compaction sorted and aligned crystals                      Interstitial Material: Two populations of IM - a high silica and K<sub>2</sub>O and a low silica, high FeO group                      Mafic Enriched Domains: Trace present</p>
	<p>GR 8b</p>	<p>Whole Rock SiO<sub>2</sub> wt.%: 46                      Plag. %: 75 %                      CPO: Strong                      An#: 37                      Interstitial Material %: 2.5 %</p>	<p>Interstitial Material SiO<sub>2</sub> wt.%: 59                      Mafic Enriched Domain %: 4.5                      Mafic Enriched Domain SiO<sub>2</sub> wt.%: 45</p>	<p><b>Mush:</b> Crystal accumulation and settling in a comparatively less evolved magma.                      Compaction: Cumulate fabric formed from moderate-strong uniaxial compression                      Interstitial Material: Very little felsic intergrain material                      Mafic Enriched Domains: High amounts of trapped silica-poor melt form MED</p>

Figure 8. Bertollett (2019) summary table of Goat Rock plutonic lithic populations. Left, schematic volcanic system adapted from Cashman et al. (2017). Potential lithic resident locations in mush indicated by red (GR8b), green (GR20), and blue (GR14) circles. Coloured circles correspond to schematic of lithic type samples: plagioclase (grey rectangles), mafic phases (black ovals), mafic enriched domains (red regions), and bright CL areas (purple regions). Right, corresponding data and interpretations for each component of plutonic lithic.

# Ōnawe

## Volcanic stratigraphy and inner harbour volcanic benches

Ōnawe represents some of the earliest stages of emergent volcanism of the Akaroa Volcanic Complex and the only insitu exposure of late stage plutonics, gabbro and syenite.

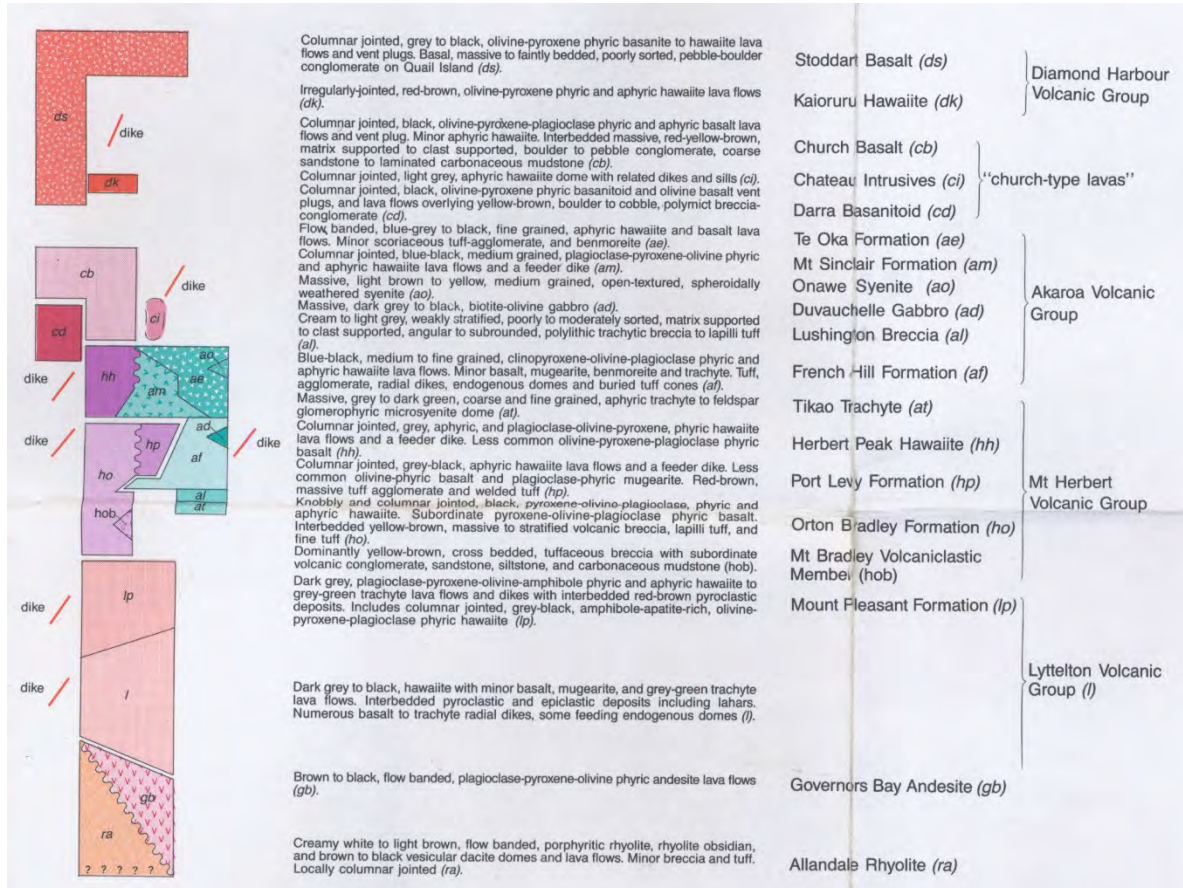


Figure 9. Sewell et al (1992) stratigraphic column for Banks Peninsula's volcanic groups.

A recently recovered core within an inner harbour borehole, extended 250 meters in depth. This volcanic stratigraphy in itself is the first recovered, sub-surface borehole within the AVC, providing insight into the volcanic stratigraphy beyond the surficial mapped volcanics and shore platform and the current interpreted stratigraphy (i.e., Dorsey, 1988; Sewell, 1988; Trent, 2010). The core intersected four main facies: lava flow sequences, altered trachytic breccia, red ash/pyroclastic horizons, and an interpreted dyke. The stratigraphy of the core offers insight into the subsurface geology beneath Takamatua Peninsula. The presence of stratified lava sequences in the core indicates that there are earlier stages of volcanism in Akaroa beyond the current interpreted stratigraphy.

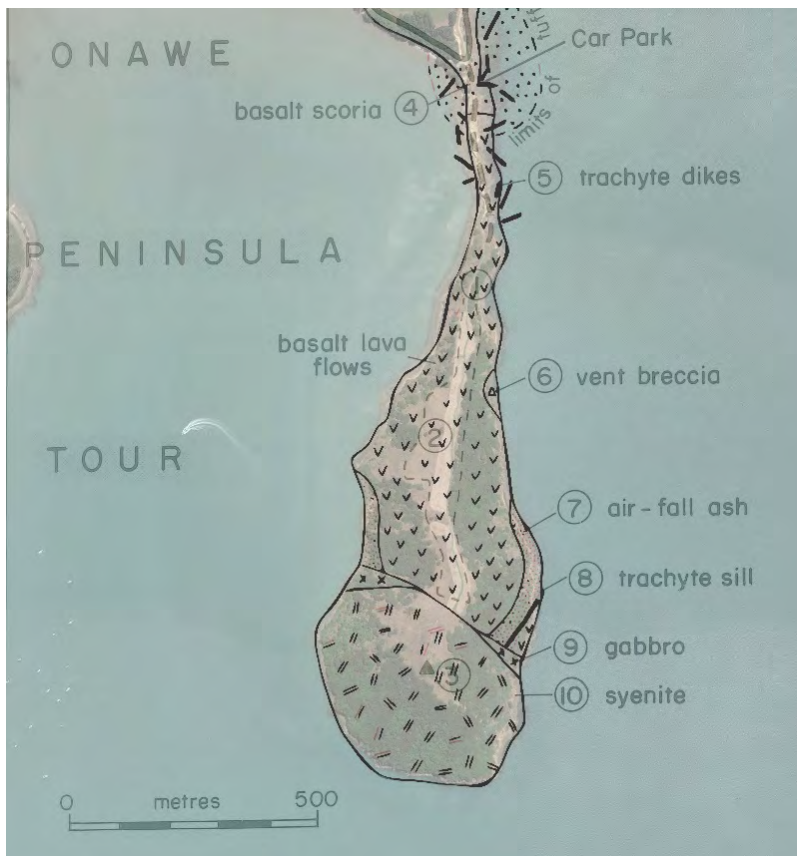


Figure 10. Geology of Ōnawe (modified from Weaver et al (1985).

### **Ōnawe Pa**

The volcanic landform of Ōnawe provided the perfect topography for a defensive pa. The site is also of historical significance for its siege and attack by Te Rauparaha in November 1831. On the 6<sup>th</sup> of November 1830 Te Rauparaha attacked local Ngai Tahu at Takapuneke, aided by Capt. Stewart of the brig Elisabeth. In response to this and ensuing attacks from Te Rauparaha further fortifications were developed at Ōnawe. The pa included three defensive areas (outer wall and two citadels), creating a virtually impregnable stronghold, and it is aspects of these we can see in the landscape today. The pa defences were never truly tested, with the pa being taken by Te Rauparaha by deceit and confusion leading to massacre and the burning of the pa.

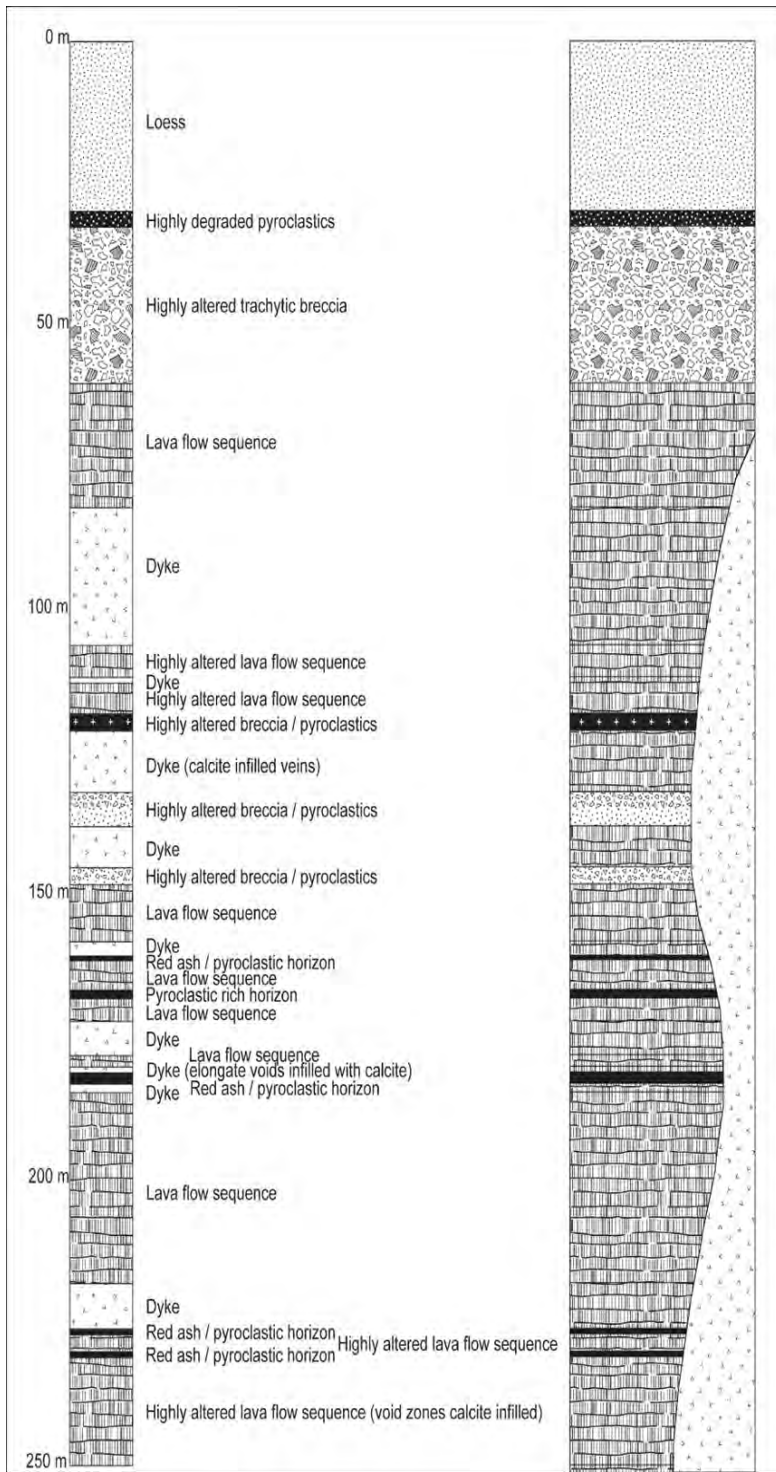


Figure 11. The summary stratigraphic facies column interpretations of the stratigraphy encountered in the Takamatua borehole (from Grande and Hampton 2019).



*Ōnawe with pa site remains draped over GoogleEarth image. Pa plan adapted from Brailsford (1981).*

### Geopark framework (Hampton 2019)

The Geopark kaupapa is one of blended elements founded on the unique geology. The Geopark will weave together knowledge of our geology, flora and fauna, archaeology, oral traditions, mātauranga Māori, heritage, communities, and conservation. On the ground the Geopark will comprise a series of Geopoints (sign posted sites of significance), which are linked together (trail, road, and sea) to form a Geosite.

Geosites of Banks Peninsula will span varying areas, allowing individual voices to tell their unique stories. This holistic framework will highlight the interconnectedness of the landscape elements, forming an educational resource that will contribute to a sustainable future for the communities of Banks Peninsula.

Initial Geosites of the Te Pātaka o Rākaihautū / Banks Peninsula Geopark will be selected on the basis that they:

- Are located on publicly accessible land, with elements of infrastructure already existing.
- Are founded on sites of geological significance.
- Cover a range of blended elements (geology, flora and fauna, archaeology, oral traditions, Mātauranga Māori, heritage and sustainability).
- Span varying areas of Banks Peninsula.

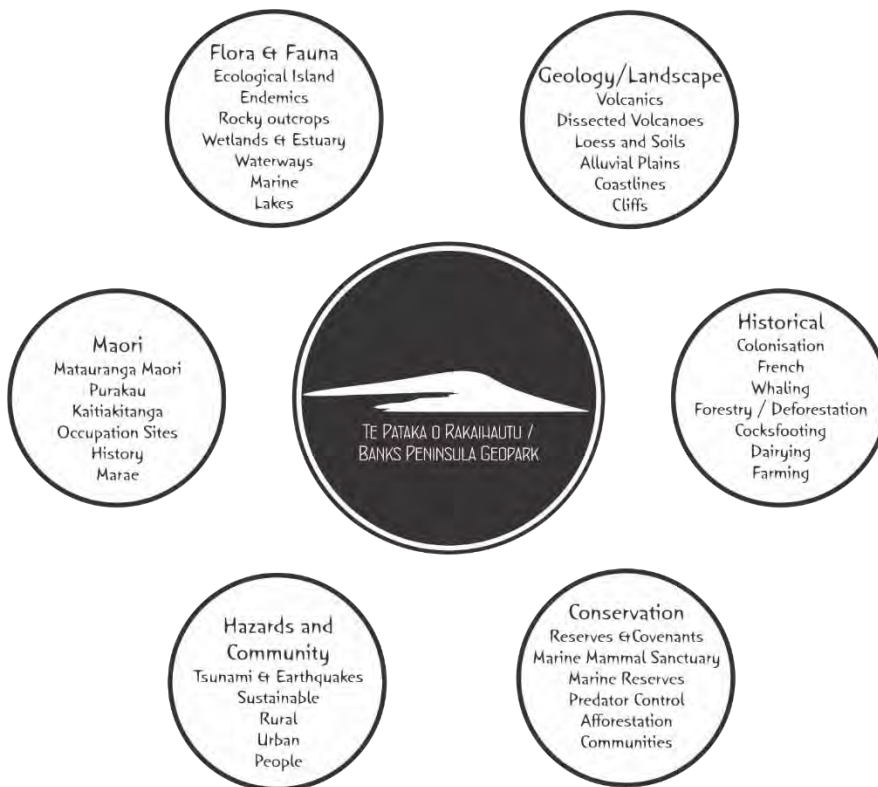


Figure 12. Holistic components within Te Pātaka o Rākaihautū / Banks Peninsula Geopark.

## Ōtepatotu Reserve

### ***Panama rock dyke and dome (Curtin, Gravley and Hampton 2012, Garvin, Albright and Gravley 2013, Gravley and Hampton and Lewis and Hampton 2016)***

Panama Rock dome is one of six trachytic domes found on the flanks of the Akaroa volcano, the other five being located at View Hill, Pulpit Rock, Ellangowan, and Devils Gap (which has 2 domes, Jr. and Sr.) (Figure 1). While these other domes are not connected to exposed feeder dikes at the surface, the example from Panama Rock and their elongate shapes parallel to the local dike trends suggest that they are similarly fed by radial dikes (Dorsey 1988). While their sharp contacts with the country rock and the lack of extrusive features such as autobreccias suggest that these domes were near-surface intrusions (Dorsey 1988), evidence from Panama Rock suggests that this specific feature may have been extruded at the surface while confined to the crater of a pre-existing scoria cone (Curtin 2012).

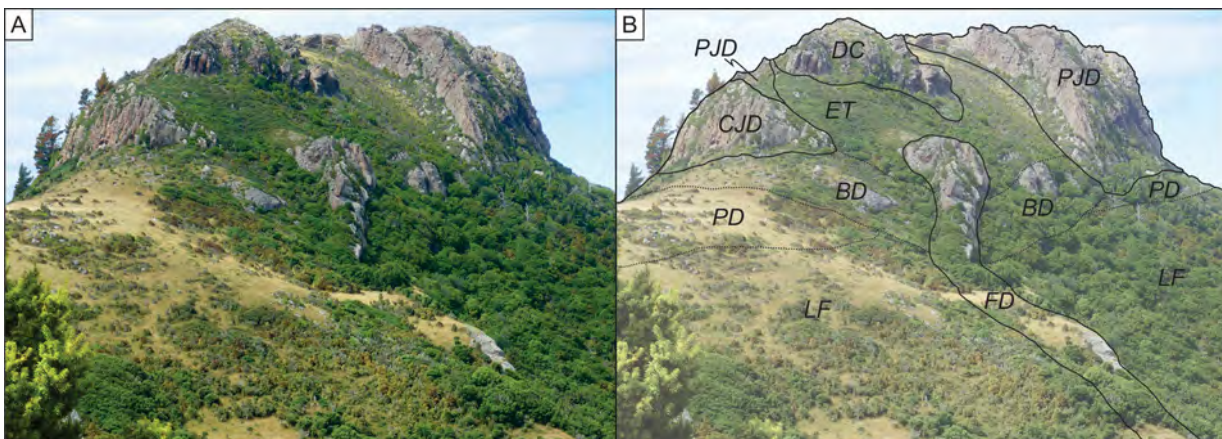


Figure 13. Panama Rock from the west showing the dike and exfoliated “onion-skin” layers of the lava dome. Near vertical columnar jointing can be seen on the northwest face, as well as a steeply sloped southern face. A) Photograph of Panama Rock. B) Annotated photograph of Panama Rock. LF, underlying lava flow sequence; FD, feeder dike propagating from west to east to the interior of the dome; PD, pyroclastic deposits; CJD, columnar jointed dome; BD, brecciated dome; PJD, platey jointed dome; DC, dome core; ET, eroded trough (from Lewis and Hampton 2016).

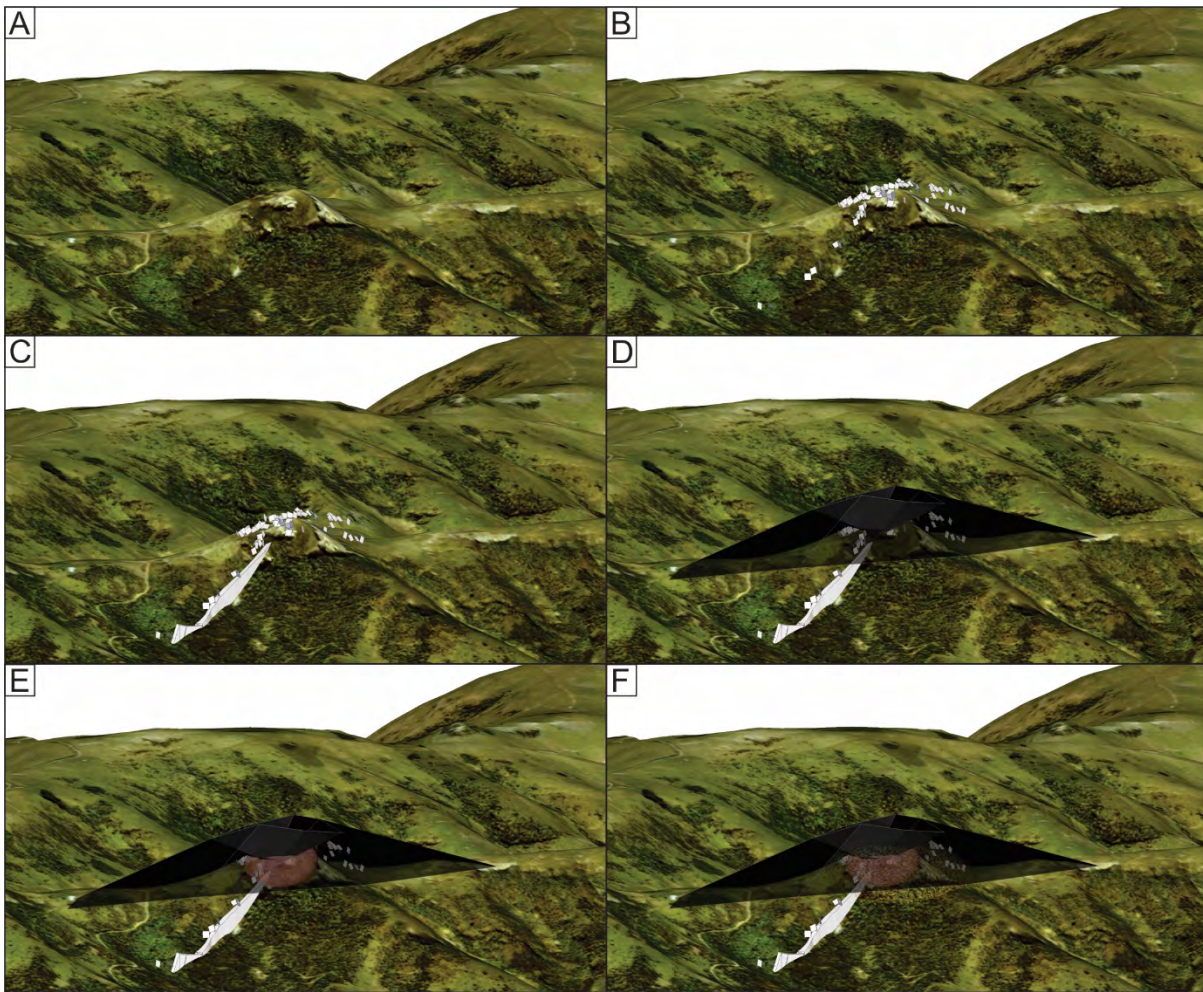


Figure 14. Geological stages of formation of Panama Rock as modelled with SketchUp. A) Current topography of the eroded Akaroa Volcanic Complex, with Panama Rock as a resistant high. B) 3D joint planes of dike and dome, the dip slope of the Akaroa Volcanic Complex is not depicted in this representation. C) Initial intrusion of basaltic dike. D) Scoria cone growth, note elongation of crater to NE and basaltic dike feeding the scoria cone system following a similar pathway as later dike. E and F) Intrusion and growth of the dome. Note in F the elongate outer dome, which underwent some rheomorphic flow, with the core of the dome as a more spherical body closely connected to the trachytic dike (from Lewis and Hampton 2016).

### ***Ridgeline eruptives (Lowden, Gravley and Hampton 2013)***

The ridgeline southwest of Panama Rock formed from a fissure system, scoria deposits and intrusive dike features, on the flanks of Akaroa Volcanic Complex. Dykes have a NE-SW orientation, and the scoria deposits include both welded and non-welded deposits with clast sizes ranging from lapilli to bombs.

The NE-SW trending structure of the dike and the non-welded scoria deposits suggest that the scoria was deposited from a Hawaiian fire fountaining fissure eruption. With the dike intruding the non-welded scoria deposits once the deposits were cool and the fissure systems pressure had lessened.

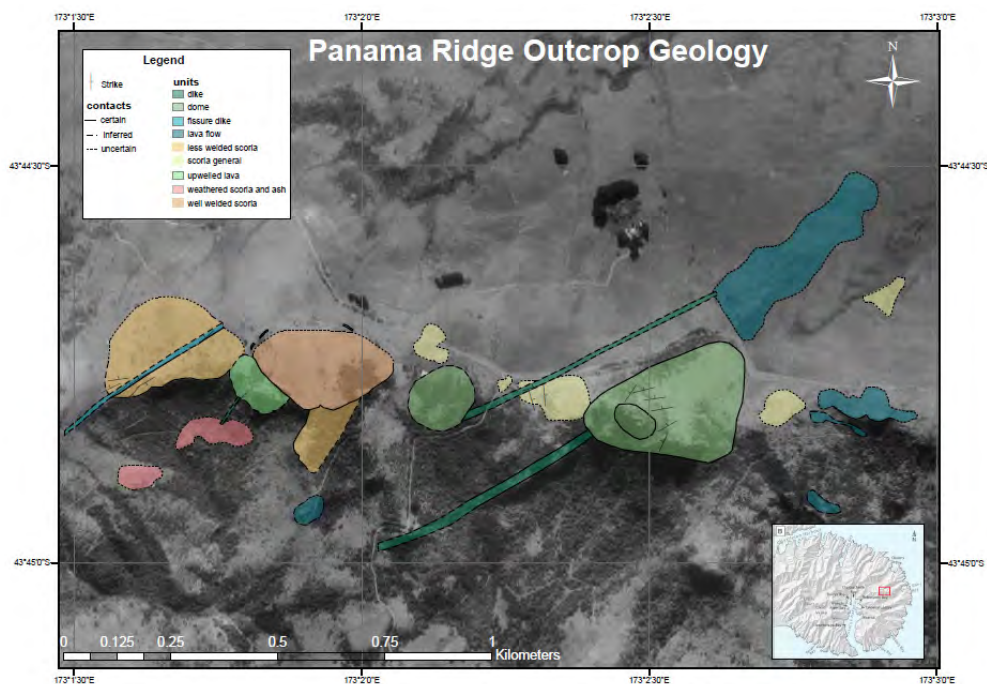


Figure 15. GIS map of Panama ridge produced by the Frontiers Abroad GIS mapping team (Lowden, Gravley and Hampton 2013).

### ***Ōtepatotu eruptive sequence (Hudziak, Hampton, and Gravley 2017)***

Ōtepatotu provides an interesting case study, as there is a progression between agglutinated material and massive to poorly bedded spatter deposits within a single unit within the remnant crater rim feature of the eroded Akaroa Volcanic Complex. The exposure rises vertically roughly 25m out of heavily vegetated terrain with the Ōtepatotu Scenic Reserve (Department of Conservation) and is a popular rock-climbing destination.

Due to the height of the cliff face, paired with the DOC status of the site, traditional observation and sampling techniques would not be possible, as removing samples from the rock face is prohibited. Different techniques had to be implemented in order to collect data in ways that would not significantly impact the rock, but would provide adequate proxies for the desired data, which would aid in identification of formation processes. Key elements recorded and measured were observation height, texture, clast shape and size, vesicularity, concentration of clasts above 5cm, and Schmidt hammer (non-invasive numerical proxy for uniaxial compressional strength (UCS)).

The character of the deposit is strongly influenced by rate of accumulation. Low accumulation rates of warm clasts such as bombs with fluid cores and viscous/ brittle rims, resulted in variously deformed clasts within a finer grained surrounding matrix. Conversely, during time of high accumulation, rates of cooling between successively impacting clasts is reduced, completely welded or even rheologic lavas can form. The largescale lack of welding throughout the bottom of the deposit and the presence of identifiable clasts indicates low accumulation rates, as clasts had sufficient time to cool preserving their shape. Above 17 m, welding is more common and identification of singular clasts is no longer possible. This is likely because material is deposited so rapidly, that clasts are unable to cool due to the subsequent deposition of more hot material, producing the welded spatter deposits observable in the upper limits of the outcrop. A direct correlation between the trends of clast size and relative abundance illustrates the relationship between the rate of cooling and accumulation rate.

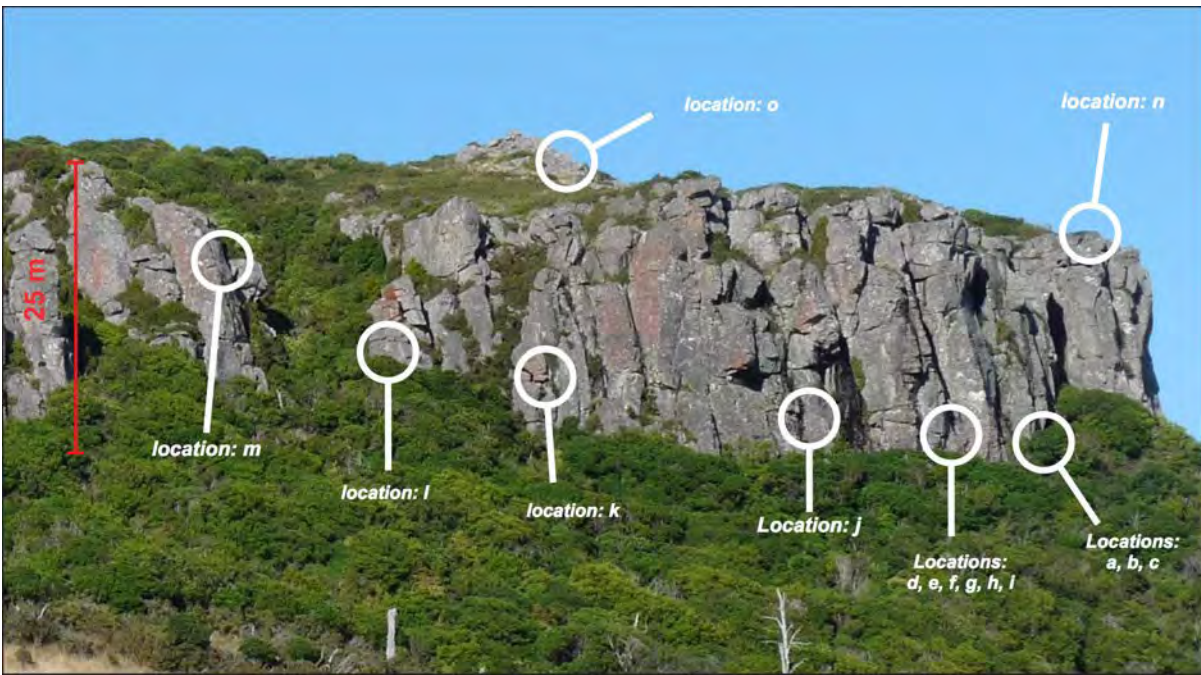


Figure 16. Photograph of the exposed cliff face at Ōtepatotu Reserve with locations of data collection denoted within white circles. Location letters correlate with letters within stratigraphic column represented (from Hudziak, Hampton, and Gravley 2017).

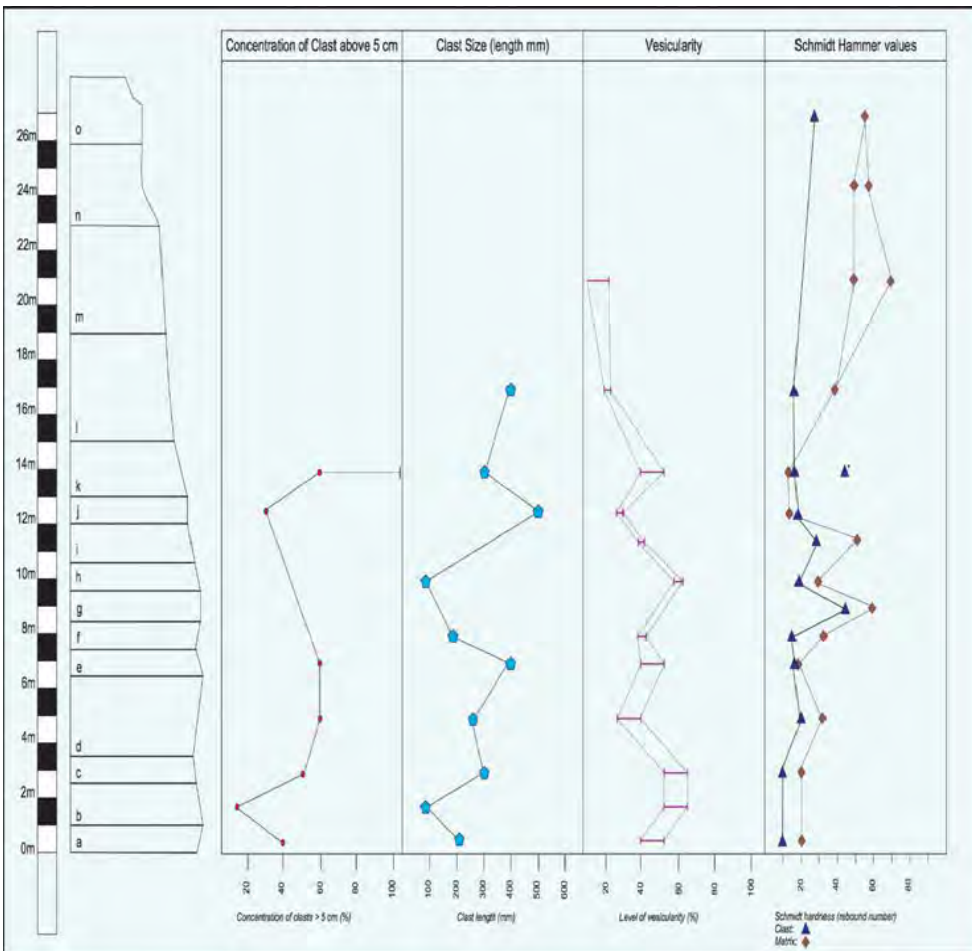


Figure 17. Visual representation and collation of data collected at the remnant crater rim feature in the eroded Akaroa Volcanic Complex, Banks Peninsula, New Zealand. Data graphed in relation to relative elevation within the lithologic column (from Hudziak, Hampton, and Gravley 2017).

## Pigeon Bay overlook

**Volcanic Benches – Quasi-planar Surfaces (Sumner and Hampton 2014, Barefoot and Hampton 2016, Worthington, Hampton and Gravley 2016, Bersson 2017, Lown and Hampton 2018, Sadowsky and Hampton, 2018, Grande and Hampton 2019)**

Volcanic geomorphic approaches may be utilized to create reconstructions and understand the growth. Quasi-planar surfaces are remnant volcanic geomorphic features preserved within the landscape, derived from original cone surfaces (Karátson et al 2016). Located throughout the degraded volcanic landscape of Banks Peninsula are planezes and quasi-planar surfaces. Unlike the QPSs of Karátson et al (2010), these QPSs are gently sloping planes, descending in elevation from the central eruptive regions, in both the eroded inner harbour and within the incised valleys and bays. These slopes are semi-continuous, due to lateral gully incision. We term these QPSs, “benches”, because the cross-sectional profile of these features are similar to quarry bench cuts.

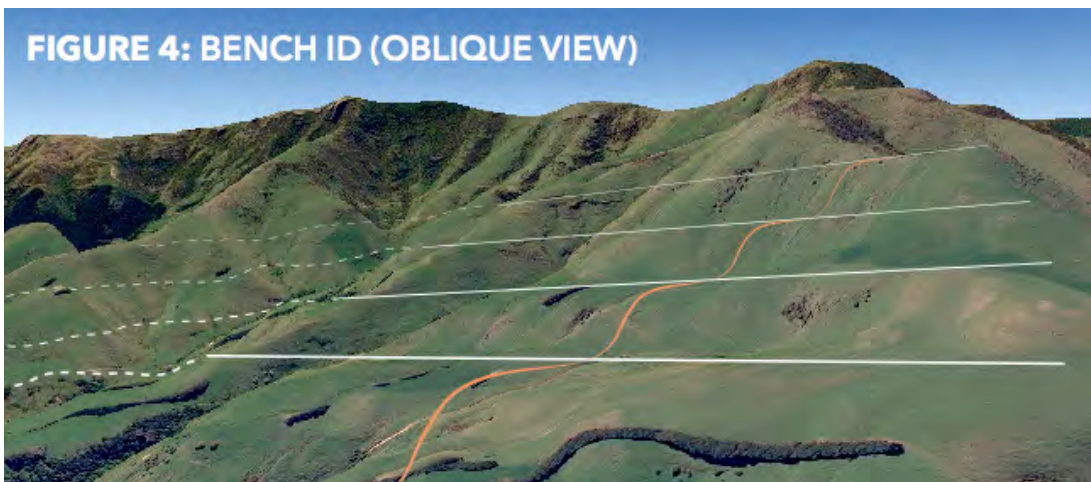


Figure 18. Oblique, Google Earth Pro, view of Bench Identification techniques based on erosional ridge/ valley side. Orange line indicates the section cut of the view. Dotted lines are an estimated projection based on inherent lava flow dip (from Worthington, Hampton and Gravley 2016).

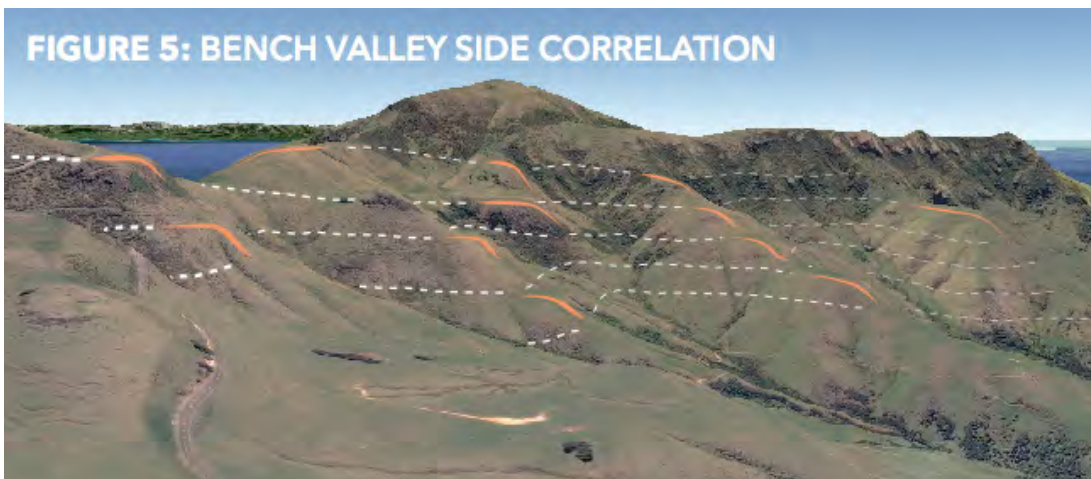


Figure 19. View of valleys side correlation methods in Google Earth Pro. Orange lines represent identified bench segments using methods from Figure 2 and Figure 4. Dotted white lines correlate these distinct segments via a projection of the inherent lava flow dip angle (from Worthington, Hampton and Gravley 2016).

### **Formation of volcanic benches (Lown, Gravley, Hampton and Villeneuve 2018)**

The eastern side of Pigeon Bay located on Banks Peninsula displays volcanic “benches” which appear to be preferentially eroded, flatter stepped-out sections of hillside that display a distinct break in slope



### **Volcanic sectors (Hobbs, Hampton, and Gravley 2012)**

Remote analysis of DTM models of both active and ancient volcanic edifices has proven useful for extrapolating past structures from imagery of current structures at a number of volcanoes (Székely & Karátson, 2004), including the adjacent Lyttelton volcano (Hampton & Cole, 2009). For long extinct cones in particular, these techniques are highly useful for identifying radial patterns of topographic (ridge and valley) and volcanic (dyke, lava flow, cone sectors) structures that are hypabyssal, constructional, and erosional in origin. Akaroa is known to host similar topographic and volcanic features which are used in this paper to evaluate patterns identify volcanic summits, eruptive centres, and secondary cone sectors.

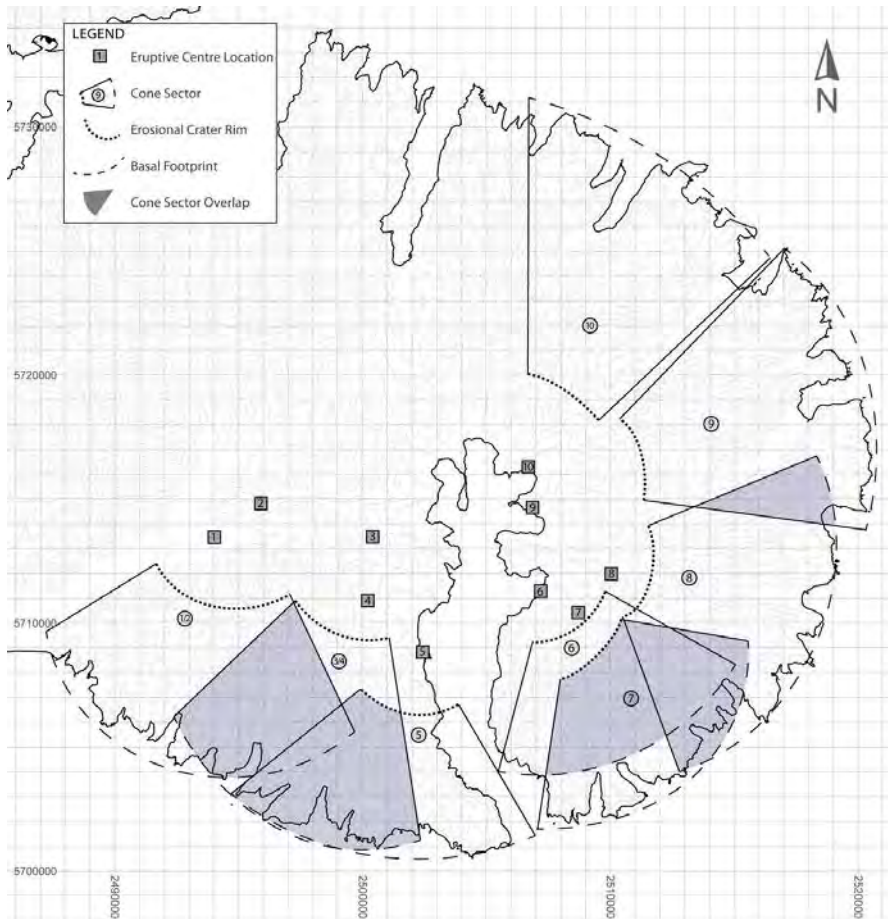


Figure 22. Cone sectors of each eruptive centre. Cones 1/2 and 3/4 represent cones for two eruptive centres (from Hobbs, Hampton and Gravley 2012).

### ***Volcanic benches as reconstruction features (Bersson and Hampton 2017)***

Using Digital Elevation Model (DEM) data, this study provides a new perspective on lava benches as markers of paleo-topography of the AVC. The methods of projection and reconstruction used were largely modelled after the methodology used by Karátson et al. (2016) in their reconstruction of paleovolcanoes on Gran Canaria, Canary Islands using quasi-planar surfaces (QPS) and planezes as topographic markers. Research was conducted in three phases: Extraction and Analysis, Classification and Interpretation of topographic markers, and reconstruction of the paleo topography using lava bench projections.

Projected lava benches create a cross-sectional view illustration of the effusive growth stages of the Akaroa Volcanic Complex. Each lava bench projection represents the surface of a volcanic growth formation. These volcanic growth formations represent at least one distinct period of effusive activity, with the top volcanic growth formation being the youngest stage of growth. The top volcanic bench projection is the most valuable for volcanic reconstruction, as it signifies the youngest, highest paleo-topography.

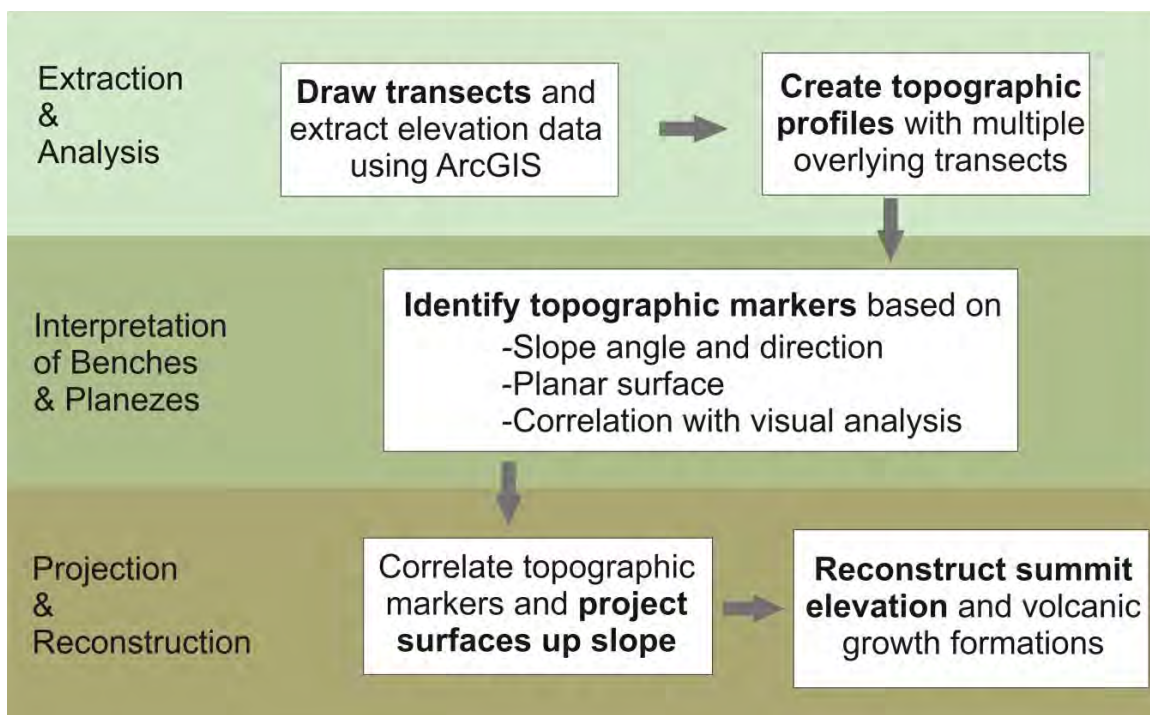


Figure 23. Flow chart detailing the progression of methods used in reconstruction (from Bersson and Hampton 2017).

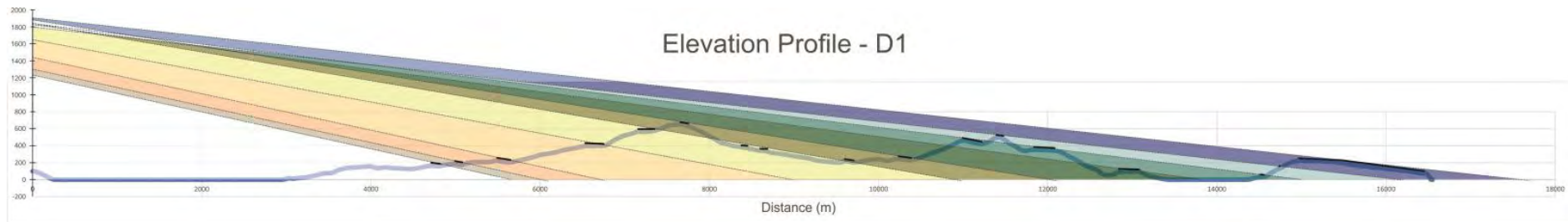


Figure 24. Each coloured section represent a constructive phase. Volcanic growth formations, separated by lava bench projections, represent effusive periods of volcanic growth. Each volcanic growth formation may be composed of multiple periods of effusive activity. The top volcanic growth formation represents the youngest growth of Akaroa (from Bersson and Hampton 2017).

### Early eruptives reconstructions (Grande and Hampton 2019)

The initiating / early stages of Akaroa's volcanic growth can be examined through mapping and analysis of quasi-planar surfaces evident within the inner harbour area. GoogleEarthPro provided a platform in which one can identify features, map, and gain perspectives that have not been readily available. It also provides a stable platform for 3d representations, data projections and analysis GoogleEarthPro was used as a base mapping tool, supporting field observations and photograph analysis. Quasi-planar surfaces were mapped, and correlated using heights, projections, and cross valley relationships. Correlated quasi-planar surfaces were then used to create topographic spot heights from which wireframe models / cone projections could be established and rendered in GoogleEarthPro. Analysis indicates that early eruptions initiated in the upper harbour with progressive cone over-growth occurred with subtle down harbour vent shifts.



Figure 25. Robinson's Bay Cone, and Takamatua Peninsula Cone projected contour intervals and lines (from Grande and Hampton 2019).

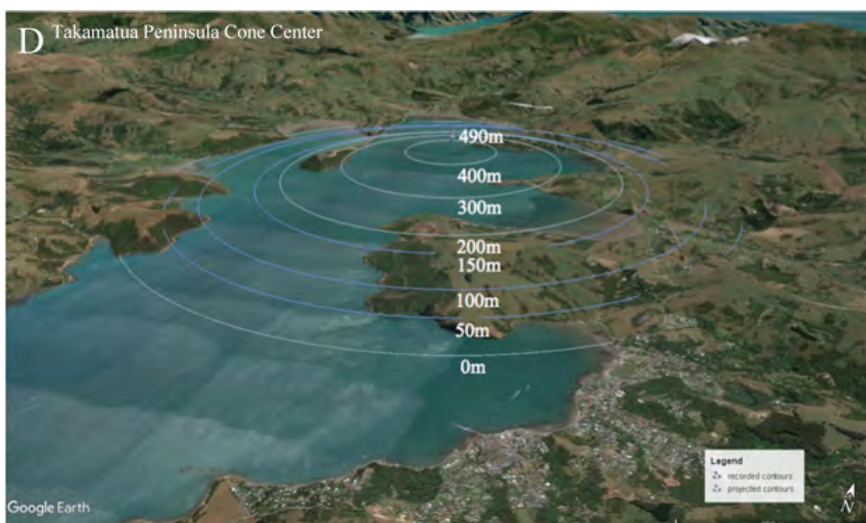


Figure 26. Reconstructed three dimensional models of Robinson's Bay Cone and Takamatua Peninsula Cone on GoogleEarthPro (from Grande and Hampton 2019).

### ***Current magmatic and volcanic schematic model***

Bertolett (2019) has provided the most recent rendering of the magmatic and volcanic systems of the Akaroa Volcanic Complex, incorporating aspects from the decade of Frontiers Abroad Aotearoa research projects. This model incorporates the development of the Akaroa as a series of overlapping cone growth phases punctuated by repeated cyclic volcanic activity record in lava flows. Buried flank eruptives and eroded bench surfaces (QPS') provide evidence of past flank topography. While the spatial distribution and stratigraphic relationship and burial of trachytic domes link to episodic trachytic intrusions within an associated period of cone growth.

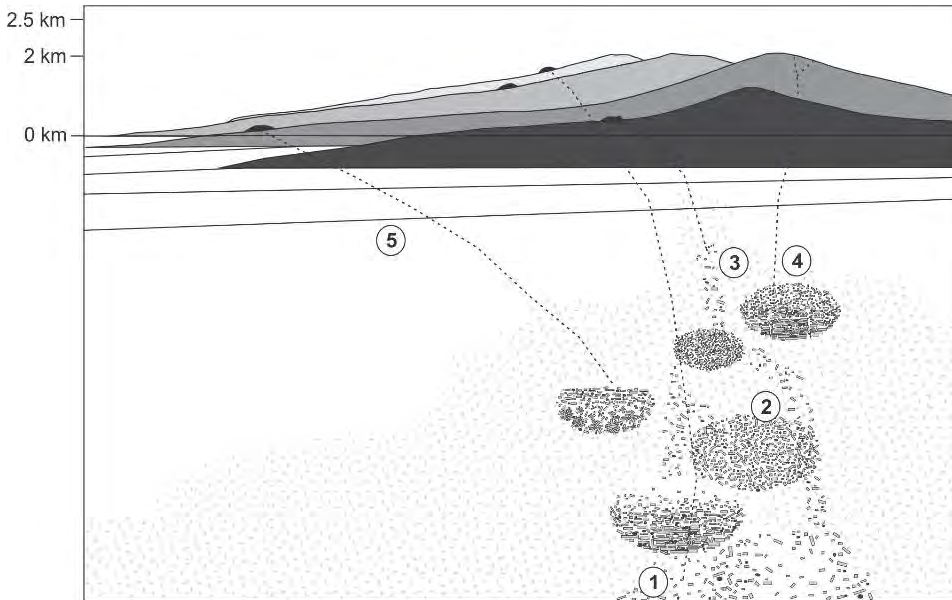


Figure 27. Bertolett (2019) schematic of progressive cone-building and magmatic structure of the AVC. Multi-staged cone building represented by greyscale cones, underlying sedimentary units that source some of the Pa Bay non crystalline lithics highlighted by shallowing dipping lines. Basement and magmatic system represented by grey ticks. Idealized mush-bodies in varying stages of crystallization, settling, compaction, etc. and their pathways represented by dotted lines. Number 1-5 designate the possible host-lithic relationships identified in this study and their relationship to the volcanic stratigraphy.

## Gebbies Pass and Kaitangita/Mansona Peninsula

### ***Gebbies Pass***

The oldest rocks of Banks Peninsula are exposed in the area of Gebbies Pass.

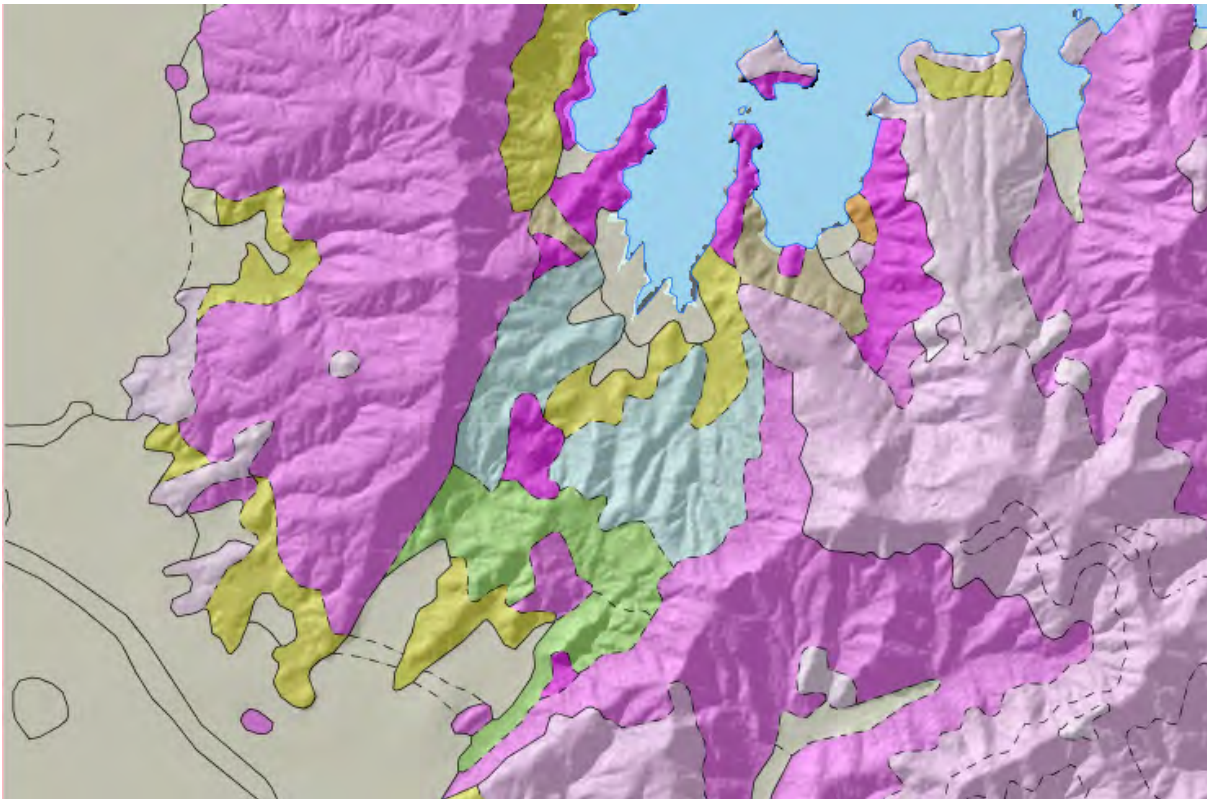


Figure 28. Geologic units exposed in Gebbies Pass. Light blue = ~250 Ma Torlesse Supergroup. Light green = ~98 Ma Gebbies Rhyolite (Mount Somers Volcanics Group). Light brown = ~65 Ma Charteris Bay Sandstone (Eyre Group). Purple = 11–9.7 Ma Lyttelton Volcanic Group. (from <https://data.gns.cri.nz/geology/>)

### ***Kaitangita / Mansons Peninsula Arc StoryMap***

Kaitangita is a predominantly pre-Lyttelton Volcanics rhyolitic peninsula. It is comprised of interbedded tuffs and breccias, domes and crosscutting dykes.

StoryMaps are a platform to virtually explore an area. This StoryMap explores the geologic history of Kaitangata/Mansons Peninsula, which is not publicly accessible due to private ownership.

<https://arcg.is/1TzzXP>

## References\*

\*References are not inclusive of Frontiers Abroad Aotearoa / Geol 356 Independent Research Projects.

- Bertolett, E. (2019). Understanding the Akaroa Magmatic System: a multi-method approach to erupted plutonic lithics. Unpublished PhD thesis. University of Canterbury.
- Brailsford, B. (1981). *The Tattooed Land: The Southern Frontiers of the Pa Maori*. Wellington, N.Z.: Reed.
- Giacomoni, P.P., Ferlito, C., Coltorti, M., Bonadiman, C., Lanzafame, G. (2014). Plagioclase as archive of magma ascent dynamics on “open conduit” volcanoes: The 2001–2006 eruptive period at Mt. Etna. *Earth-Science Reviews* 138: 371–393
- Hampton, S.J., Cole, J.W. (2009). Lyttelton Volcano, Banks Peninsula, New Zealand: Primary volcanic landforms and eruptive centre identification. *Geomorphology* 104(3–4): 284–298. <https://doi.org/10.1016/j.geomorph.2008.09.005>
- Karátson, D, Telbisz, T, Singer, B.S. (2010). Late-stage volcano geomorphic evolution of the Pleistocene San Francisco Mountain, Arizona (USA), based on high-resolution DEM analysis and  $^{40}\text{Ar}/^{39}\text{Ar}$  chronology. *Bulletin of Volcanology* 72: 833–846.
- Karátson, D., Yepes, J., Rodríguez-Peces, M., Fornaciai, A. (2016). Reconstructing eroded paleovolcanoes on Gran Canaria, Canary Islands, using advanced geomorphometry. *Geomorphology* 253: 123–134.
- Lewis, G.M., Hampton, S.J. (2015). Visualizing volcanic processes in SketchUp: An integrated geo-education tool. *Computers & Geosciences* 81: 93–100.
- Renjith, M.L. (2014). Micro-textures in plagioclase from 1994–1995 eruption, Barren Island Volcano: Evidence of dynamic magma plumbing system in the Andaman subduction zone. *Geoscience Frontiers*, 5(1): 113–126.
- Sewell, R.J. (1988). Late Miocene volcanic stratigraphy of central Banks Peninsula, Canterbury, New Zealand; *New Zealand Journal of Geology and Geophysics* 31: 41–64.
- Sewell, R.J., Reay, M.B., and Weaver, S.D. (1992). *Geology of Banks Peninsula*. Institute of Geological & Nuclear Sciences 1:100,000 geological map 3. Institute of Geological & Nuclear Sciences, Lower Hutt, New Zealand.
- Timm, C., Hoernle, K., Van Den Bogaard, P., Bindeman, I., Weaver, S.D. (2009). Geochemical evolution of intraplate volcanism at Banks Peninsula, New Zealand: Interaction between asthenospheric and lithospheric melts. *Journal of Petrology* 50(6): 989–1023. doi: 10.1093/petrology/egp029.
- Viccaro, M., Giacomoni, P.P., Ferlito, C., Cristofolini, R. (2010). Dynamics of magma supply at Mt. Etna volcano (Southern Italy) as revealed by textural and compositional features of plagioclase phenocrysts. *Lithos* 116(1): 77–91
- Weaver, S.D., Sewell, R.J., Dorsey, C. (1985). *Extinct volcanoes: a guide to the geology of Banks Peninsula*. Geological Society of New Zealand Guidebook 7. Geological Society of New Zealand, Lower Hutt. 48 p.

# FIELD TRIP 6: A WALKING TOUR OF CHRISTCHURCH CBD REBUILD

Thursday 26 November 2021

Leaders: Clark Fenton and Brandy Alger, University of Canterbury



## Introduction

To many the Garden City is defined by the 2010–2011 Canterbury earthquake sequence (CES). Images of crumbling masonry, vast swaths of suburban land inundated by liquefaction ejecta, the labours of the Student Volunteer Army, and the collapsed gable of the spire-less Christ Church Cathedral are images conjured up by many when they think of Ōtautahi (Figure 1). A decade on from the start of the CES this tour is an opportunity to highlight the new face of the City and reflect on the scientific and engineering advances that have resulted from these events. Christchurch has grown from earthquake-induced adversity to be the most seismically-resilient city in New Zealand through the implementation of the latest, often Kiwi-developed, structural and geotechnical engineering solutions.



Figure 1. Visions of Christchurch!

## Near-Surface Geology

The Christchurch urban area lies on the coastal periphery of the Canterbury Plains. The plains are a series of coalescing alluvial fans and braid plains deposited by east-flowing rivers draining the Southern Alps. These rivers, fed by meltwater during Pleistocene glacial cycles, prograded eastward, beyond the current shoreline. In the postglacial period, the shoreline has fluctuated, with a general westward marine transgression, to reach its current location. The resulting ground profile is a series of inter-fingering coarser alluvial and finer marine sequences. Christchurch is located on an area that was originally predominantly coastal swamp, lying behind a series of coast-parallel beach dunes. The spring-fed Heathcote and Avon rivers drain the area of the city and its immediate surroundings through the Avon-Heathcote estuary. The landscape of the City and its immediate surroundings has been subject to considerable change due to drainage and infilling of channels and hollows since the establishment of the Pākehā settlement in the 1850s (Figure 2).

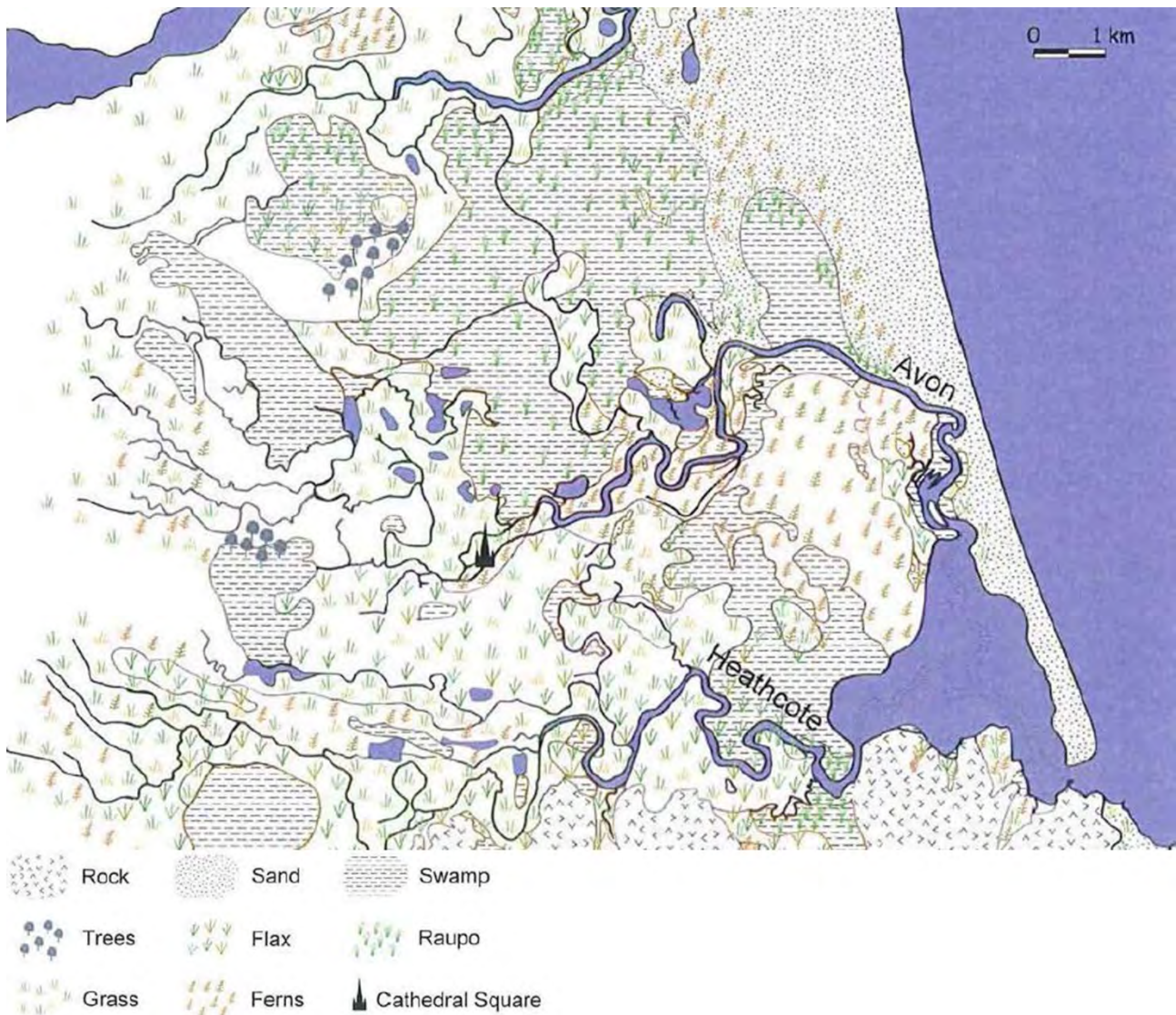


Figure 2. Waterways, wetlands and vegetation cover in and around Christchurch in 1856 (CCC, 2003)

The near-surface geology of Christchurch is dominated by the Springston Formation in the west and the Christchurch Formation in the east (Figure 3). The latter grades in to the Pegasus Bay Formation in the offshore. The Christchurch Formation is a sequence of beach, estuarine, lagoon, dune and coastal swamp deposits. This extends as far inland as Riccarton and Fendalton. The most recent deposits are dominated by dunes and inter-dune swamps. Further west the predominantly fine-grained Christchurch formation inter-fingers with the alluvial gravels, sands and silts of the Springston Formation.

### The 2010-2011 Canterbury Earthquake Sequence (CES)

The 2010–2011 Canterbury earthquake sequence (Figure 4) started with the 4th September 2010 M7.1 Darfield earthquake (e.g., Gledhill et al., 2011). This event and three subsequent earthquakes of  $M \geq 5.9$ , caused widespread damage across Ōtautahi. Most damaging was the 22nd February 2011 M6.2 Christchurch earthquake (e.g., Kaiser et al., 2012) that resulted in 185 fatalities. All of these earthquakes occurred on previously unrecognised faults.

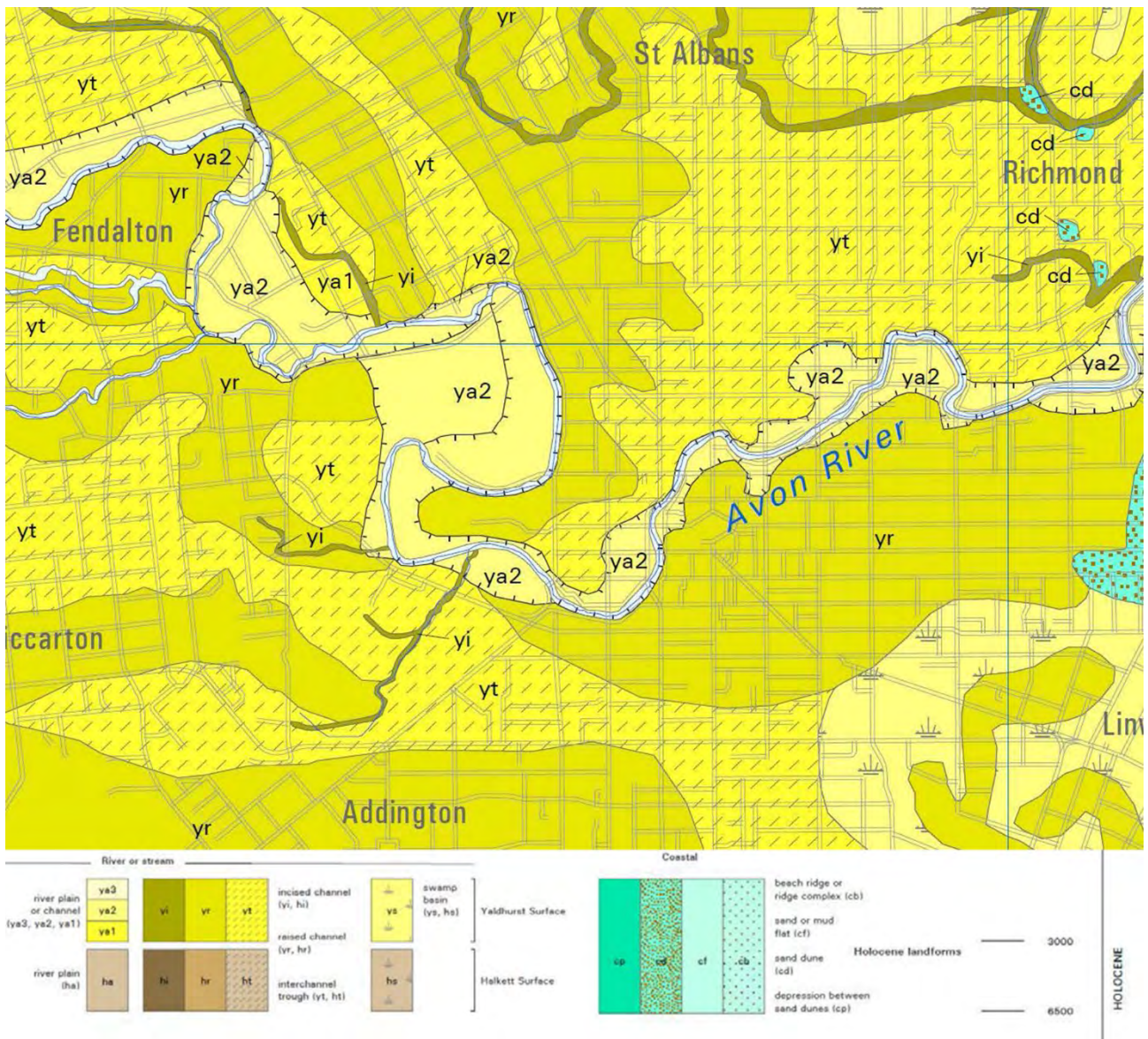


Figure 3. Geological map of central Christchurch (Begg et al., 2015).

The initial 2010 Darfield earthquake was the only event involving surface rupture. This caused significant damage to agricultural land, structures and lifelines. (e.g., Van Dissen et al., 2011). Ground shaking in the Darfield earthquake resulted in widespread liquefaction in eastern Christchurch and in isolated areas throughout the region (Cubrinovski et al., 2011b). Building damage was mostly limited to unreinforced masonry structures (Dizhur et al., 2010).

The 22<sup>nd</sup> February 2011 M6.2 Christchurch earthquake caused major damage to commercial and residential buildings of various ages and construction styles (Buchanan et al., 2011; Clifton et al., 2011; Kam et al. 2011). The collapse of two buildings, the CTV and Pyne Gould buildings in the CBD, resulted in 133 of the 185 fatalities during this earthquake. The widespread liquefaction across the City was the main cause of damage to residential houses, bridges, and underground lifelines (Cubrinovski et al., 2011a). Rockfall and cliff collapse occurred in many parts of the Port Hills on the southern side of the City (Massey et al., 2014). The 13<sup>th</sup> June 2011 M6.0 earthquake caused further damage to previously damaged buildings and triggered further liquefaction and rockfall.

M5.8 and M5.9 earthquakes on 23<sup>rd</sup> December 2011 triggered further liquefaction across the City and rockfall activity in the Port Hills. Several smaller aftershocks also caused localized liquefaction (e.g., Quigley et al., 2013) and limited rockfall, and building damage.

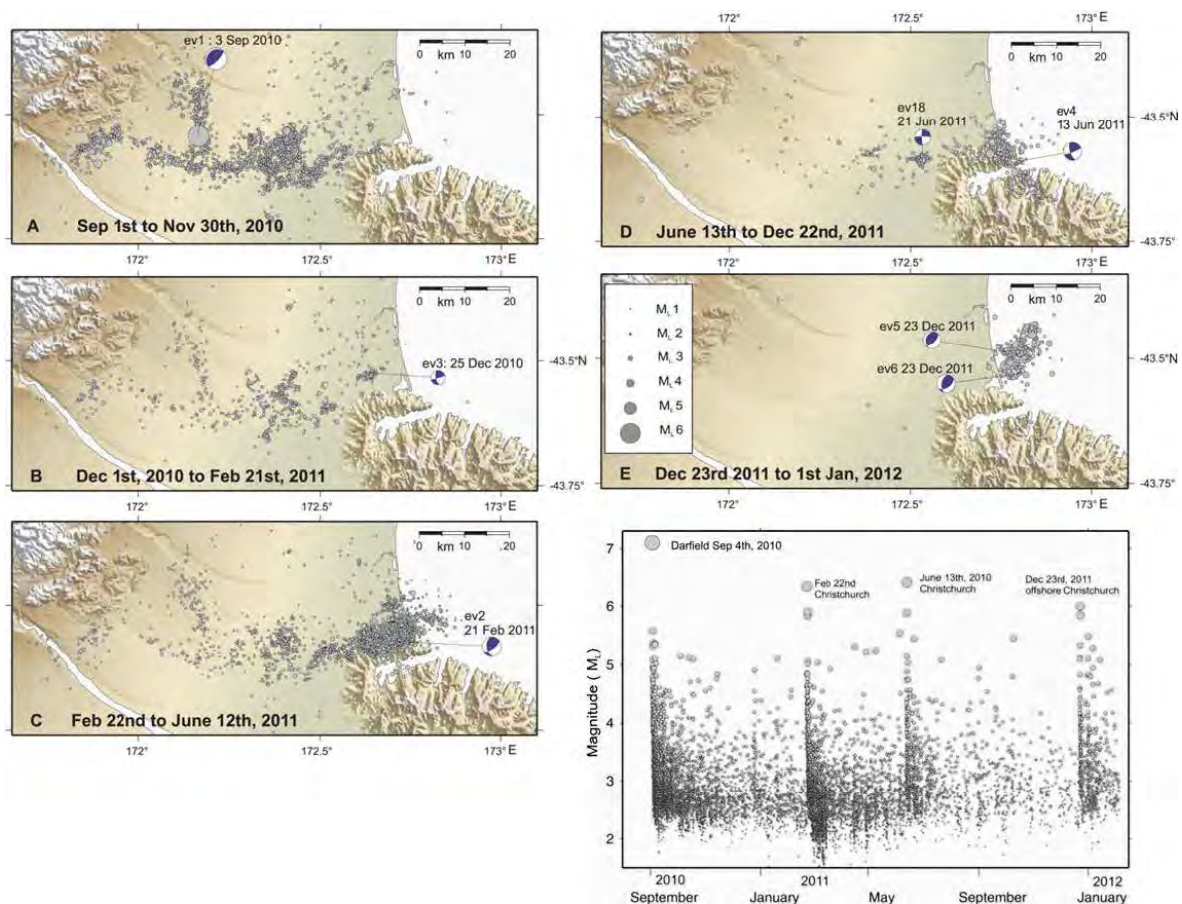


Figure 4. The 2010–2011 Canterbury Earthquake Sequence. Starting with the 4<sup>th</sup> September 2010 Darfield earthquake, the locus of activity has moved progressively eastward.

## Tectonic Setting

In the central part of the South Island oblique continental convergence of  $38 \text{ mmyr}^{-1}$  is accommodated between the Pacific and Australian plates (DeMets et al., 2010). The Alpine Fault, located about 140 km to the west of Christchurch accommodates as much as three-quarters of the total plate motion. In the northern South Island, plate motion is largely taken up by the strike-slip faults of the Marlborough Fault System (MFS). The zone of active plate boundary deformation has widened eastwards into the Canterbury Plains during the Quaternary (Forsyth et al., 2008). The strain rate across this region corresponds to about  $2 \text{ mmyr}^{-1}$ . Although active faults have been mapped in the foothills of the Southern Alps to the west of the Canterbury Plains. The thick cover of recent alluvium across the Plains has obscured evidence of (low slip-rate) active tectonic structures. Prior to the CES active tectonic structures in the immediate vicinity of Christchurch were largely unknown.

## Historical Seismicity

Despite the Canterbury region's relatively low seismicity levels prior to the CES, several historical events have generated low-to-moderate ground shaking in Christchurch. Magnitude (M) 6–7 earthquakes have occurred in the Southern Alps and in the foothills to the west and north of the region in the past 150 years. The 1888 M7.1 North Canterbury, 1901 M6.9 Cheviot, 1929 M7.0 Arthur's Pass, 1944 M6.7 Arthur's Pass and 1995 M6.2 Cass earthquakes have been felt across the region (e.g., Pettinga et al., 2001). Moderate-sized events have also occurred in the Christchurch region, most notably a shallow earthquake in 1869 c. 10

km from Christchurch city centre and an event further south in 1870 located near Lake Ellesmere. Both of these events occurred on unknown (buried) faults and produced shaking of intensity MM VII in Christchurch (Pettinga et al. 2001).

It should be noted that the 1888 North Canterbury earthquake toppled the upper 8 m of Christ Church Cathedral spire. This was further damaged in the 1901 Cheviot earthquake. Along with the toppling of a number of stone crosses during the 1922 M6.4 Motunau earthquake, the old cathedral has not had a happy seismic history!

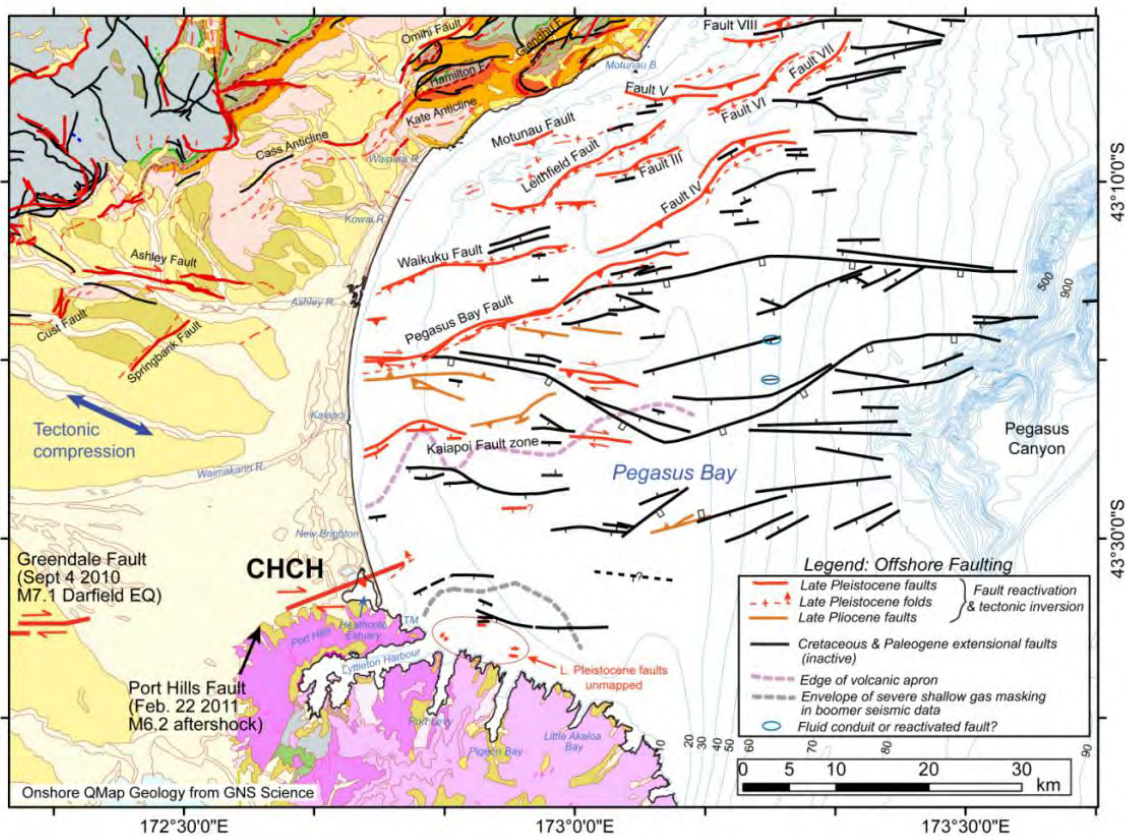


Figure 5. Recently recognised active seismic sources in the Christchurch region (Barnes et al., 2016).

## Seismic Sources

Tectonic and seismological evidence indicates that the CES is a relatively rare cluster of activity for this region characterised by long recurrence intervals. The 2010 Darfield earthquake rupture was complex, occurring on intersecting and subsidiary blind thrust faults as well as the dominant east–west strike-slip Greendale Fault (Beavan et al., 2010). Faults in the foothills of the Southern Alps generally strike northeast–southwest, representative of the current stress field, whereas older Early Cretaceous faults found offshore are oriented east–west (Barnes et al., 2016). The orientation of the Greendale Fault and other faults in Canterbury has suggested that the recent earthquakes may have occurred on reactivated east–west-trending Cretaceous faults (Figure 5). The extinct basaltic shield volcano of Banks Peninsula south of Christchurch may have also played a role in concentrating the stress field following the Darfield earthquake (Reyners, 2011).

## Ground Motions

The largest ground motions in central Christchurch occurred during the 22<sup>nd</sup> February 2011 Christchurch earthquake (Table 1), primarily as a result of its close proximity to the earthquake source. Severe ground motions were recorded at numerous strong motion stations over the multiple events of the CES. Peak ground accelerations (PGAs) of up to 1.41 g (horizontal) and 2.21 g (vertical) were recorded at Heathcote Valley School on the south side of the City. In the central City PGA values ranging from 0.37–0.52 g were recorded during the 22<sup>nd</sup> February 2011 earthquake.

Table 1. Strong ground motions recorded across Christchurch during the four largest earthquakes in the CES (from Bradley et al., 2014).

Station name	Code	Site class <sup>1</sup>	4 September 2010 M <sub>w</sub> 7.1 <sup>5</sup>			22 February 2011 M <sub>w</sub> 6.2 <sup>5</sup>			13 June 2011 M <sub>w</sub> 6.0 <sup>5</sup>			23 December 2011 M <sub>w</sub> 5.9 <sup>5</sup>		
			R <sub>rup</sub> <sup>2</sup> (km)	PGA <sup>3</sup> (g)	PGV <sup>4</sup> (cm/s)	R <sub>rup</sub> <sup>2</sup> (km)	PGA <sup>3</sup> (g)	PGV <sup>4</sup> (cm/s)	R <sub>rup</sub> <sup>2</sup> (km)	PGA <sup>3</sup> (g)	PGV <sup>4</sup> (cm/s)	R <sub>rup</sub> <sup>2</sup> (km)	PGA <sup>3</sup> (g)	PGV <sup>4</sup> (cm/s)
Canterbury Aeroclub	CACS	D	11.7	0.20	39.2	12.8	0.21	20.0	16.2	0.14	9.7	16.7	0.08	9.8
Christchurch Botanic Gardens	CBGS	D	14.4	0.16	36.2	4.7	0.50	46.3	7.6	0.16	26.0	10.2	0.21	22.4
Christchurch Cathedral College	CCCC	D	16.2	0.22	53.8	2.8	0.43	56.3	–	–	–	8.7	0.18	22.3
Christchurch Hospital	CHHC	D	14.7	0.17	38.3	3.8	0.37	50.9	6.8	0.22	31.6	10.0	0.22	21.0
Cashmere High School	CMHS	D	14.0	0.24	31.3	1.4	0.37	44.4	7.1	0.18	28.4	12.0	0.17	19.2
Hulverstone Dr Pumping Station	HPSC	E	21.7	0.15	39.3	3.9	0.22	36.7	5.5	0.26	34.7	3.2	0.26	41.5
Heathcote Valley School	HVSC	C	20.8	0.61	28.8	4.0	1.41	81.4	3.6	0.91	55.3	9.7	0.44	22.3
Kaipoi North School	KPOC	E	27.6	0.34	35.7	17.4	0.20	18.9	19.4	0.10	11.2	–	–	–
Lincon School	LINC	D	5.9	0.44	74.4	13.6	0.12	12.7	21.0	0.06	12.1	25.9	0.07	6.5
Lyttelton Port	LPCC	B	22.1	0.29	19.1	7.1	0.92	45.6	5.8	0.64	32.6	12.4	0.44	22.8
New Brighton Library	NBLC	D	–	–	–	–	–	–	4.1	0.21	36.8	–	–	–
North New Brighton School	NNBS	E	23.1	0.21	35.6	3.8	0.67	35.1	5.6	0.20	31.8	–	–	–
Papanui High School	PPHS	D	15.3	0.22	54.8	8.6	0.21	36.7	10.4	0.12	19.3	10.5	0.14	18.6
Pages Rd Pumping Station	PRPC	E	19.3	0.21	44.9	2.5	0.63	72.8	3.7	0.34	60.3	–	–	–
Christchurch Resthaven	REHS	D	15.8	0.25	42.6	4.7	0.52	65.4	6.8	0.26	42.5	8.8	0.25	43.8
Riccarton High School	RHSC	D	10.0	0.21	39.3	6.5	0.28	29.8	11.8	0.19	17.6	14.6	0.16	16.9
Rolleston School	ROLC	D	2.2	0.34	73.7	19.6	0.18	8.4	26.8	0.05	5.7	30.6	0.06	3.6
Shirley Library	SHLC	D	18.6	0.18	43.0	5.1	0.33	67.8	6.3	0.18	34.5	6.1	0.28	24.0
Styx Mill Transfer Station	SMTC	D	17.5	0.18	36.1	10.8	0.16	27.6	12.0	0.08	13.0	10.4	0.15	13.0
Templeton School	TPLC	D	3.0	0.27	55.6	12.5	0.11	11.3	19.1	0.06	7.8	22.2	0.08	5.2

<sup>1</sup> As defined by the New Zealand Loadings Standard, NZS1170.5 (2004), that is, B = rock, C = shallow soil, D = deep or soft soil, and E = very soft soil.

<sup>2</sup> Closest distance from fault plane to site based on Beavan et al. (2010, 2011, 2012).

<sup>3</sup> Peak ground acceleration.

<sup>4</sup> Peak ground velocity.

<sup>5</sup> Moment magnitudes from GeoNet (<http://www.geonet.org.nz/>), the corresponding USGS estimates for these events are: 7.0, 6.1, 5.9, 5.9 (<http://earthquake.usgs.gov/earthquakes/>). Ground motion parameters are geometric mean horizontal definition.

## Building Damage

Many buildings were severely damaged during the September 2010 and February 2011 earthquakes, predominantly unreinforced masonry buildings. Many of these structures were damaged by ground shaking as well as ground deformation, including liquefaction-induced ground deformation causing differential settlement and tilting. A variety of buildings and infrastructure were affected, including residential housing, health care and schooling facilities, the central business district, iconic landmarks and heritage buildings. The greatest impact was in the east of the city (Figure 6) where liquefaction-induced ground deformation was greatest (Figure 7).

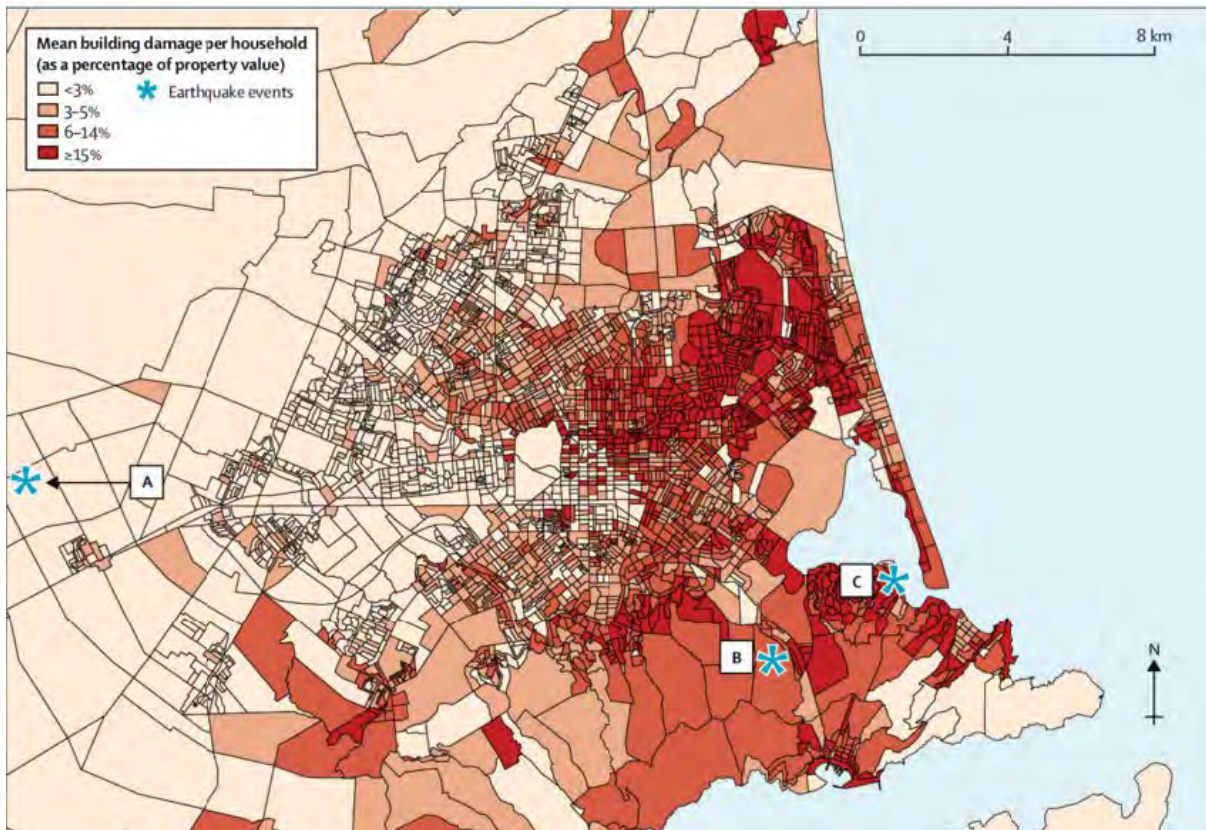


Figure 6. Earthquake damage from the Canterbury earthquake sequence. Map shows mean assessed-damage costs per household as a proportion of property value. Stars indicate the three most damaging earthquake events in the first year of the Canterbury earthquake sequence: (A) September 4<sup>th</sup>, 2010 M7.1 (centred off the map in Darfield, 40 km west of Christchurch); (B) February 22<sup>nd</sup>, 2011 M6.3; and (C) June 13<sup>th</sup>, 2011 M6.3 (from Teng et al., 2017).

New Zealand not only has stringent building codes, but they are also enforced (unfortunately this is not the case in all seismically-active regions). However, Christchurch had many old buildings which predate these regulations. The original building codes date back to 1935, but earthquake design really only started in 1965. The codes were further strengthened in 1976 with the concept of ‘controlled failure’, and strengthened again in 1984 and 1992. The codes focus on the standards that have to be met, rather than specifying precise building procedures. This is to encourage new and innovative building methods that can meet the required standards.

The lessons from the M7.1 ‘dress rehearsal’ on 4<sup>th</sup> September 2010 were straightforward: old houses and commercial buildings constructed in the early 20<sup>th</sup> century, or in some cases in the 19<sup>th</sup> century, which relied on single or double brick for their structural integrity, performed poorly. More modern houses, with concrete slab-on-grade foundations in areas suffering liquefaction, were often subject to cracking of the slab and/or excessive tilting due to differential settling or lateral spreading.

The damage in the CBD in the 22<sup>nd</sup> February earthquake includes modern buildings built from the 1960s to the 1990s that were untouched by the larger but more distant September 2010 event. Until the mid-1980s, the design of most structures was non-ductile. Strength was accomplished through rigidity rather than ductility, a feature of modern design used to absorb the energy of larger earthquakes. Modern design standards emphasise life safety by preventing catastrophic failure rather than preventing any damage.

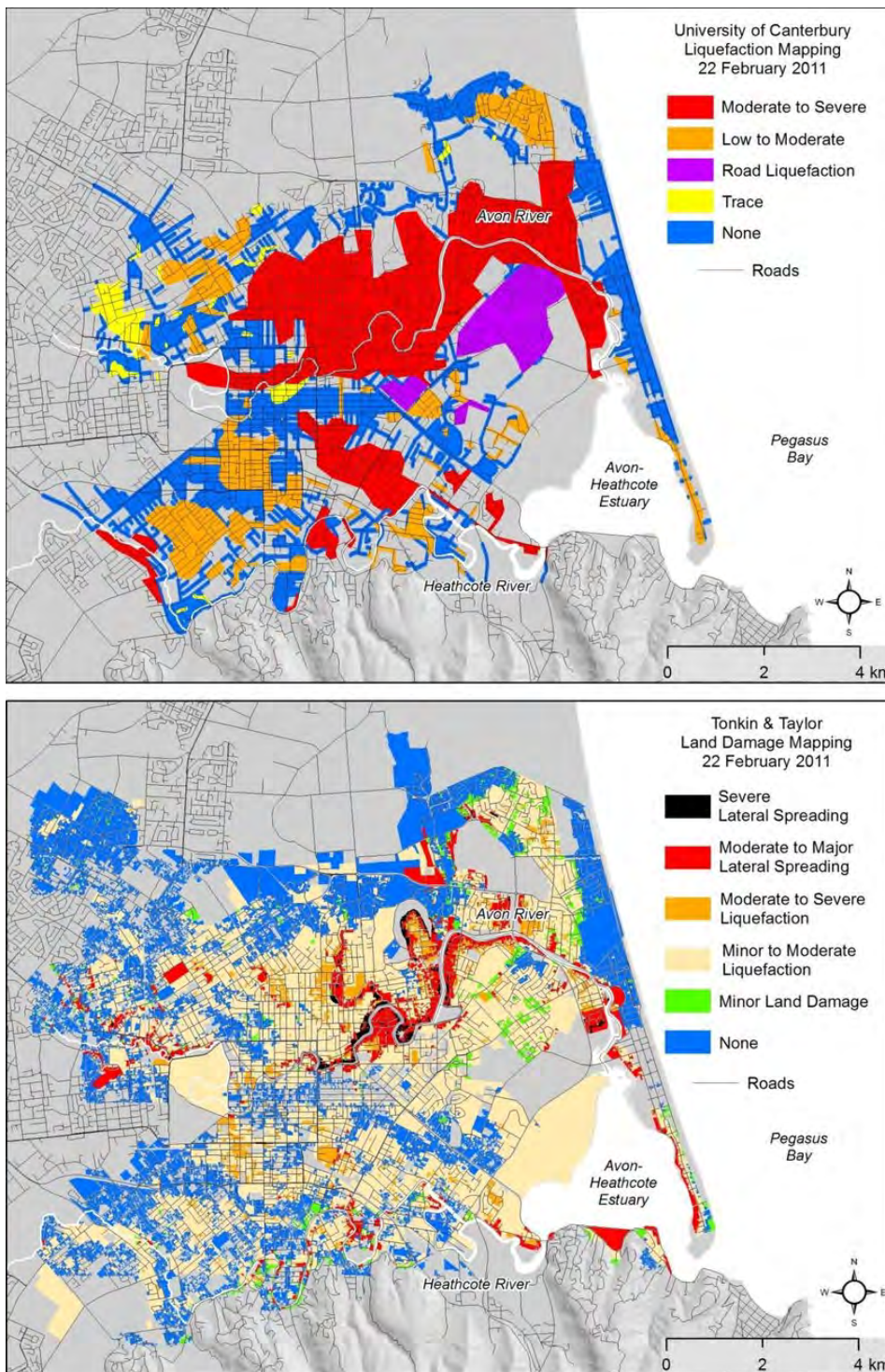


Figure 7. Liquefaction and land damage mapping for the 22<sup>nd</sup> February 2011 Christchurch earthquake. Top: Area wide interpretations of liquefaction occurrence based on street reconnaissance drive-through conducted by the University of Canterbury (Cubrinovski et al., 2011a,b). Bottom: Property- based land damage assessments conducted by Tonkin and Taylor for the Earthquake Commission (Cubrinovski et al., 2014).

Following the CES many buildings in the CBD were removed (see Appendix), thus clearing the way for extensive rebuilding. Although not yet complete, the rebuild of the CBD has resulted in a modern, earthquake-resilient city that utilises the latest in ground improvement techniques to reduce liquefaction-related ground deformation and innovative structural engineering to improve life safety in future seismic events.

## Lesson Learned and New Technology

The observations made during and the research following the CES has led to many advances in both geotechnical and structural earthquake engineering. The understanding of behaviour of the ground during earthquakes was subject to considerable revision. Prior to the CES it was generally understood that loose, granular soils following liquefaction, would densify and would then be unlikely to liquefy again! The CES events demonstrated repeated liquefaction at single locations. Some of these sites liquefied again during the M5.9 14th February 2016 earthquake!

Methods of ground improvement have been tested and are now a requirement in areas identified as being susceptible to liquefaction (Figure 8).

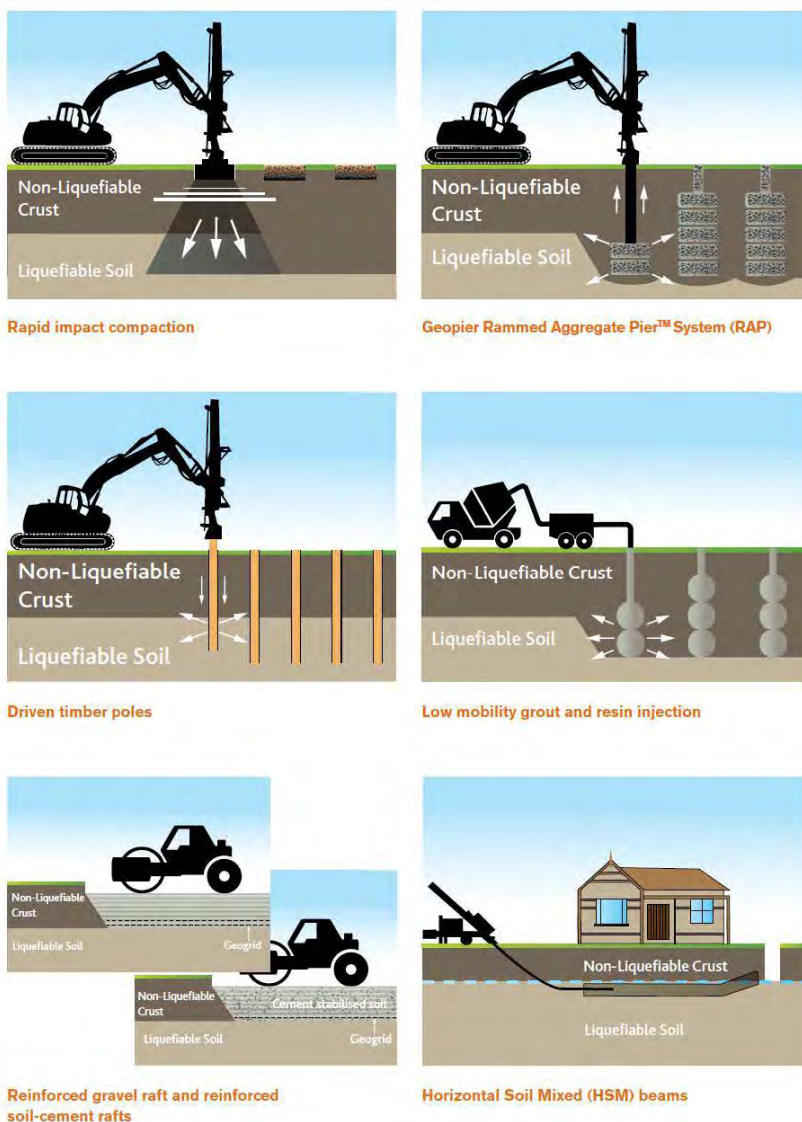


Figure 8. Ground improvement methods trialled and implemented across Christchurch following the CES (EQC 2015)

Thresholds for rockfall triggering and the calibration of sophisticated run-out models have been improved using empirical rockfall debris mapping from numerous sites in the Port Hills. Better understanding of rockfall hazard has led to better land use planning and the implementation of rockfall protection measures in the most vulnerable areas.

Observations of structural response have improved both design and construction standards. The inclusion of sacrificial structural elements, including various forms of cross-bracing, have become the norm in new construction (Figure 9). In addition, work on retrofitting existing structures now includes the latest in bracing (Figure 10) and base-isolation technology (Figure 11).

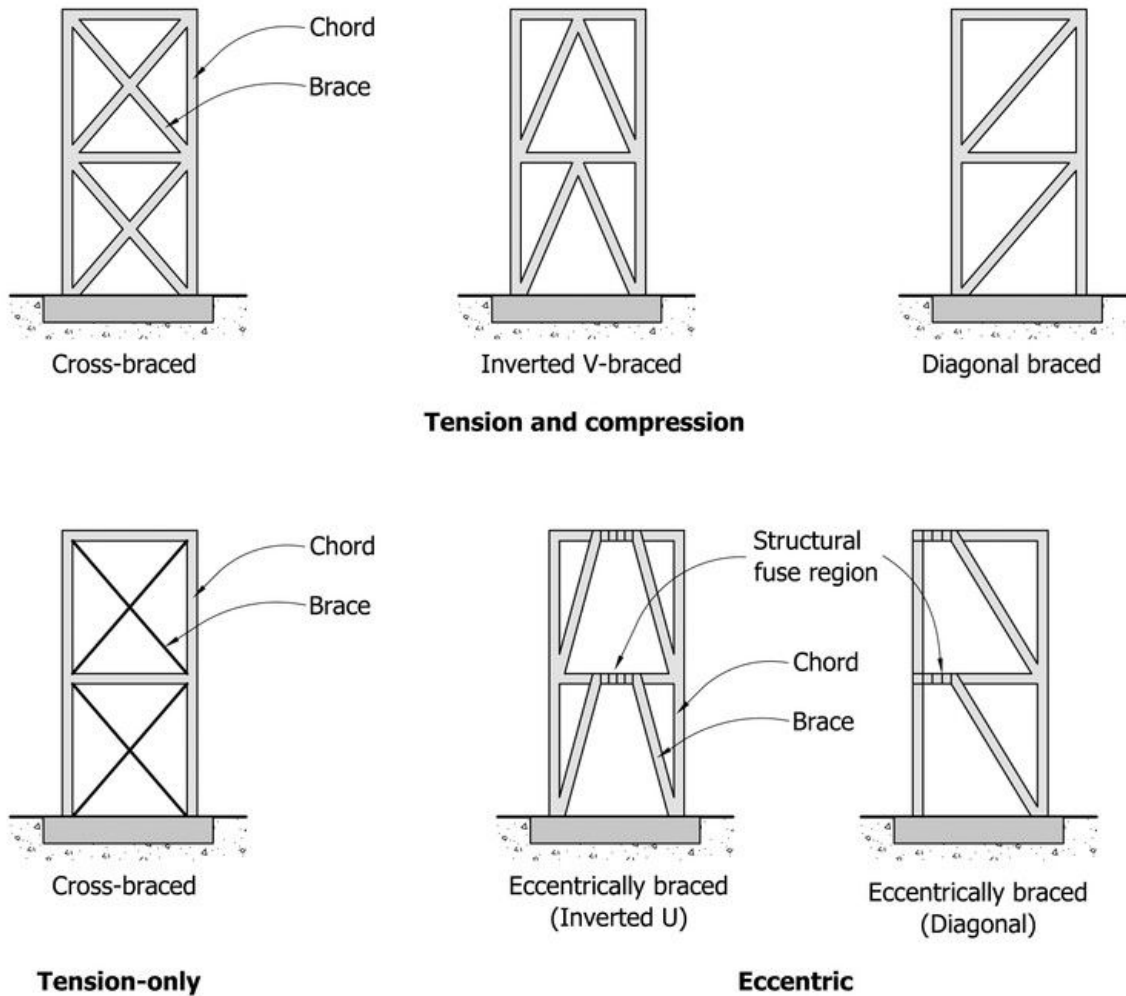
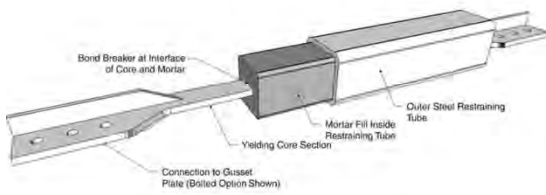


Figure 9. Common building cross-bracing strategies.

A buckling-restrained brace (BRB) is a structural brace in a building, designed to allow the building to withstand cyclical lateral loadings from earthquakes. It consists of a slender steel core, a concrete casing designed to continuously support the core and prevent buckling under axial compression, and an interface region that prevents undesired interactions between the two.



Fluid viscous dampers typically consist of a cylinder with an internal piston that allows transfer of silicone oil between two chambers through orifices in the piston head. The devices become active during dynamic events when the displacement induced creates a relative velocity between each end of the device, and the energy input is converted to heat.

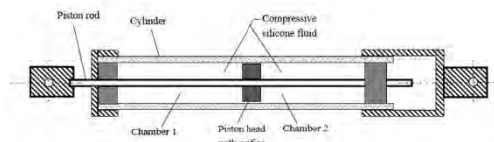


Figure 10. Common bracing elements found in new build structures across Christchurch. BRBs are also commonly used to retrofit older buildings in order to improve seismic performance.

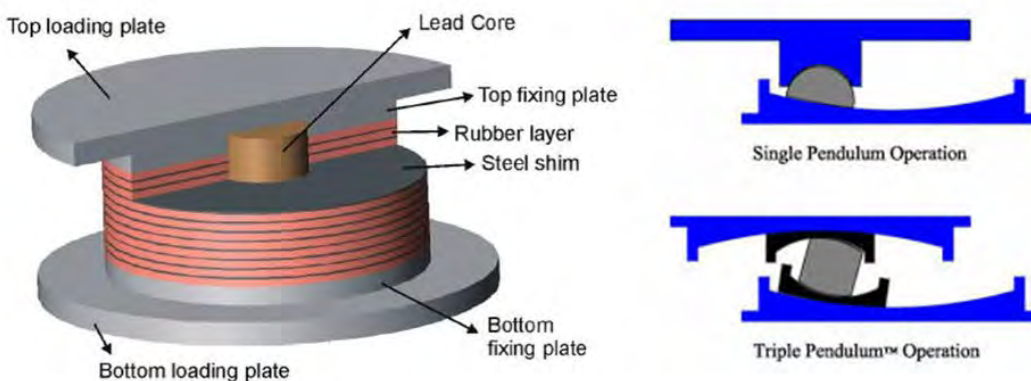
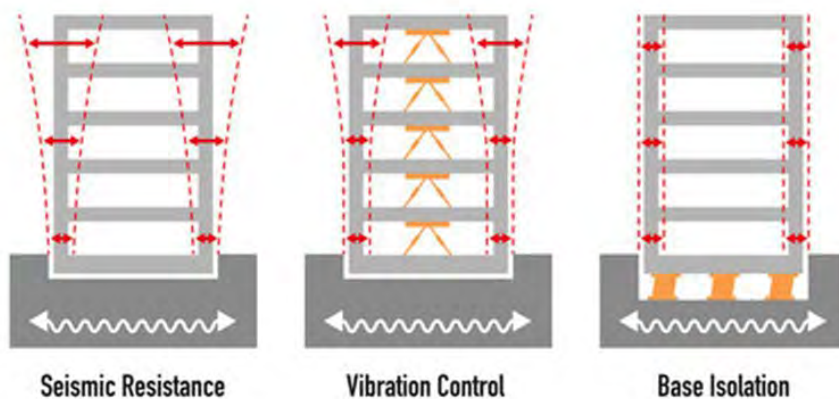


Figure 11. Base isolation strategies. Lead rubber bearing base isolation (left) and triple friction pendulum base isolation (right). Both methods allow a building to move independently of the ground reducing the movement of the structure.

## References

- Barnes, P.M., Ghisetti, F.C., and Gorman, A.R. (2016). New insights into the tectonic inversion of North Canterbury and the regional structural context of the 2010–2011 Canterbury earthquake sequence, New Zealand. *Geochemistry Geophysics, Geosystems* 17: 324–345, doi:10.1002/2015GC006069.
- Beavan, R.J., Samsonov, S., Motagh, M., Wallace, L.M., Ellis, S.M., Palmer, N.G. (2010). The Darfield (Canterbury) earthquake: geodetic observations and preliminary source model. *Bulletin of the New Zealand Society for Earthquake Engineering* 43(4): 228–235.
- Begg, J.G., Jones, K.E., Barrell, D.J.A. (2015). Geology and geomorphology of urban Christchurch and eastern Canterbury. GNS Science geological map 3.
- Bradley, B.A., Quigley, M.C., Van Dissen, R.J., Litchfield N.J. (2014). Ground Motion and Seismic Source Aspects of the Canterbury Earthquake Sequence. *Earthquake Spectra* 30(1):1-15.
- Buchanan, A., Carradine, D., Beattie, G.J., and Morris, H. (2011). Performance of houses during the Christchurch earthquake of 22 February 2011. *Bulletin of the New Zealand Society for Earthquake Engineering* 44: 342–357
- CCC [Christchurch City Council] (2003). Waterways, wetlands and drainage guide. Ko Te Anga Whakaoroa mō ngā Arawai Rēpō.
- Clifton, C., Bruneau, M., MacRae, G.A., Leon, R.T., Fussell, A. (2011). Steel Structures Damage from the Christchurch earthquake series of 2010 and 2011. *Bulletin of the New Zealand Society for Earthquake Engineering* 44: 297–318.
- Cubrinovski M., Bray J.D., Taylor M., Giorgini S., Bradley B., Wotherspoon L., Zupan J. (2011a). Soil liquefaction effects in the central business district during the February 2011 Christchurch earthquake. *Seismological Research Letters* 82: 893–904.
- Cubrinovski, M., Bradley, B., Wotherspoon, L., Green, R., Bray, J., Wood, C., Pender, M., Allen, J., Bradshaw, A., Rix, G., Taylor, M., Robinson, K., Henderson, D., Giorgini, S., Ma, K., Winkley, A., Zupan, J., O'Rourke, T., DePascale, G., Wells, D. (2011b). Geotechnical aspects of the 22 February 2011 Christchurch earthquake. *Bulletin of the New Zealand Society for Earthquake Engineering* 44: 205–226.
- Cubrinovski, M., Hughes, M., Bradley, B., Noonan, J., Hopkins, R., McNeill, S., English, G. (2014). "Performance of Horizontal Infrastructure in Christchurch City through the 2010-2011 Canterbury Earthquake Sequence. Civil & Natural Resources Engineering Research Report 2014–02. University of Canterbury, March 2014. <https://ir.canterbury.ac.nz/handle/10092/9492>.
- DeMets, C., Gordon, R.G. and Argus, D.F. (2010). Geologically current plate motions. *Geophysical Journal International* 181: 1–80.
- Dizhur, D., Ismail, N., Knox, C., Lumantarna, R., and Ingham, J. M. (2010). Performance of unreinforced and retrofitted masonry buildings during the 2010 Darfield earthquake, *Bulletin of the New Zealand Society for Earthquake Engineering* 43: 321–339
- EQC (2015). Residential Ground Improvement: Findings from trials to manage liquefaction vulnerability report, 38 p. <https://www.eqc.govt.nz/summary-of-gips-findings>

- Forsyth P.J., Barrell D.J.A., Jongens R. (2008). Geology of the Christchurch area, scale 1:250000. Institute of Geological & Nuclear Sciences Limited, 1:250,000 Geological Map 16, 1 sheet + 67 p, Lower Hutt, New Zealand. GNS Science.
- Gledhill, K., Ristau, J., Reyners, M., Fry, B. and Holden, C. (2011). The Darfield (Canterbury, New Zealand) Mw 7.1 Earthquake of September 2010: A Preliminary Seismological Report. *Seismological Research Letters* 82(3): 378–386.
- Kaiser, A., Holden, C., Beavan, J., Beetham, D., Benites, R., Celentano, A., Collett, D., Cousins, J., Cubrinovski, M., Dellow, G., Denys, P., Fielding, E., Fry, B., Gerstenberger, M., Langridge, R., Massey, C., Motagh, M., Pondard, N., McVerry, G., Ristau, J., Stirling, M., Thomas, J., Uma, S.R., Zhao, J. (2012). The Mw6.2 Christchurch earthquake of February 2011: preliminary report. *New Zealand Journal of Geology and Geophysics* 55(1): 67-90.
- Kam, W.Y., Pampanin, S., and Elwood, K.J. (2011). Seismic performance of reinforced concrete buildings in the 22 February Christchurch (Lyttelton) earthquake, *Bulletin of the New Zealand Society for Earthquake Engineering* 44: 239–278.
- Massey C.I., McSaveney, M.J., Taig, T., McSaveney, M.J., Richards, L., Litchfield, N.J., Rhoades, D.A., McVerry, G.H., Lukovic, B., Heron, D.W., Ries, W., Van Dissen, R.J. (2014). Determining Rockfall Risk in Christchurch Using Rockfalls Triggered by the 2010–2011 Canterbury Earthquake Sequence. *Earthquake Spectra* 30(1): 155–181.
- Pettinga, JR, Yetton, MD, Van Dissen, RJ and Downes, G. (2001). Earthquake source identification and characterisation for the Canterbury region, South Island, New Zealand. *Bulletin of the New Zealand Society for Earthquake Engineering* 34(4): 282–317.
- Quigley, M. C., Bastin, S., and Bradley, B. A. (2013). Recurrent liquefaction in Christchurch, New Zealand, during the Canterbury earthquake sequence. *Geology* 41: 419–422.
- Reyners, M. (2011). Lessons from the destructive Mw 6.3 Christchurch, New Zealand, Earthquake. *Seismological Research Letters* 82(3): 371–372.
- Teng, A., et al. (2017). Living in areas with different levels of earthquake damage and association with risk of cardiovascular disease: a cohort-linkage study. *The Lancet Planetary Health* 1: e242- e253.
- Van Dissen R , Barrell D , Litchfield N , Villamor P , Quigley M et al. (2011) . Surface rupture displacement on the Greendale Fault during the Mw7.1 Darfield (Canterbury) earthquake, New Zealand, and its impact on man-made structures. *Proceedings of the Ninth Pacific Conference on Earthquake Engineering*, 14–16 April 2011 University of Auckland, Auckland, New Zealand: 9PCEE.

## Christchurch CBD Rebuild Walking Tour

Christchurch has undergone a remarkable transformation in the decade following the 2010–2011 Canterbury Earthquake Sequence. This tour aims to highlight some of the innovative earthquake engineering employed in the rebuild of the Central Business District (CBD). The field trip starts at the Art Gallery, which acted as the centre for emergency operations during the earthquake sequence. The sites visited cover everything from completely new construction to retrofitting of older, often heritage buildings. The itinerary is not fixed; anyone wishing to use this field guide at some later date is encouraged to use this as a rough guide and let their curiosity be the guide. The city is in a state of constant change and there is always something new to look at! Once you know the basic elements involved in structural earthquake engineering, it is fun wandering around the new builds and seeing which earthquake-resistant measures have been employed!

For those wanting a good overview of the earthquakes and their effects on the city, the Quake City interactive exhibition at 299 Durham Street North is highly recommended.

The following field trip stops are just a number of the highlights that illustrate some of the challenges and approaches to rebuilding a city following a major earthquake. The location of each site is shown on Figure 12.

### **1. Art Gallery Te Puna o Waiwhetū (retrofit): Montreal Street, between Gloucester & Worcester Streets.**

The Art Gallery opened on 10th May 2003. The façade is designed in the form of koru and mimics the meanders of the Avon River. Te Puna o Waiwhetū relates to life giving properties of the artesian spring on which the gallery sits. The building served as the Emergency Operations Centre during 2010–11 Canterbury Earthquakes. The ground beneath the building suffered severe liquefaction causing the building to suffer differential settlement, reaching a maximum of 182 mm in some areas. Post-earthquake restoration included re-supporting and re-leveling the 33,000-tonne building while the building held valuable artworks and staff members. Jet grouting was employed to install 124 columns, 4 m in diameter, beneath the building to provide a solid foundation from which the building could then be lifted and relevelled. Lifting occurred at a rate of a few millimetres per day, all the while being monitored and modelled by custom designed sensors, until the building reached its original position. The foundation now comprises 140 triple friction base isolators. It is the first base isolation retrofit project in New Zealand to use triple pendulum double concave sliding isolators. These are observed in the underground parking structure (access from Montreal Street). Also of note is the seismic gap that surrounds the building, allowing the building to move independently of any seismic ground motion. The cover plates over this gap is seen in the gallery courtyard. The gap itself is seen from the parking structure—look up towards the margins of the parking structure! Like most of the CBD, the Art Gallery is situated on Holocene alluvium (Figure 12), mostly loose to medium dense sand overlying sandy gravel.

### **2. Art Centre Te Matatiki Toi Ora (retrofit/rebuild): Worcester Boulevard**

The Art Centre comprises 23 separate buildings, 21 of which are classified as Category One NZ Historic Places. The Student Union Building (formerly Duxe Deluxe) is designated Category Two. The Gothic Revival buildings were designed by Benjamin Mountfort. The land on which the Arts Centre is located was acquired by the provincial government in 1873 for the location of Canterbury College (now University of Canterbury). Built in 1877 this was also the site of both Boys' and Girls' High Schools. The buildings are entirely unreinforced masonry, mostly Port Hills basalt for the rough-hewn blocks, Halswell and Hoon Hay basalts and Port Hills trachyte for the lower course blocks and pillars, and Oamaru limestone for lintels, sills and other architectural detailing.

Julius von Haast lectured at Canterbury College from 1873 and he was appointed Chair of Geology in 1876. The university started moving out of this site to its current home in Ilam in 1961. The site was gifted to the city in 1973 and is currently held in trust for the people of Canterbury.

The 4<sup>th</sup> September 2010 Darfield earthquake caused extensive damage. Collapsing chimneys damaged the Great Hall, the Observatory Tower and the Clock Tower. The then Arts Centre director Ken Franklin commented that strengthening work in 1985 prevented additional damage. The buildings had been insured for NZ\$95 million, and this was increased to NZ\$120m in January 2011! The 22<sup>nd</sup> February 2011 Christchurch earthquake caused further, extensive damage, but no people were injured. All historic buildings became inaccessible and the entire complex was closed until the first restored and strengthened building, the Registry, reopened in 2013.

The initial cost estimate to repair the cumulative earthquake damage was NZ\$100m. This was revised to more than NZ\$200m and estimated to take 15 years to complete. Under the guidance of a new chief executive the rebuild and retrofit programme was accelerated. The costs escalated to NZ\$290m making it one of the largest heritage restoration projects in the world.

Each building throughout the campus is largely unique and has required bespoke solutions. Particular consideration was required when balancing heritage constraints with the cost of implementing strengthening works. Overall there is little visible evidence of the strengthening and restoration. Look carefully and you will see that the original stone in the chimneys, towers and finials have been replaced with lighter, stronger engineered materials. Much of the stonework is merely lightweight stone façade over a steel or timber frame.

Post-tensioned tendons (high-specification stainless-steel cables), both horizontal and vertical, can be seen on the exterior of the Teece Museum (the former Chemistry Building). This building had been part of the 1985 strengthening programme and performed well during the CES. The post-tensioning system was renewed following the 2011 earthquakes.

Elsewhere plywood diaphragms and concrete ring beams have been used to prevent out-of-plane movement in a number of buildings. Where interior heritage elements had to be preserved (e.g., vaulted ceilings, ornate plaster work) alternative methods of strengthening have been used.

The Great Hall, with its impressive vaulted ceiling and dramatic stained glass window, opened in 1882 and reopened in 2016. Both the Great Hall and Clock Tower were first to be restored due to their historical significance. It should be noted that the Great Hall also had seismic retrofitting pre-2011.

What you won't see are vertical post-tension bars; they are cored through the existing walls. They are anchored top and bottom to increase shear and rocking capacities of the panels. New reinforced concrete walls were constructed within the original wall matrix: the inner heritage fabric and the wall core were deconstructed, concrete was cast against the external fabric and then the inner heritage layer was reinstated. Horizontal bars were cored into the existing wall matrix to provide additional shear capacity and transfer of forces to adjacent strengthened elements. Within the Great Hall you will only see a few relatively unobtrusive steel strengthening elements around the stained glass windows.

Buildings with interiors of lower heritage value, such as the Registry building, allowed for a slightly more intrusive strengthening approach. Glass Fibre Reinforced Polymer (GFRP) was applied to the masonry surface and embedded steel vertical straps added to provide additional capacity. Plaster finishes were then reinstated to hide the underlying strengthening.

The complex configuration of the old Boys' High Building, with nine gable-end roofs of differing orientations, is strengthened by a ceiling-level steel x-braced diaphragm (a network of exposed internal steel cross-braces at eaves level). In addition the original stone of the reinstated gable-end walls have been replaced by light-weight engineered stone facade.

### **3. Wynn Williams House (rebuild): 47 Hereford Street**

Wynn Williams House is a new six storey building that replaced a 1930's lightly reinforced concrete eight storey building known as St Elmo Courts. The original concrete structure was demolished in April 2011 after suffering significant earthquake damage.

The new building combines lead rubber bearing base isolation and post-tensioned timber and concrete two-way seismic frames, claimed to be a world first in seismic design. During development of the design, base isolation was considered as a cost-saving alternative to providing individual dissipative devices at the beam-column joints.

The building is supported on 16 base-isolated precast concrete columns. Post-tensioned laminated veneer lumber (LVL) beams form a major part of the primary structure, providing seismic resistance through the use of rocking connections at the ends of the beams, as well as gravity load balancing through the use of steel tendons. Note the steel caps on the exterior of the building.

The LVL beams are partially exposed in the building, giving an aesthetic appeal to the internal space. This design demonstrates how moderately tall structures can utilise engineered wood products and base-isolation, items that are often considered to be expensive, to result in very cost-effective construction.

The building has a basement that sits below the local water table requiring a continuous drainage system. A 7-storey lift goes from the top floor down to the basement level. The basement holds the base isolators and therefore is not isolated. To avoid the lift breaking between the ground and basement floor in the event of an earthquake, the lift hangs from the main structure and is isolated from the basement by a seismic gap. The stairwells also hang from the main structure and can withstand 400mm of movement relative to the building.

### **4. Christchurch City Council Civic Offices Te Hononga (monitoring):**

In October 2007 Christchurch City Council selected the NZ Post building in Hereford Street as the preferred site for its new Civic Building. The existing building, designed in 1965 and completed in 1981, was redeveloped to provide office space for approximately 1,200 staff and was completed in August 2010.

Following the earthquakes, the building was evacuated for several months making progress of earthquake recovery across the city more difficult. Following the earthquakes the building was equipped with a seismic monitoring system. Sensor points throughout building and connected to central recording system instantly analyses and reports shaking levels against building specific thresholds. This allows immediate stay/evacuate decisions to be made. Building status information is sent to the building owner, manager, and engineer.

### **5. Pita Te Hori Centre (new build): 93 Cambridge Terrace**

The Pita Te Hori Centre, located on the former King Edward Barracks site, comprises of two L-shaped five-storey office buildings, a six-level car park and a large landscaped garden called Ngā Mara a Te Wera, or the Garden of Te Wera. The site has strong spiritual, cultural and historical significance to Ngāi Tūāhuriri and Ngāi Tahu as well as a long history with both the military and the police.

Named to commemorate the first Upoko Rūnanga (council chair) of Ngāi Tūāhuriri, Pita Te Hori was a Ngāi Tahu chief who had strong influence on the area occupied during Ngāi Tahu settlement in pre-European times.

The office buildings are named Iwikau and Te Uriti. Iwikau was the chief of Pakiaka, the main village in Tuahiwi where the chief resided in the nineteenth century. Te Uriti is an earlier name for Tuahiwi.

The history of the site with the military began in 1864 when the Canterbury Provincial Council set aside part of the land as a parade ground for the volunteer army service. The King Edward Barracks were erected in 1905 and used until the army withdrew from the site in 1993. The Barracks were dismantled in 1997. The Christchurch Central Police Station was also located on the site for 142 years with the first building built in 1873. Additions were made in 1906 however with an increase in population a new police station was opened in 1973. This building was demolished in May 2015. The Pita Te Hori Centre was officially opened on 10 August, 2017.

Iwakau, located at the corner of Cambridge Terrace and Cashel Street, has triple friction base isolators. Unlike the other base-isolated building observed so far, the seismic gap for this building is located at the top of the first storey rather than at ground level. This design was driven by construction and cost considerations. Similar to Wynn Williams House, the lift core and staircases are suspended from the building frame, maintaining base isolation. Look for the seismic gap as you walk through the lobby.

Both Iwakau and Te Uruti Buildings use buckling restraint braces to improve seismic performance. These are clearly seen through the windows of both buildings.

#### ***6. Traffic Control Seismometers (monitoring): throughout the CBD***

Originally Christchurch only had four GNS seismometers, located at Christchurch Hospital, the Botanic Gardens, Cathedral College, and Resthaven Rest Home. The experience of recent earthquakes, both in New Zealand and overseas, shows that detailed knowledge of the spatial variability of earthquake ground shaking can greatly improve earthquake response, possibly reducing injuries and fatalities.

EQRNet is 'Seismic Resilience as a Service', a new generation solution to deliver defendable, evidence-based decision-making information to increase certainty and reduce risk. EQRNet is developed and operated by Canterbury Seismic Instruments Ltd (CSI).

A 10-sensor trial of EQRNet was installed in November 2017, demonstrating the variability in earthquake source proximity, direction, and local ground conditions means that earthquake shaking levels across a city like Christchurch are hugely variable.

With a CCC Smart Cities grant CSI installed 150 accelerometers around Christchurch. There are 80 located in the CBD. These are housed in the light green boxes located at traffic intersections.

EQRNet instantly compares every building's design limits to the shaking beneath it. Critical buildings have additional sensors to measure how the structure responds to the ground shaking. Results are sent immediately to the building manager's phone, and to the structural engineer and city-wide data is instantly available for emergency management teams. Public data lets individuals to manage their own personal earthquake response.

#### ***7. Bridge of Remembrance (rebuild/retrofit): Cashel Street at Oxford Terrace***

The Bridge of Remembrance is a war memorial honouring those lost in the world wars and in conflicts with Vietnam, Borneo, Korea and Malaya. The memorial opened in 1924 and suffered considerable damage in the February 2011 earthquake. Repairs were conducted from May 2013 through to September 2015 costing NZ\$6.7 million. It was reopened and rededicated on ANZAC day, 2016.

Differences in the soil conditions beneath the bridge caused differential settlement. Repairs included micro piles to level south side and extending the original 4 m deep piles to 26 m. Concrete footings were widened to reduce rocking of the Triumphal Arch. The hollow arch elements were strengthened with steel boxes and sliding joints and a post tension were added to improve the seismic response of the entire arch structure.

#### ***8. PwC Centre (new build): 60 Cashel Street***

The PwC Centre in Christchurch is the first new post-earthquake office building in the CBD, opening in May 2018. This integrates its earthquake structural engineering elements as part of the architectural detailing. Buckling Restraint Braces (BRBs) are an obvious feature of the structure. Leaving these visible lends a feeling of strength and safety to the building. Once hidden, it is now common to see such earthquake resistant design features to be prominently displayed and incorporated into the architectural aesthetic.

### **9. Te Pae Christchurch Convention Centre (new build): Oxford Terrace at Armagh Street**

The Wood Bagot and Warren & Mahoney designed Te Pae draws inspiration from the braided rivers of the Canterbury Plains, the neo-gothic architecture of Christchurch city and the patterns and colours that are part of the local Ngāi Tahu iwi tradition. The sweeping curves of the exterior façade mimics the anastomosing channels of Canterbury's braided rivers. The cross-hatched fibre cement tile cladding tiling represents harakeke weaving.

Currently under constructions, Te Pae is a moment resisting steel frame with buckling restraint bracing. The location, adjacent to the Ōtākaro-Avon River, indicates that this site is underlain by low density, water-saturated, recent alluvial deposits (Figure 13), mainly fine overbank and point bar sands. This site is in the medium to high liquefaction susceptibility zone as designated by CCC hazard maps.

### **10. Isaac Theatre Royal (rebuild/restoration): 145 Gloucester Street**

Construction of the Theatre Royal began in 1906 and the theatre was opened in 1908. The theatre underwent several upgrades in 1928 (to upgrade for film screening), 1998-2000 (refurbishing and seismic retrofitting), and 2004-2005 (refurbishment and rebuild of back of house and stage house).

The theatre was subjected to severe shaking during the earthquakes of 22nd February and 13th June 2011 and sustained considerable damage; this damage was exacerbated by the constant and frequent aftershocks throughout 2011 and subsequent significant earthquake on 23rd December 2011. The Back of House and Stage House (built in 2004/05) suffered only moderate damage and were repaired, but the 1908 auditorium and 1928 foyer spaces were not considered repairable in their original form, due to the dangerous nature of the original un-reinforced masonry walls.

The structural earthquake strengthening carried out in 1999/2000 prevented complete collapse of the theatre and enabled the retrieval and salvage of key heritage items and stabilisation of the Edwardian façade prior to deconstruction. All heritage fabric was retained, restored and/or reinstated. The restoration work included new foundations and structural strengthening of the original 1908 heritage façade; complete replacement of the auditorium, foyers, and western egress; and restoration and reinstatement of the original key heritage items.

The Theatre re-opened on 17th November 2014. The project was significantly more elaborate in design and complexity than originally estimated, with the theatre essentially being rebuilt from façade to proscenium arch. The rebuild and restoration had significant challenges throughout, making it one of the most intricate building projects in the CBD with an overall rebuild cost of NZ\$40M.

### **11. Town Hall (retrofit): 86 Kilmore Street**

The Town Hall was opened in 1972. It was designed by Sir Miles Warren and Maurice Mahoney of Warren and Mahoney Architects with acoustic assistance from Professor Harold Marshall. The main auditorium is world-renown for the quality of its acoustics. It has been argued that its design was the birth of modern-day music hall acoustics.

The original cost of the Town Hall was about \$4 million, equivalent to \$51 million today. \$500,000 was raised by public subscription and the remainder contributed by the regional Canterbury local bodies.

The Town Hall was closed as a result of significant damage caused by the 22nd February 2011 earthquake from liquefaction and the related lateral spreading of the ground towards the Ōtākaro-Avon River. In October 2012, a staff report recommended that only the main auditorium be saved, with the rest of the building to be demolished. However, on 22nd November 2012, Christchurch councillors voted unanimously to rebuild it at a cost of \$127.5 million, only \$68.9 million of which would be covered by insurance.

On 11th June 2015 confirmation was given by the Christchurch City Council on the decision for the repairs of the Christchurch town hall to proceed. Work started in November 2015 with the foundations. Ground improvement included 1,097 interlocked jet-grout columns forming a grid of cells beneath the footprint of the building. The cells will reduce the potential for lateral movement resulting from soil liquefaction. Jet grouting was complicated by the need to work in the confined spaces around and beneath the existing protected building. Ground improvement works took 11 months.

The restoration was initially expected to be completed mid-2018, but the first part did not officially open until February 2019.

On 4<sup>th</sup> September 2020, the Town Hall was designated a Category I Historic Place by Heritage New Zealand, reflecting the building's "outstanding international and national significance".

### ***12. Oi Manawa Canterbury Earthquake National Memorial: Oxford Terrace at Montreal Street***

The official memorial to the 185 people who died on 22<sup>nd</sup> February 2011. Ngāi Tahu gifted the name Oi Manawa which means 'tremor or quivering of the heart'. It also refers to the shaking of earthquake tremors and is symbolic of the trauma experienced as a result of the earthquakes.

An unofficial memorial, 185 White Chairs, is located on Madras Street adjacent to the Transitional Cathedral (13).

### ***13. ChristChurch Cathedral (demo and rebuild): Cathedral Square***

ChristChurch Cathedral was built between 1864 and 1904 in the centre of the city, surrounded by Cathedral Square. It became the cathedral seat of the Bishop of Christchurch, who is in the New Zealand tikanga of the Anglican Church in Aotearoa, New Zealand and Polynesia.

Earthquakes have repeatedly damaged the building (mostly the spire): in 1881, 1888, 1901, 1922, and 2010. The 22nd February 2011 Christchurch earthquake destroyed the spire and the upper portion of the tower, and severely damaged the rest of the building. A lower portion of the tower was demolished immediately following the earthquake to facilitate search and rescue operations. The remainder of the tower was demolished in March 2012. The badly damaged west wall, which contained the rose window, partially collapsed in the 13th June 2011 earthquake and suffered further damage in the December 2011 earthquakes.

The Anglican Church decided to demolish the building and replace it with a new structure, but various groups opposed the church's intentions, with actions including taking a case to court. While the judgements were mostly in favour of the church, no further demolition occurred after the removal of the tower in early 2012. Government expressed its concern over the stalemate and appointed an independent negotiator and in September 2017, the Christchurch Diocesan Synod announced that ChristChurch Cathedral will be reinstated after promises of extra grants and loans from local and central government. By mid-2019 early design and stabilisation work had begun.

Since 15 August 2013 the cathedral community has worshipped at the Cardboard Cathedral (14).

### ***14. Transitional Cathedral (new build): Hereford Street at Madras Street***

The Cardboard Cathedral, formally called the Transitional Cathedral is the transitional pro- cathedral of the Anglican Diocese of Christchurch. The Cardboard Cathedral was designed by the Japanese architect Shigeru Ban and opened in August 2013. It is located on the site of St John the Baptist Church.

The A-frame building is 21 m high. Materials used include 600 mm diameter cardboard tubes, timber and steel. The roof is of polycarbon, with eight shipping containers forming the walls. The foundation is concrete slab. The architect wanted the cardboard tubes to be the structural elements, but local manufacturers could not produce tubes thick enough and importing the cardboard was rejected. The 96 tubes, reinforced with laminated wood beams, are coated with waterproof polyurethane and flame retardants with 50 mm gaps allowing natural light to filter inside. Instead of a replacement rose window, the building has triangular pieces of stained glass. The building seats around 700 people and serves as a conference/concert venue as well as a cathedral.

The Wizard of New Zealand, one of the strongest critics of the Diocese for wanting to demolish ChristChurch Cathedral, who had been a daily speaker in Cathedral Square, called the design "kitsch".

Lonely Planet named Christchurch one of the "top 10 cities to travel to in 2013" in October 2012, and the cathedral was cited as one of the reasons that makes the city an exciting place.

### ***15. Cashel Street & Surroundings (new build galore!)***

The rebuilt of Christchurch, both in the CBD and beyond, means that you are confronted with an ever-changing landscape. A plethora of seismic design options and wide-ranging architectural styles are on display. This is well displayed in the central shopping thoroughfare of Cashel Street and is a reflection of where the new Christchurch is heading.

If time allows, additional CBD highlights include the Bus Interchange (Tuam Street at Colombo Street), the Justice Plaza (Tuam Street at Durham Street) and Ao Tawhiti (St Asaph Street at Colombo Street). These all incorporate the latest in earthquake structural engineering and a modern architectural aesthetic that incorporates the bicultural heritage of Ōtautahi.

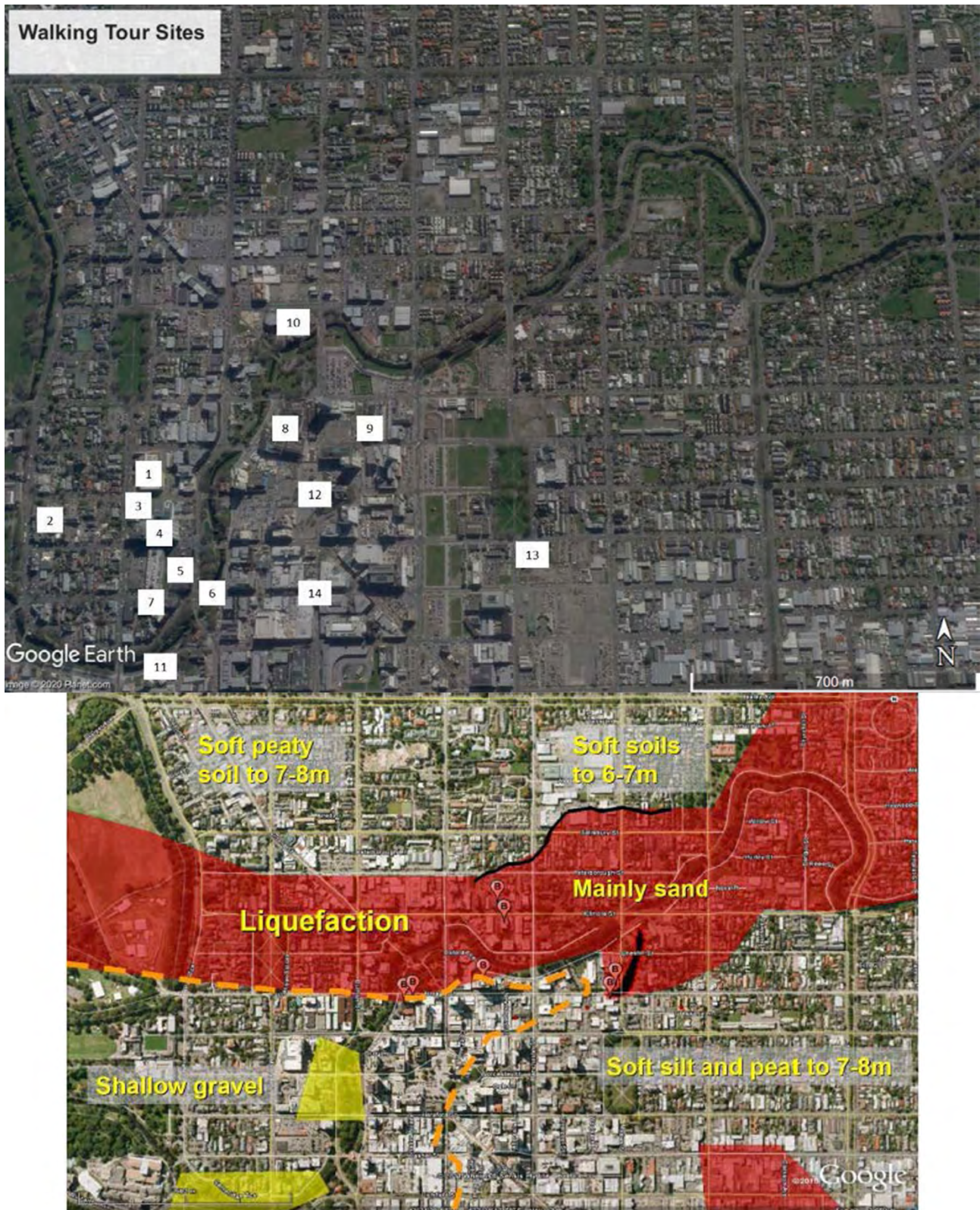


Figure 12. Aerial image showing the location of field trip stops (Google, 2020). Lower image shows the general ground conditions and areas of recorded liquefaction (Cubrinovski, 2013).

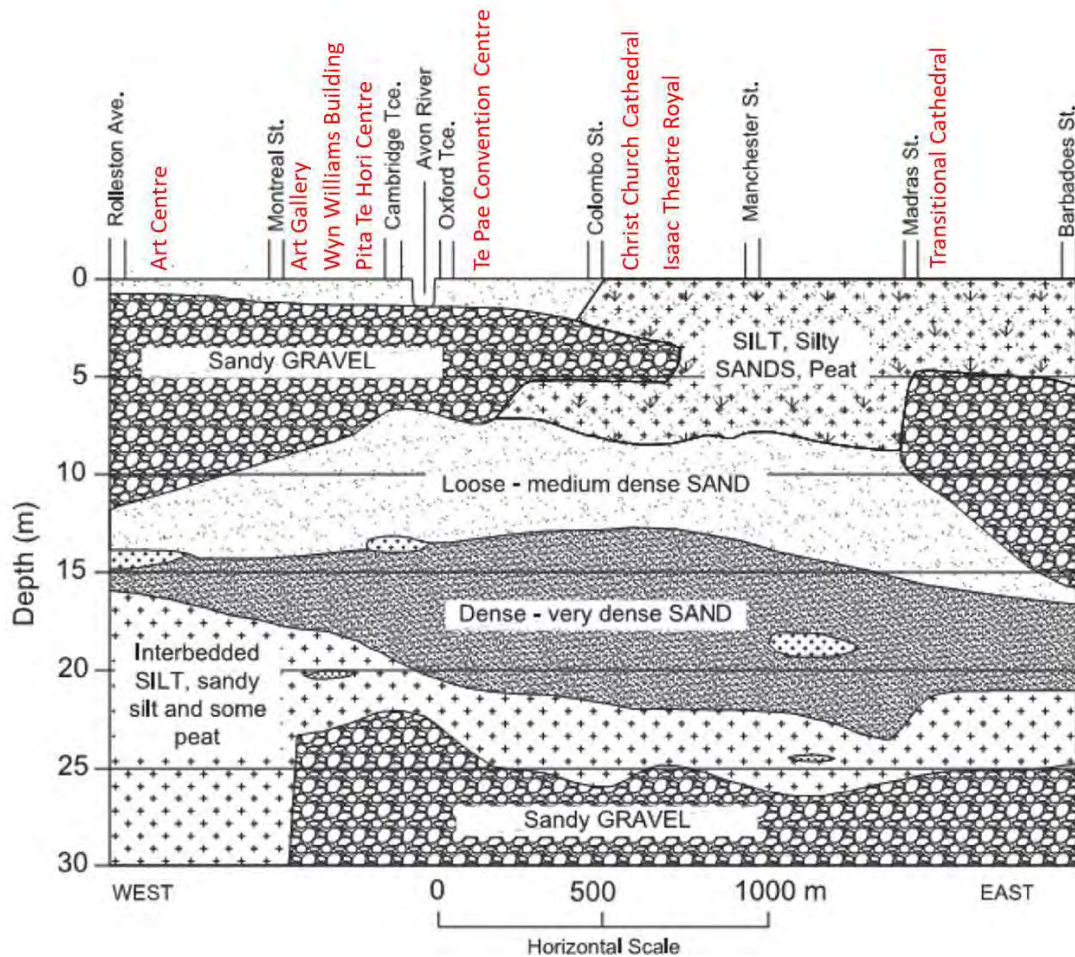


Figure 13. West to east cross section along Hereford Street showing the near-surface ground conditions in the CBD. The location of the main field trip stops are shown in red. Modified from Elder & McCahon (1990).

### References

- Cubrinovski, M. (2013). Liquefaction-Induced Damage in The2010-2011 Christchurch (New Zealand) Earthquakes. International Conference on Case Histories in Geotechnical Engineering 1. <https://scholarsmine.mst.edu/icchge/7icchge/session12/1>
- Elder, D., McCahon, I. (1990). Near surface groundwater hydrology and excavation dewatering in Christchurch, Proceeding of Groundwater and Seepage Symposium, Auckland, New Zealand, May 1990.

**Appendix: Google Earth Images highlighting the changes in the CBD during and following the CES**

